Volume 1 | Issue 1 | 2021

WORLD JOURNAL OF MEDICAL INNOVATIONS

www.worldjmi.com

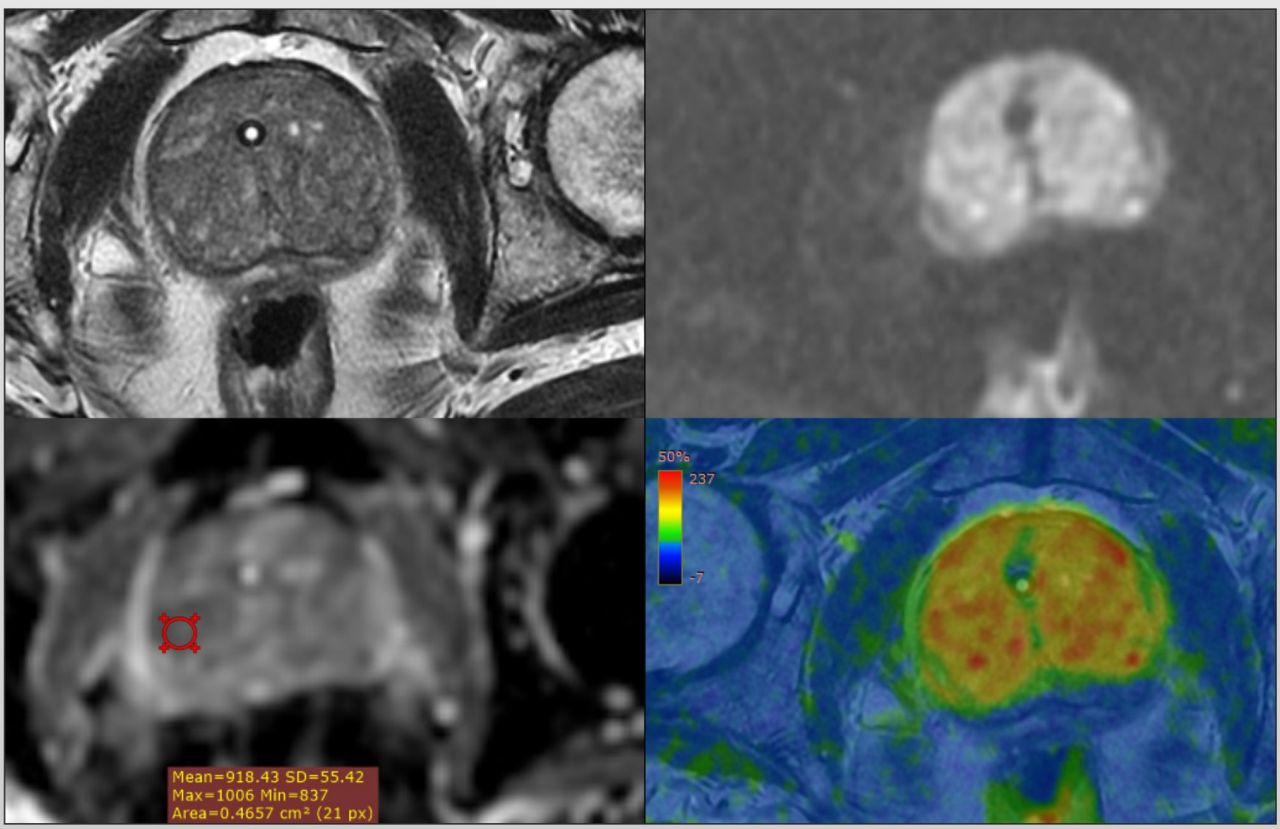

Open-access peer-reviewed international journal

WORLD JOURNAL OF MEDICAL INNOVATIONS

Volume 1 | Issue 1 | 2021

WORLD JOURNAL OF MEDICAL INNOVATIONS

2021, Volume 1, Issue 1

Editorial Board

Aims & Scope

WJMI strongly supports research that will benefit medical science and discourages the publication of articles that merely represent pre-established and repetitive facts. The journal covers all the sub-specialties of Medicine including:

- Anatomy
- Biomedical data science
- Biostatistics
- Biotechnology
- Case Study
- Cell Biology
- Clinical Trials
- Cytology
- Dentistry
- Dermatology
- Endocrinology
- General Medicine
- Genetics
- Gynecology
- Haematology
- Immunology
- Medical Biotechnology
- Microbiology
- Molecular Biology
- Nephrology
- Neurology
- Oncology
- Ophthalmology
- Organ transplantation
- Orthopedics
- Pathology
- Pediatrics
- Pharmacology
- Public health & hygiene
- Radiology
- Surgery
- Telemedicine/digital health
- Tropical diseases
- Tropical diseases
- Urology

And other medical sciences.

WORLD JOURNAL OF MEDICAL INNOVATIONS

2021, Volume 1, Issue 1

Table of Contents

WORLD JOURNAL OF MEDICAL INNOVATIONS

Malignant pleural mesothelioma with cardiac and renal metastases: a case report confirmed at autopsy

Vasylyk Volodymyr[1], Matskevych Viktoriya[2], Mytsyk Yulian[3], Lenchuk Tetiana[2], Kindrativ Elvira[4]

[1]*Pathology Department, Municipal Non-profit Enterprise «Regional Clinical Hospital of Ivano-Frankivsk Regional Council», Ivano-Frankivsk, Ukraine.*
[2]*Department of radiology and radiation medicine, Ivano-Frankivsk National Medical University, Ivano-Frankivsk, Ukraine.*
[3]*Department of Urology, Danylo Halytsky Lviv National Medical University, Lviv, Ukraine.*
[4]*Department of Pathomorphology, Ivano-Frankivsk National Medical University, Ivano-Frankivsk, Ukraine.*

Article info

PATHOLOGY

Case report

Article history:
Accepted August 17, 2021

Published online
December 5, 2021

Keywords:
mesothelioma,
malignant,
neoplasm metastasis,
myocardium,
kidney

Abstract

Objectives. The presentation of case report of cardiac and renal metastases from malignant pleural mesothelioma. Material and methods. An 80-year-old male with epithelioid mesothelioma for 9 years, without asbestos exposure was admitted to hospital with multiorgan failure manifested by acute respiratory heart and renal failure. Patient died despite the resuscitation. An autopsy followed by histological examination was performed. Results. The autopsy revealed a whitish lesion up to 6.6 cm and a lot of whitish lesions measuring 0.4 cm in diameter with irregular shape throughout the visceral pleura. Left ventricular wall of the heart was with solid whitish irregularly shaped lesion placed intramurally up to 0.6 cm in diameter and left ventricular free wall was 1.6, accordingly. Right ventricular free wall was 0.6 cm. A solid whitish lesion up to 1.1 cm in diameter was found in the middle third of left kidney as well. Histologically the visceral pleura lesion was presented by epithelioid mesothelioma consisted of tubules, papillae, solid and adenomatoid pathomorphism. Some sections of the myocardium of left ventricle and cortex of left kidney were with tumor cells presence. Conclusions. A case report of unusual metastatic lesion is presented to enrich an already existing literature database. Attention should be paid to the antemortem searching of clinically asymptomatic metastases.

Corresponding author. Viktoriya Matskevych, Department of radiology and radiation medicine, Ivano-Frankivsk National Medical University, Halytska str., 2, Ivano-Frankivsk, 76000, +38(050)9685152, vmatskevych@ifnmu.edu.ua

Introduction.

Malignant pleural mesothelioma (MPM) is a relatively rare variant of cancer, arises from multipotential mesothelial cells of the pleura, closely related to previous asbestos exposure with an unfavorable prognosis for survival [1, 2, 3]. MPM occurs in elderly people (median age 70 years) and is more common in males than females with a ratio of 3:1, respectively [4]. Histological variants of MPM are presented by three subtypes: epithelioid (60%), sarcomatoid (10-20%) and biphasic (20-30%), which are often difficult for the pathologist to distinguish because of disease's rarity and noninformative tissue samples obtained during life-time diagnostics [5,6]. The invasion of surrounding organs is typical for MPM, and more rarely distant metastases occur [7]. There are a few reported cases of unusual sites for MPM

metastases, namely salivary glands, pancreas, stomach, duodenum, ileum, and rectum [8].

Objectives.

The presentation of case report of cardiac and renal metastases from malignant pleural mesothelioma.

Material and methods (Case presentation).

An 80-year-old male, who had an anamnesis of MPM for 9 years, was admitted to hospital with multiorgan failure manifested by acute respiratory failure (type I), heart failure, renal failure. The patient was not a smoker. Also, he did not have prior asbestos and extra-radiation exposure. Ischemic heart disease was a concomitant disease. The diagnosis of MPM was suspected on contrast-enhanced computed tomography scan and confirmed by lifetime pleural biopsy performed during thoracoscopic surgery followed by histology of postoperative biomaterial (epithelioid pattern) and immunohistochemical stains (CK 5/6 +, calretyn +, WT-1 +). Patient had combined treatment, including a platinum-based therapy and palliative care in the last year of his life. The intensive treatment was carried out, despite which clinical death occurred at the emergency medical department. Resuscitation was performed but had no effect and biological death was recorded. The body was sent for the autopsy to Pathology Department. The basis of data processing was the written consent of the legally authorized person of the deceased patient. Autopsy findings. The descendent was an elderly male of average built. During the external examination no external injury was present. The skin was clean with pale conjunctivae. Lower extremities were without edema. Visceral and parietal pleura tightly fused to throughout on both right and left sides during macroscopical examination of thoracic cavity. There was a solid whitish lesion in the visceral pleura at the level of lower lobe of right lung which reached 6.6 cm and visually invaded the lung tissue (Figure 1A).

Figure 1. Macropathologic autopsy findings: A. Part of visceral pleura with adjacent lung tissue. On the right - a whitish lesion with indistinct margins. B. Left ventricular wall with whitish lesion placed intramurally of heterogeneous structure with indistinct margins. C. Part of left kidney with subcapsular whitish lesion up to 1.1 cm in diameter.

There were a lot of whitish lesions measuring 0.4 cm in diameter with irregular shape throughout the visceral pleura. Abdominal cavity was without pathological contents, peritoneum was smooth. Gross examination of the blood vessels revealed yellowish areas of aorta's intima with multiplication of small plaques up to 0.4 cm in size some of which were with calcifications. The orifices of the mesenteric and renal arteries were passable. The pericardial cavity contained up to 50 ml of serous yellowish liquid. The heart measures were 13 x 10 x 8 cm. The myocardium was brown with a few small whitish lesions up to 0.1 cm. Right ventricular free wall thickness was 0.6 cm and left ventricular free wall was 1.6, accordingly. There was a solid whitish irregularly shaped lesion placed intramurally up to 0.6 cm in diameter (Figure 1B). Heart valves were not changed. The intima of coronary vessels was yellowish and the patency of them was preserved. The parietal thrombi and partly liquid and coagulated blood were determined in heart chambers. Bronchial wall thickening was not observed. The mucous membranes of the trachea and main bronchi were edematous covered by semi-liquid bloody mucus. During the section it was found the upper lobes and middle lobe of both lungs were variegated; lower lobes had large areas of reddish consolidation with a few pinkish zones on the front surface of lungs. The moderate amount of foamy bloody fluid was seen in the section of lungs. A solid whitish lesion up to 1.1 cm in diameter was found in the middle third of left kidney (Figure 1C). The structure of right kidney was unchanged. There were no visible tumor, infarction or obvious abnormalities in the liver, esophagus, stomach, pancreas, biliary tract, small and large intestine, thyroid, adrenal glands, spleen. The polymerase-chain reaction for acute severe respiratory syndrome coronavirus 2 of postmortem biomaterial of trachea, bronchi, and lungs was negative as well as antigen rapid test performed in the emergency department.

Histologic features. During the microscopic examination of lung tissues alveolar edema with focal inflammatory infiltration, formation of microvascular thrombosis was revealed. The lesion of visceral pleura tissue is presented by epithelioid mesothelioma with combination of tubules, papillae, solid and adenomatoid components (Figure 2A). Small fibrotic foci in the myocardium, moderate thickening and sclerosis of blood vessels walls with perivascular fibrosis were seen in paraffin-embedded myocardial tissue. Some sections from the heart and left kidney were with tumor cells presence (Figure 2B and 2C). Histopathological studies of right kidney, liver, pancreas, spleen, and stomach were unremarkable.

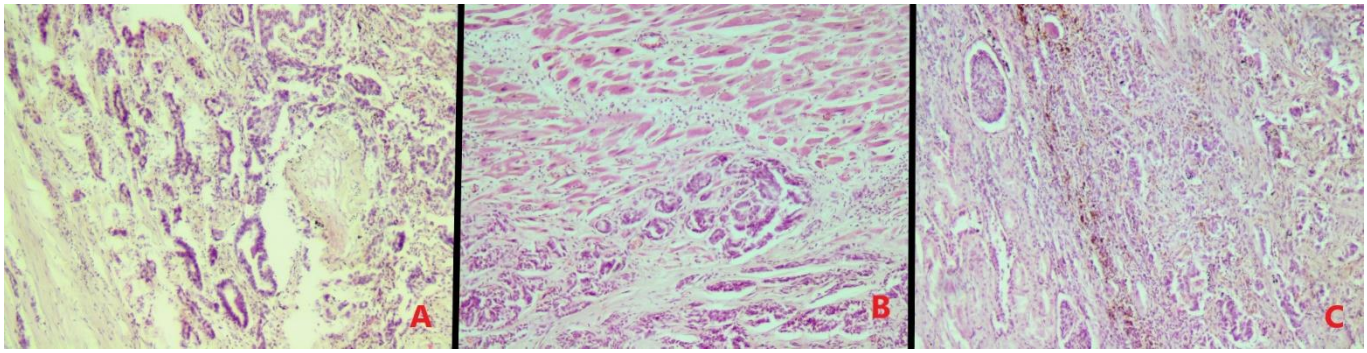

Figure 2. Histologic findings (hematoxylin and eosin-stained section; original magnification x 20 A. Epithelioid malignant mesothelioma: prominent tubular and papillar architecture, solid areas and adenomatoid structures are visualised. B. Myocardial tissue with invasion of malignant mesothelioma's metastatic lesion. C. Left kidney cortex with metastatic lesion of malignant mesothelioma.

Case Discussion.

In the present case we report about postmortem metastatic findings of the lifetime confirmed MPM. Since the antemortem diagnostics was performed in full and the determination of survival, treatment sensitivity and prognosis were definitely not our task, the routine staining methods were used. Also, electron microscopy is used occasionally in equivocal cases and not recommended for daily practice because of time- and resource-consuming and is no more useful with immunohistochemistry [9,10]. Autopsy is the gold standard for retrospective analysis of lifetime video-assisted thoracoscopic surgery and allows to find metastases not visualized antemortem [11, 12]. The difficulty in lifetime identifying MPM metastases, especially distant ones, is a major cornerstone in the search of improvement and development of new radiological protocols and has long-term significance. Since there still remains a paucity of documentation of the radiology patterns of MPM metastatic spread, just autopsy case reports and their analysis is main source of metastatic spread pathway especially in unusual, rare locations [13]. In series of S. Wadler et al., of 19 autopsies, invasion to the heart was determined in 14 (74%), with more than half to the pericardium and more than one quarter to the myocardium layer [14].

In fact, secondary cardiac tumors are 30 times as frequent as the primary ones [15]. The overall prevalence of cardiac metastasis ranges between 2.3% to 18.3% considering the theory of possibility of any malignancy to metastasize into the heart [16]. Cardiac metastases thereby are often not detected until necropsy. Most of them are clinically silent and can be suspected just during life-threating conditions like fatal cardiac tamponade or pericardial constriction. Since MPM is one of the most aggressive type of cancer the direct invasion of tumor cells into pericardial sac is possible pathway. Lymphatic spread is typical for pericardial metastases as well. Hematogenous pathway prevails for myocardial metastases placement. A case series and cohort study of cardiac metastases spreading into cardiac cavity demonstrate the pathways including invasion of lung parenchyma and permeating the vessels following by tumor embolus into left atrium via pulmonary vein. For the right-sided cardiac metastases appearance the superior vena cava should be involved and used as a pathway for tumor spreading into right atrium [17, 18]. The incidence of renal metastases detected in autopsy series is estimated between 2.36-12.6% and has a much higher prevalence than clinically antemortem ones found [19]. The exact mechanism of tumor spread to the kidneys is not sufficiently known. First pathway is hematogenous when cancer cells detached from primary location can go to the

arterial circulation following by directly to the kidney. Other mechanism is well-known as "metastasis from metastasis" and includes multiple steps: primary tumor spreads cells to one organ, then some metastatic cells are detached from there and disseminate kidneys. Also, there is pathway when some cancer cells skip some organ on the way and go specifically to another one [20]. All abovementioned different mechanisms of cancer spreading explains current unusual case with absence involving of lungs, but present cardiac and renal secondary lesions. An available literature analysis of reported cases is presented in Table I. As can be seen in previous 9 reports the median age was 68 years old with significant male predominance over female with a ratio 6:3, respectively. 8 cases were an autopsy analysis, and 1 case was the result of biopsy. 7 case reports of metastatic spreading to the heart and 2 cases of kidney secondary lesions were revealed with different histologic types of MPM.

Table I. Case reports of malignant pleural mesothelioma metastases.

№	Reference	Sex	Age (years)	Asbestos exposure	Histologic type of MPM	Cardiac metastases	Renal metastases	Location of metastases according to autopsy / biopsy
1	Olds J et al (1974) [21]	F*	63	NM*	NM	+*	-*	Left ventricle with obstruction of mitral valve
2	Walters L, Taxy J (1983) [22]	M*	70	NM	Biphasic	+	-	Right atrium with occlusion of the tricuspid orifice
3	Grellner W, Staak M (1995) [23]	M	54	+	Biphasic	+	-	Pericardium, heart.
4	Ishiyama Yet al (1998) [24]	F	78	-	NM	+	-	Tumor embolus in the left atrium
5	Sencottaiyan N et al (2006) [25]	M	71	+	Sarcomatoid	+	-	Left ventricular endocardium
6	Ushio R et al (2015) [26]	M	73	+	Epithelioid with deciduoid features	+	+	Left kidney
7	Zardawi S et al (2015) [27]	M	67	+	Biphasic	-	+	Left kidney cortex
8	Kabbash M et al (2020) [28]	M	71	NM	Epithelioid	+	-	Cardiac interventricular septum with the involvement of the endocardium
9	Fukui T et al (2021) [29]	F	62	-	Biphasic	+	-	Heart
10	Present case	M	80	-	Epithelioid	+	+	Myocardium of left ventricular wall. Left kidney cortex

*"+" present. "-" absent. M – male. F – female. NM – not mentioned.

Conclusions.

A case report of unusual metastatic lesion is presented to enrich an already existing literature database. Attention should be paid to the antemortem searching of clinically asymptomatic metastases.

References.

[1] Bibby AC, Tsim S, Kanellakis N, [et al.]. Malignant pleural mesothelioma: an update on investigation, diagnosis and treatment. Eur Respir Rev 2016; 25: 472-486.

[2] Schumann SO, Kocher G, Minervini F. Epidemiology, diagnosis and treatment of the malignant pleural mesothelioma, a narrative review of literature. J Thorac Dis 2021; 13(4): 2510-2523.

[3] Tertemiz KC, Alpaydin AO, Gurel D, [et al.]. Multiple distant metastases in a case of malignant pleural mesothelioma. Respir Med Case Rep 2014; 13: 16-18.

[4] Nadal E, Bosch-Barrera J, Cedrés S, [et al.]. SEOM clinical guidelines for the treatment of malignant pleural mesothelioma. Clin Transl Oncol 2021; 23: 980–987.

[5] Thomas A, Karakattu S, Cagle J, [et al.]. Malignant pleural mesothelioma epidemiology in the United States from 2000 to 2016. Cureus 2021; 13(4): e14605.

[6] Moser S, Beer M, Damerau G, [et al.]. A case report of metastasis of malignant mesothelioma to the oral gingiva. Head Neck Oncol 2011; 3: 21.

[7] Hamaoka M, Nakagawa M, Nakahara H, [et al.]. Intussusception caused by small intestine metastasis of malignant pleural mesothelioma: a case report. J Surg Case Rep 2021; 2: rjab003.

[8] Mitsimponas N, Petounis A. Pancreatic metastasis from malignant pleural mesothelioma. An extremely rare site of metastasis in a patient with a very prolonged survival of seven years. Curr Probl Cancer Case Rep 2021; 4: 100077.
[9] Scherpereel A, Opitz I, Berghmans T, [et al.]. ERS/ESTS/EACTS/ESTRO guidelines for the management of malignant pleural mesothelioma. Eur Respir J 2020; 58(1): 1-31.
[10] Husain A, Colby T, Ordonez N, [et al.]. Guidelines for Pathologic Diagnosis of Malignant Mesothelioma 2017 Update of the Consensus Statement from the International Mesothelioma Interest Group. Arch Pathol Lab Med 2018; 142: 89–108.
[11] Barbieri P, Consonni D, Schneider M. Accuracy of pleural biopsy for the diagnosis of histologic subtype of malignant pleural mesothelioma: Necropsy-based study of 134 cases. Tumori 2021.
[12] Finn M, Brims F, Gandhi A, [et al.]. Postmortem findings of malignant pleural mesothelioma: A two-center study of 318 patients. Chest 2012; 142(5): 1267-1273.
[13] Collins D, Sundar R, Constantinidou A, [et al.]. Radiological evaluation of malignant pleural mesothelioma – defining distant metastatic disease. BMC Cancer 2020; 20: 1210.
[14] Wadler S, Chahinian P, Slater W, [et al.]. Cardiac abnormalities in patients with diffuse malignant pleural mesothelioma. Cancer 1986; 58(12): 2744-2750.
[15] Jafri S, Ali N, Farhat S, [et al.]. The tell-tale heart: A case of recurrent vulvar carcinoma with cardiac metastasis and review of literature. Gynecol Oncol Rep 2017; 21: 20-23.
[16] Bussani R, De-Giorgio F, Abbate A, [et al.]. Cardiac metastases. J Clin Pathol 2007; 60(1): 27-34.
[17] Goldberg A, Blankstein R, Padera R. Tumors metastatic to the heart. Circulation 2013; 128: 1790-1794.
[18] Reynen K, Kockeritz U, Strasser R. Metastases to the heart. Ann Oncol 2004; 15(3): 375-381.
[19] Zhou C, Urbauer D, Fellman B, [et al.]. Metastases to the kidney: a comprehensive analysis of 151 patients from a tertiary referral centre. BJU Int 2016; 117(5): 775-782.
[20] Cazacu S, Sandulescu L, Mitroi G, [et al.]. Metastases to the kidney: a case report and review of literature. Curr Health Sci J 2020; 46 (1): 80-89.
[21] Olds J, Langley J, [et al.]. Mitral Valve Obstruction and Pulmonary Congestion Due to Malignant Mesothelioma. *Arch Intern Med* 1974;134(1):142–144.
[22] Walters L, Taxy J. Malignant mesothelioma of the pleura with extensive cardiac invasion and tricuspid orifice occlusion. Cancer 1983; 52(9): 1736-1738.
[23] Grellner W, Staak M. Multiple skeletal muscle metastases from malignant pleural mesothelioma. Pathol Res Pract 1995; 191(5): 456-460.
[24] Ishiyama Y, Hisanaga S, Asada Y, [et al.]. Malignant mesothelioma of the pleura with a large tumor embolus in the left atrium: an autopsy case. Intern Med 1998; 37(7): 614-617.
[25] Senkottaiyan N, Seacord L, Fulling K, [et al.]. Sarcomatous pleural mesothelioma metastatic to left ventricular endocardium. Angiology 2006; 57(4): 517-521.
[26] Ushio R, Yamamoto M, Shibata Y, [et al.]. An autopsy case report of malignant pleural mesothelioma with deciduoid features. Intern Med 2015; 54(22): 2915-2917.
[27] Zardawi S, Li B, Zauderer M, [et al.]. Localized malignant pleural mesothelioma with renal metastasis. Oxf Med Case Reports 2015; 1: 170-172.
[28] Kabbash M, Edmund J, [et al.]. Intracardiac involvement by primary malignant mesothelioma: a report of two cases. J Thorac Oncol 2020; 15(2): 25-27.
[29] Fukui T, Okubo T, Tanimoto N, [et al.]. Malignant pleural mesothelioma in a patient with pneumothorax: a cumbersome subtype both clinically and pathologically. Thorac Cancer 2021; 12(6): 974-977.

WORLD JOURNAL OF MEDICAL INNOVATIONS

Superior mesenteric artery aneurysm due to fibromuscular dysplasia: diagnosis and surgical treatment

Kobza Ihor[1], Kobza Taras[2], Mota Yuliya[1], Zborivskiy Yaroslav[2], Vovk Volodymyr[3]

[1]*Department of Surgery №2, Danylo Halytsky Lviv National Medical University, Lviv, Ukraine.*
[2]*Communal Noncomercial Enterprise of Lviv Regional Council Lviv Regional Clinical Hospital, Lviv, Ukraine.*
[3]*Department of Pathological Anatomy and Forensic Medicine, Danylo Halytsky Lviv National Medical University, Lviv, Ukraine.*

Article info

SURGERY

Case report

Article history:
Accepted August 17, 2021

Published online
December 11, 2021

Keywords:
superior mesenteric artery, aneurysm, fibromuscular dysplasia, diagnosis, surgical treatment

Abstract

Objectives. Improvement of diagnosis and surgical treatment of superior mesenteric artery aneurysms. Material and methods. The peculiarities of the clinical course, diagnosis and surgical treatment of superior mesenteric artery aneurysm were analyzed in 64-year-old patient. Results. In our observation, in a 64-year-old patient, by clinical examination, laboratory and diagnostic imaging the diagnosis of superior mesenteric artery branch aneurysm was confirmed, that has become a direct indication for surgical intervention - resection of aneurysm. Pathomorphologically fibromuscular dysplasia was detected. Follow-up: 3, 6 months after surgical treatment the patient has no complaints, at the control ultrasound examination magistral blood flow through superior mesenteric artery is detected, aneurysmatic expansions are not visualized. Due to the rarity of pathology, the results of surgical treatment of superior mesenteric artery aneurysms in literature are limited to a small number of observations. Most of them indicate on an infectious etiology of the disease – mycotic aneurysms. According to the U.S. registry for fibromuscular dysplasia, celiac and mesenteric arteries were involved in 37.5% of all cases, in the form of stenosis, dissection or visceral artery aneurysm. When the diagnosis of superior mesenteric artery aneurysm is confirmed there is no alternative to timely surgical treatment. Open surgical intervention traditionally remains a «gold» standard for superior mesenteric artery aneurysm repair and includes a resection of aneurysm or resection in combination with revascularization. Conclusions. Superior mesenteric artery aneurysm is a rare clinical condition that may be complicated by rupture with fatal bleeding and mesenteric ischaemia. This clinical case demonstrates that timely diagnosis and adequate surgical treatment of superior mesenteric artery aneurysm allow to prevent the occurrence of life-threatening complications and achieve complete recovery of the patient.

Corresponding author. Yuliya Mota, Department of Surgery №2, Danylo Halytsky Lviv National Medical University, Lviv, 79000, +38(096)8379925, yuliamota@gmail.com

Introduction.

Superior mesenteric artery aneurysm (SMAA) is a rare clinical pathology, with a 5,5% rate due to visceral artery aneurysms [1]. SMAAs are divided into: true aneurysms (saccular or fusiform), pseudoaneurysms, dissecting aneurysms. Unlike other visceral aneurysms, the most common etiology of SMAAs is the infection, associated with bacterial endocarditis. Other causes of SMAAs include: atherosclerosis, fibromuscular dysplasia, hypertension, cystic medianecrosis, collagenosis, posttraumatic etiology et al [1-3]. Clinical course of the disease is often asymptomatic, manifesting rupture or mesenteric ischemia [1,4]. With active introduction of diagnostic imaging – computed tomography angiography (CTA) / magnetic resonanse imaging (MRI), when the diagnosis of SMAA is confirmed, there is no alternative to timely surgical treatment [5].

Objectives.

Improvement of diagnosis and surgical treatment of SMAAs.

Material and methods (Case presentation).

We consider expedient to share the following clinical case-report because of the rarity of this pathology, peculiarities of the clinical course, diagnosis, and surgical treatment. The 64-year-old woman 01.02.2021 was admitted to the Vascular surgery department of Lviv Regional Clinical Hospital presenting of SMAA, periodic increase of blood pressure up to 150/90 mm Hg. From anamnesis: the disease is diagnosed incidentally when ultrasound examination of the abdominal cavity was performed. Objectively: the patient's status is good. Vital signs are stable and within normal limits. The pulsation of the main arteries is determined. The ultrasound examination of abdominal aorta and visceral vessels: superior mesenteric artery (SMA) – 7,5 mm in diameter, magistral blood flow through SMA is determined, peak systolic velocity – 80 cm/s. Above SMA by 3,0 cm distal from its origin – saccular aneurysmatic expansion is visualised, within 16,0 mm in diameter, without thrombotic masses inside (probably branch of SMA). US-signs of SMA branch aneurysm (Figure 1).

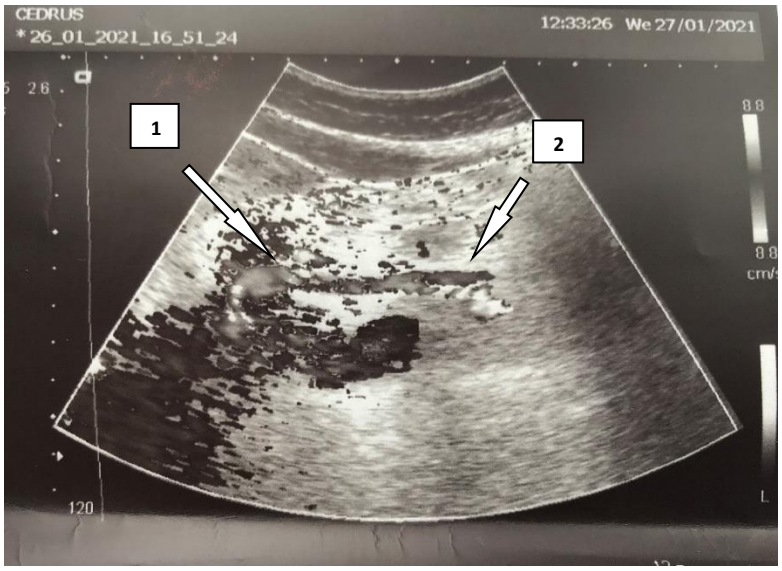

Figure 1. Ultrasonography of visceral arteries: 1 – Superior mesenteric artery aneurysm; 2 – Superior mesenteric artery.

The abdominal CTA revealed: at the distance of 68,0 mm from SMA origin – aneurysmal expansion on a thin stalk 9.0 mm in length, 18,0x12,0 mm in diameter (Figure 2). Transthoracic echocardiography didn't reveale any valvular lesions or vegetations.

So, the diagnosis of SMA branch aneurysm, 18,0x12,0 mm in diameter, has become a direct indication for surgical intervention – resection of aneurysm. 02.02.2021p. 11^{00} – 14^{10} Surgical operation - under general anesthesia the resection of SMA branch aneurysm was performed.

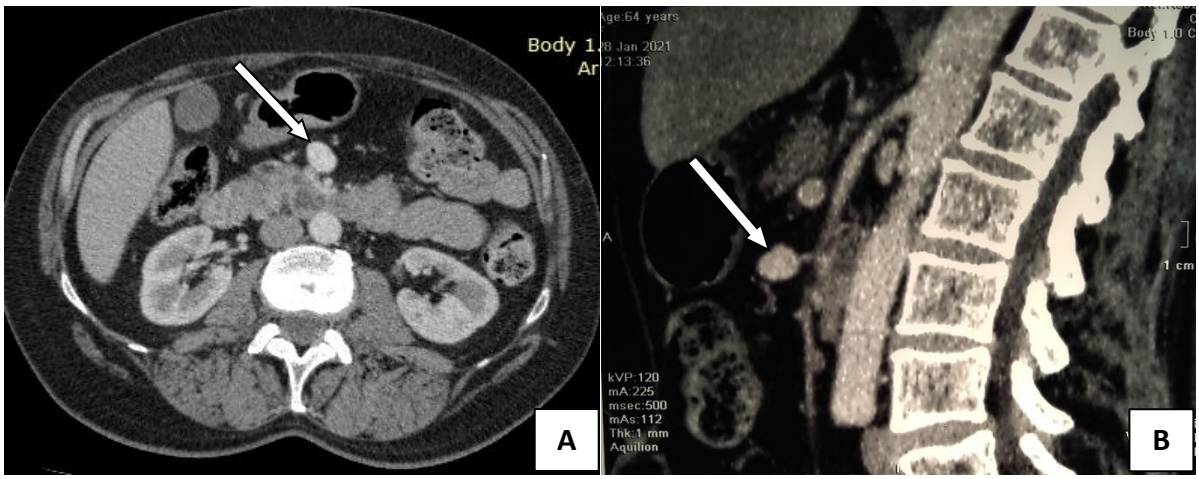

Figure 2. Computed tomography angiography of the abdomen: A, B –branch aneurysm of the superior mesenteric artery.

«Mercedes» laparotomy. T-shaped incision of the posterior leaf of the peritoneum. Novocaine blockade of the mesentery root. At the root of the mesentery, the SMA is mobilized on 3,0 cm distal from it's origin of the aorta, within 7,0 cm in length. A pulsating aneurysm of the SMA branch, 20,0x15,0 mm in diameter, was detected. Systemic heparinization. By the lateral clamping of the SMA the aneurysm was mobilized from inflammatory surrounding tissues. The aneurysm was resected and sent for pathomorphological examination. The blood flow through SMA is restored. Intestines – without visual signs of ischemia, with active peristalsis. Hemostasis. Suturing of laparotomy wound. Aseptic bandage. (Figure 3). Pathomorphological results: fibromuscular dysplasia (FMD) (Figure 4).

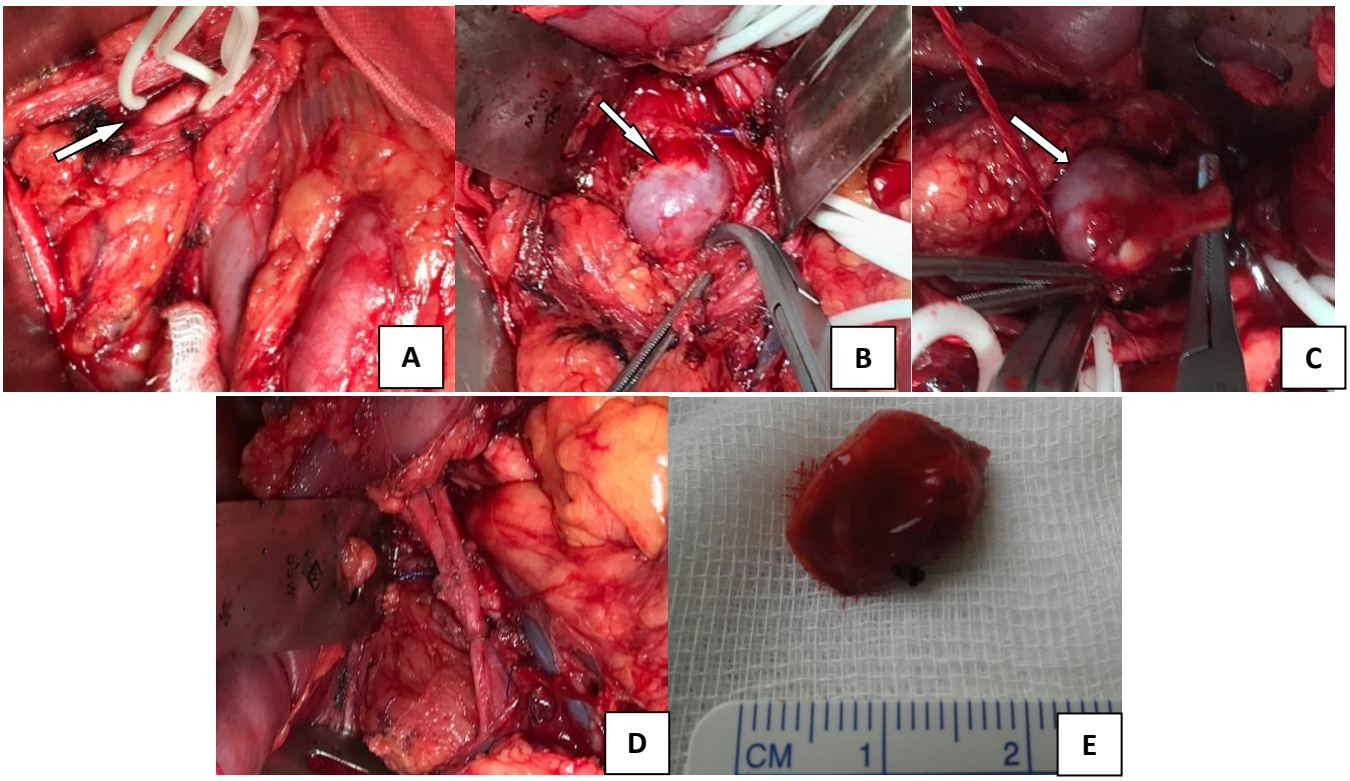

Figure 3. Intraoperative photos: A – mobilized superior mesenteric artery; B,C – branch aneurysm of the superior mesenteric artery; D – the blood flow through superior mesenteric artery is restored; E – resected aneurysm.

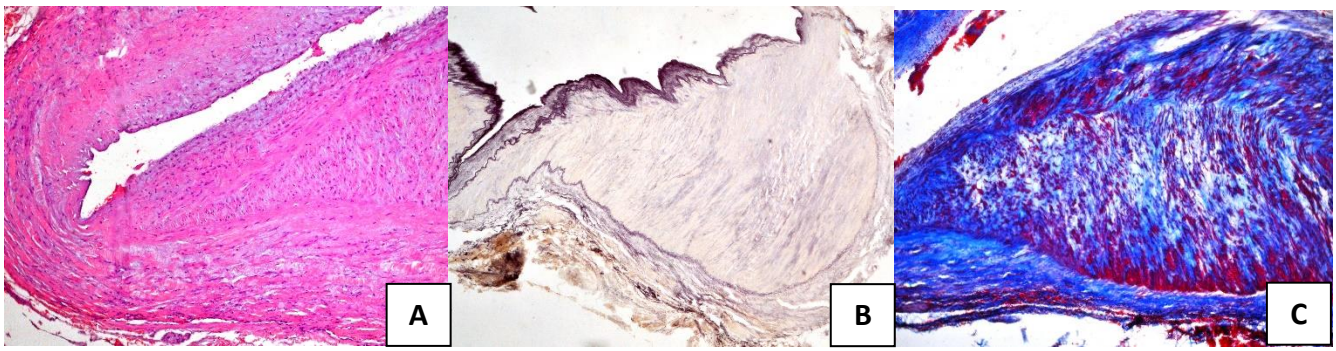

Figure 4. Histologic sections – FMD of SMA: A – the wall of the artery is thickened with the formation of fibro-muscular plaque. H&E stain, x100; B – expressed subintimal hyperplasia of arterial wall. Hart's stain for elastic fibers, x100; C – expressed hyperplasia of smooth muscle cells and connecting tissue cells of the arterial wall. Masson's trichrome stain, x100.

In the postoperative period signs of ileus, edematous pancreatitis were observed. The patient was consulted by a general surgeon with relevant recommendations, received adequate infusion-transfusion corrective therapy, anticoagulants, antibiotic therapy, prokinetics. Against the background of the conservative therapy, the patient's status – with positive dynamics. Postoperative wound healed by primary tension. Patient was discharged 18.02.2021 in a good status with recommendations of a general surgeon observation. Follow-up: 3, 6 months after surgical treatment the patient has no complaints, at the control ultrasound examination magistral blood flow through SMA is detected, aneurysmatic expansions are not visualized.

Results and case discussion.

In our observation, in a 64-year-old patient, by clinical examination, laboratory and diagnostic imaging the diagnosis of SMA branch aneurysm was confirmed, that has become a direct indication for surgical intervention – resection of aneurysm. Pathomorphologically FMD was detected. Due to the rarity of this pathology, the results of surgical treatment of SMAAs in the literature are limited to a small number of observations. Most of them indicate on an infectious etiology of the disease – mycotic aneurysms, that account for 60% of all SMAAs [1,6,7]. Predisposing factor in the formation of SMAAs also is FMD – nonatherosclerotic, non-inflammatory disease, unknown etiology, in which microscopically segmental development of fibrosis and hyperplasia of the media cells were observed [8-10]. According to the U.S. registry for FMD, celiac and mesenteric arteries were involved in 37.5% of all cases, in the form of stenosis, dissection, or visceral artery aneurysm [8]. Furthermore, SMAAs, also found predominantly in women, but less frequently associated with other dysplasias and were generally sacciform [11]. Abdominal ultrasound, CT, MRI-angiography are all feasible methods for the diagnosis of SMAAs, but CTA is the «gold» standard and provide the best diagnostic information as regards location, evidence of rupture, presence of collateral flow, that are important for choice of surgical treatment [1,5]. In this clinical case the disease is diagnosed incidentally during ultrasonography of abdominal cavity. Further before surgery the CTA was performed to determine the accurate diagnostic information regards relationship between the aneurysm and related blood vessels. Manifestations of SMAAs differ, often with asymptomatic course. Abdominal pain is the most common symptom of SMAAs that may indicate on increase in the size and risk of rupture of the aneurysm [1,4,6]. Therefore the Society for Vascular surgery clinical practice guidelines on the management of visceral aneurysms recommends repair of all true SMAAs and pseudoaneurysms as soon as the diagnosis is made regardless of size [5]. Open surgical intervention traditionally remains a «gold» standard for SMAAs repair and includes a resection of aneurysm or resection in combination with revascularization. Direct revascularization of the SMA is recommended at aneurysm of the SMA trunk or its bifurcation and involves performing primary anastomosis, saphenous vein interposition or aortomesenteric bypass grafting [1,6,7,12,13]. With the active development of endovascular treatment, successful cases of SMAAs stenting and embolization have been reported in the literature [1, 2, 4, 6]. However, according to some authors, endovascular surgery has certain disadvantages due to the complex anatomy of SMAAs, including technical difficulties of catheterization of the aneurysmal «neck», intraoperative migration of stents, stratification or rupture of aneurysms, embolization [1, 6]. Moreover, a recent meta-analysis discovered that the endovascular approach was associated with shorter hospital

days and lower rates of cardiovascular complications, but higher rates of reintervention for visceral artery aneurysm were also reported [14].

Thus, the performed surgical treatment – SMA branch aneurysm resection saved the patient's life and prevented the development of fatal complications.

Conclusions.

Superior mesenteric artery aneurysm is a rare clinical condition that may be complicated by rupture with fatal bleeding and mesenteric ischaemia. This clinical case demonstrates that timely diagnosis and adequate surgical treatment of superior mesenteric artery aneurysm allow to prevent the occurrence of life-threatening complications and achieve complete recovery of the patient.

References.

[1] Wang L, Shu C, Li Q, [et al.]. Experience of managing superior mesenteric artery aneurysm and its midterm follow-up results with 18 cases. Vascular 2021; Aug; 29 (4): 516-526.

[2] Zilun L, Henghui Y, Yang Z, [et al]. The management of superior mesenteric artery aneurysm: experience with 16 cases in a single center. Ann Vasc Surg 2017; Jul; 42: 120-127.

[3] Pasha SF, Gloviczki P, Stanson AW, [et al]. Splanchnic artery aneurysms. Mayo Clin Proc 2007; 82: 472-479.

[4] Stone WM, Abbas M, Cherry KJ, [et al.]. Superior mesenteric artery aneurysms: is presence an indication for intervention? J Vasc Surg 2002; Aug; 36 (2): 234-7.

[5] Chaer RA, Abularrage CJ, Coleman DM, [et al.]. The Society for Vascular Surgery clinical practice guidelines on the management of visceral aneurysms. J Vasc Surg 2020 Jul; 72 (1S): 3S-39S.

[6] de Troia A, Mottini F, Biasi L, [et al.]. Superior mesenteric artery aneurysm caused by aortic valve endocarditis: the case report and review of the literature. Vasc Endovascular Surg 2016; Feb; 50 (2): 88-93.

[7] Jacobs CR, Fatima J, Scali ST, [et al]. Surgical treatment of true superior mesenteric artery aneurysms. Ann Vasc Surg 2021; Feb; 71: 74-83.

[8] Kadian-DodovD, GornikHL,Gu X, [et al]. Dissection and aneurysm in patients with fibromuscular dysplasia: findings from the U.S. registry for FMD. J Am Coll Cardiol 2016; 68: 176e85.

[9] Ko M, Kamimura K, Sakamaki A, [et al]. Rare mesenteric arterial diseases: fibromuscular dysplasia and segmental arterial mediolysis and literature review. Intern Med 2019; Dec; 58 (23): 3393-3400.

[10] Silvestri V, Sapienza P, Ossola P, [et al]. Ruptured superior mesenteric artery aneurysm due to fibromuscular dysplasia: a rare vascular presentation in a patient with schizophrenia. Ann Vasc Surg 2019 Jul; 58: 384.

[11] Cormier F, Cormier JM. Trente-huit cas de lésions dysplasiques de l'artère mésentérique supérieure [Thirty-eight cases of dysplasia of the superior mesenteric artery]. J Mal Vasc 2005; Jul; 30 (3): 150-61.

[12] Bespaev AT, Abuov SM, Kyrgyzbaev SZh, [et al]. Surgical treatment of an aneurysm of the upper mesenteric artery. Angiol Sosud Khir 2015; 21 (3): 149-52. [Russian].

[13] Hogendoorn W, Schlösser FJ, Sumpio BE. A giant superior mesenteric artery aneurysm mimicking an abdominal aortic aneurysm. Aorta (Stamford) 2013; Jun; 1 (1): 52-6.

[14] Barrionuevo P, Malas MB, Nejim B, [et al]. A systematic review and meta-analysis of the management of visceral artery aneurysms. J Vasc Surg 2019; 70: 1694–1699.

WORLD JOURNAL OF MEDICAL INNOVATIONS

The mineral waters of Skhidnytsia spa town and their therapeutic benefits in patients after renal surgical procedures for renal cell cancer

Pasichnyk Serhiy [1], Mytsyk Yulian[1], Hozhenko Anatoly [2], Myrka Oleg [3]

[1]*Department of Urology, Danylo Halytsky Lviv National Medical University, Lviv, Ukraine.*
[2]*Ukrainian Research Institute of Transport Medicine of the MoH of Ukraine, Odessa, Ukraine.*
[3]*Communal Institution of Lviv Regional Council "Lviv Regional Rehabilitation Hospital" Skhidnytsia, Ukraine.*

Article info

UROLOGY

Original paper

Article history:
Accepted August 17, 2021

Published online
December 22, 2021

Keywords:
the mineral waters of Skhidnytsia,
renal cell cancer,
rehabilitation,
nephrectomy,
chronic kidney disease

Abstract

Objectives. To evaluate the effect of medicinal water of the Skhidnytsia region on rehabilitation of patients after nephrectomy for renal cell carcinoma of the kidney complicated by chronic kidney disease. Materials and methods. The study was conducted from 2007 to 2014. The investigators have reviewed medical records of 116 patients with renal cell cancer and concomitant chronic kidney disease. All patients have had radical nephrectomy with a therapeutic intent. All patients were randomized into two treatment groups. The first group enrolled 67 patients (31 males and 36 females); this patient subpopulation was dominated by patients diagnosed with urinary syndrome, which lasted over 3 months. Only 12 patients had glomerular filtration rate < 90 ml/sec. The patients in the first group did not have any spa resort treatment in the postoperative period. The second group enrolled 49 patients (21 males and 28 females). As in the case with patients of the first group, most patients in the second group have had urinary syndrome for more than three months. Glomerular filtration rate < 90 ml/sec was observed only in 13 patients of the second group. All patients of the second group have had spa resort treatment in the setting of the spa town of Skhidnytsia. Results. The duration of follow-up was 2 years. The patients returned to the spa town every six months, for a total of 4 spa resort treatment courses. The mean duration of each course was 17.9±1.3 days. Changes in creatinine level and glomerular filtration rate with time were assessed once every 6 months in both groups, for a total of 4 follow-up visits.

Corresponding author. Serhiy Pasichnyk, Department of Urology, Danylo Halytsky Lviv National Medical University, Lviv, 79010, Ukraine. +38(067)718519, pasichnykdoctua@gmail.com

Introduction.

Kidney cancer (KC) is the third by prevalence (after prostate cancer and urinary bladder cancer) among all urological cancers and the 10th among all malignancies [1, 2, 3]. KC includes many pathomorphologically diverse variants of malignant neoplastic transformation of renal tissue. Chronic kidney disease (CKD) results from kidney damage. The most frequent causes of CKD include increased blood pressure, diabetes, infectious and inflammatory kidney disease, impaired urine outflow and renal masses. One of the early signs of emerging CKD is the so-called urinary syndrome [4].

In a broad sense, urinary syndrome (UrS) includes all qualitative and quantitative changes in urine, and in a more specific sense, it includes changes in urinary sediment, such as proteinuria, hematuria and leukocyturia. As already mentioned, urinary syndrome is regarded as one of the most important signs of urinary system disorders, stemming from laboratory-proven (statistically significant) and obvious deviation of urinary composition from normal [5, 6]. Isolated renal syndrome may develop in primary or secondary glomerulonephritis, as well as in other kidney diseases [4, 7]. However, preventing and slowing down the progression of existing CKD increases the need for adequate rehabilitation therapy in the postoperative period [8, 9, 10, 11]. Thus, as already mentioned above, the effect of mineral waters of the Skhidnytsia region in metaphylaxis of development and progression of CKD in patients with kidney cancer who have had radical nephrectomy is currently an open question, which is not fully understood [11, 12, 13, 14, 15].

Objectives.

To evaluate the effect of medicinal water of the Skhidnytsia region on rehabilitation of patients after nephrectomy for renal cell carcinoma of the kidney complicated by CKD.

Material and methods.

The study was conducted from 2007 to 2014. The investigators have reviewed medical records of 116 patients with renal cell cancer and concomitant CKD. All patients have had radical nephrectomy with a therapeutic intent. All patients were randomized into two treatment groups (Table1). The first group enrolled 67 patients (31 males and 36 females); this patient subpopulation was dominated by patients diagnosed with urinary syndrome, which lasted over* 3 months. Only 12 patients had glomerular filtration rate (GFR) < 90 ml/sec. The patients in the first group did not have any spa resort treatment in the postoperative period. The second group enrolled 49 patients (21 males and 28 females). As in the case with patients of the first group, most patients in the second group have had urinary syndrome for more than three months. GFR < 90 ml/sec was observed only in 13 patients of the second group. All patients of the second group have had spa resort treatment (SRT) in the setting of the spa town of Skhidnytsia. In addition to a comprehensive program of physical therapy, exercise therapy and therapeutic diet, all SRT patients were taking “Naftusia” medicinal water. A comprehensive study of waters from Source No. 25 and Source No. 26 conducted by Ukrainian Research Institute for Medical Rehabilitation and Spa Medicine in 1995 has informed the development of recommendations and regimens for use of the above waters in chronic pyelonephritis, cystitis and in patients after renal surgery. It was according to the aforementioned regimen that patients in this study were receiving mineral waters as part of their rehabilitation program. Thus, patients were referred to SRT already on Day 7 to Day 10 after minimally invasive surgical interventions, and on Day 12 – Day 15 after open surgery. Based on the research, the authors have developed a technique, where recommended use of mineral water was 10 to 15 milliliters per kilogram of body weight. It is recommended to take the water (either cold or warmed to 18–20 ℃) an hour before a meal, 5 times a day.

Table 1. Patient distribution across the groups.

Group 1 (n = 67)	M (n = 31)	UrS* > 3 mos.	(n = 7)
		GFR**< 90 ml/sec	(n = 24)
	F (n = 36)	UrS > 3 mos.	(n = 5)
		GFR < 90 ml/sec	(n = 31)
Group 2 (n = 49)	M (n = 21)	UrS > 3 mos.	(n = 4)
		GFR < 90 ml/sec	(n = 17)
	F (n = 28)	UrS > 3 mos.	(n = 9)
		GFR < 90 ml/sec	(n = 19)

* Urinary syndrome for more than 3 months; ** Glomerular filtration rate; M – male; F – female

The duration of follow-up was 2 years. The patients returned to the spa town every six months, for a total of 4 SRT courses. The mean duration of each course was 17.9±1.3 days. Changes in creatinine level and GFR with time were assessed once every 6 months in both groups, for a total of 4 follow-up visits. We calculated glomerular filtration rate from the Cockcroft-Gault formula, measured in milliliters per minute per 1.73 m^2 of area (ml/min/1.73 m^2.

Results and discussion.

At the onset of study participation, i.e. shortly after surgical treatment, there were no statistically significant intergroup differences in terms of the above assessment criteria. Median serum creatinine levels in Group 1 and Group 2 were 92.6±1.7 mmol/l and 90.3±2.1 mmol/l, (p> 0.05). Mean glomerular filtration rates in Group 1 and Group 2 were 72.3±5.8 ml/min/1.73 m^2 and 74.5±4.7 ml/min/1.73 m^2, respectively (p> 0.05). Changes in investigational parameters with time in both patient groups once every 6 months of follow-up are reflected in Tables 2 and 3.

Table 2. Changes in serum creatinine levels with time.

Months	Creatinine level, mmol/l		p
	Group 1	Group 2 (SRT)	
0	92.6±1.7	90.3±2.1	>0.05
6	118.3±2.3	96.2±0.9	<0.05
12	125.6±2.9	102.8±1.6	<0.05
18	129.8±3.2	98.6±2.3	<0.05
24	132.4±3.8	105.4±3.1	<0.05

As seen from Table 2, the use of medicinal mineral waters as part of rehabilitation program in KC patients slows down their increase in creatinine levels. During the 24-month follow-up, the overall increase in creatinine level was 39.8±1.9 mmol/l in the patient group with no rehabilitation SRT and 15.1±2.4 mmol/l in the group of patients who had rehabilitation SRT. Visual presentation of the results obtained is given in Fig. 1.

Figure 1. Changes in creatinine level with time

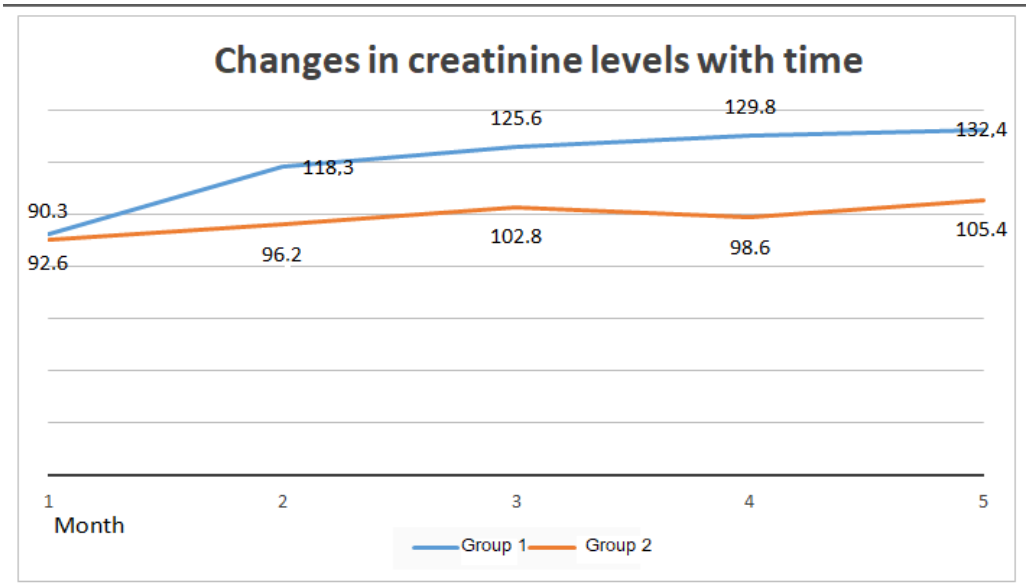

The changes in glomerular filtration rate in both patient groups are presented in Table 3. The analysis of results summarized in Table 3 shows that the use of medicinal mineral waters as part of rehabilitation program in KC patients slows down the reduction in GFR. During the 24-month follow-up, the mean reduction in GFR was 26.7± 3.4 ml/min/1.73 m^2 in the patient group with no rehabilitation SRT and 9.2±2.7 in the group of patients who had rehabilitation spa resort treatment in the postoperative period. Visual presentation of the results obtained is given in Fig. 2.

Table 3. Changes in glomerular filtration rate with time.

Months	Glomerular filtration rate, ml/min/1.73 m²		p
	Group 1	Group 2 (SRT)	
0	72.3±5.8	74.5±4.7	>0.05
6	59.8±4.6	72.6±3.1	<0.05
12	54.3±5.0	70.4±2.9	<0.05
18	49.4±3.2	68.7±3.6	<0.05
24	45.6±4.3	65.3±5.4	<0.05

Figure 2. Changes in GFR with time

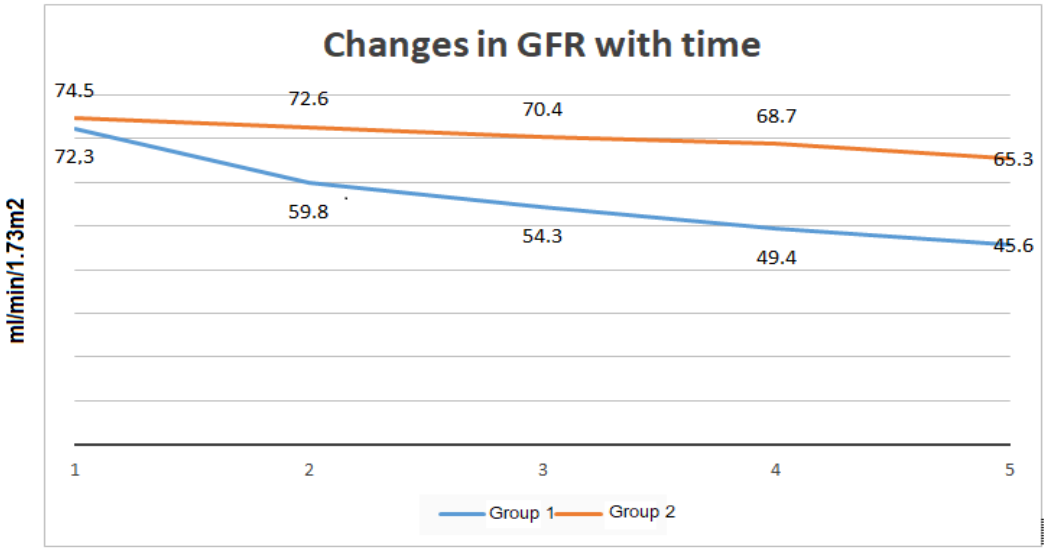

Analysis of the data presented in Table 4 suggests that radical nephrectomy leads to progression of existing urinary syndrome and reduction of GFR below 90 ml/sec already in the first 6 months after the surgical treatment. The use of rehabilitation SRT had no effect on progression of urinary syndrome.

Table 4. Progression of urinary syndrome after radical nephrectomy.

Months	Group 1 (n = 67)				Group 2 (n = 49)			
	M (n = 31)		F (n = 36)		M (n = 21)		F (n = 28)	
	UrS* > 3 mos.	GFR** < 90 ml/sec	UrS* > 3 mos.	GFR < 90 ml/sec	UrS* > 3 mos.	GFR < 90 ml/sec	UrS* > 3 mos.	GFR < 90 ml/sec
0	7	24	5	31	4	17	9	19
6	2	29	1	35	2	19	4	24
12	1	30	0	36	0	21	1	27
18	0	31	0	36	0	21	0	28
24	0	31	0	36	0	21	0	28

***** Urinary syndrome for more than 3 months; ****** Glomerular filtration rate; M – male; F – female

Conclusions.

During 24 months after surgical treatment, study patients experienced progression of creatinine levels. Creatinine level was higher by 24.7±1.2 mmol/l in the patient group after surgical treatment for KC. During the 24-month follow-up, CKD progression was more intense in the group of patients who had no rehabilitation multi-modality treatment with the use of medicinal mineral waters after their surgical treatment for KC. Radical nephrectomy leads to progression of existing urinary syndrome and reduction of GFR below 90 ml/sec already in the first 6 months after the surgical treatment. The use of rehabilitation SRT had no effect on progression of urinary syndrome.

with no rehabilitation SRT after surgical treatment for KC. Concerning CKD progression, mean GFR was lower by 17.5±2.4 ml/min/1.73 m^2 in 24 months after surgical treatment in the patient group with no rehabilitation SRT

References.

[1] Alyaev YuG, Grigoryan ZG. Bilateral asynchronous kidney cancer. Oncourology [Onkourologiya] 2010; 2: 15 [Russian].

[2] Fedorenko ZP, Hulak LO, Ryzhov AYu. The specific features of development of incidence of genitourinary cancers in Ukraine after the Chernobyl nuclear accident. Oncourology [Onkourologiya] 2013; 1 (9): 12 [Ukrainian].

[3] Fedorenko ZP, Hulak LO, Mykhailovych YuY, [et al.]. Cancer in Ukraine, 2015 – 2016. The Bulletin of the National Cancer Registry of Ukraine, 18, Kyiv, 2017 [Ukrainian].

[4] Evenski A, Ramasunder S, Fox W, [et al.]. Treatment and survival of osseous renal cell carcinoma metastases. J Surg Oncol 2012; 106: 850-855.

[5] Moskvina LV, Andreeva YuYu, Malkov PG, [et al.]. The clinically significant morphological parameters of renal cell carcinoma. Oncology [Onkologiya] 2013; 4: 34-39 [Russian].

[6] Hosokawa Yu, Tanaka N, Mibu H, [et al.]. Follow – up study of unilateral renal function after nephrectomy assessed by glomerular filtration rate per functional renal volume. World J Surg Oncol 2014; 12 (59): 4-6.

[7] Huang WC, Levey AS, Serio AM, [et al.]. Chronic kidney disease after nephrectomy in patients with renal cortical tumors: a retrospective cohort study. Lancet Oncol 2006; 7 (9): 735-740.

[8] Hamilton SKD, Stewart GD, McNeill A, [et al.]. Renal function after unilateral Nephrectomy. SUMJ 2014; 3 (2): 22 -31.

[9] Chapman D, Moore R, Klarenbach S, [et al.]. Residual renal function after partial or radical nephrectomy for renal cell carcinoma. Can Urol Assoc J 2010; 4 (5): 337-343.

[10] Ahn JS, Kim HJ, Jeon HG, [et al.]. Predictive preoperative factors for renal insufficiency in patients followed for more than 5 years after radical nephrectomy. Korean J. Urol 2013; 54: 303-310.

[11] Li L, Lau WL, Rhee CM, [et al.]. Risk of chronic kidney disease after cancer nephrectomy. Nat Rev Nephrol 2014; 10: 135-45.

[12] Muzaale AD, Mussie AB, Wang MC, [et al.]. Risk of end – stage renal disease following live kidney donation. JAMA 2014; 311: 579-586.
[13] Simmons MN, Hillyer SP, Lee BH, [et al.]. Functional recovery after partial nephrectomy: effects of volume loss and ischemic injury. J Urol 2012; 187: 1667-1673.
[14] James MT, Hemmelgarn BR, Wiebe M, [et al.]. Glomerular filtration rate, proteinuria, and the incidence and consequences of acute kidney injury: a cohort study. Lancet 2010, 376: 2096-2103.
[15] Jemal A, Tiwari RC, Murray T, [et al.]. Cancer statistics, 2004. CA Cancer J Clin 2004; 54: 8 – 29.

WORLD JOURNAL OF MEDICAL INNOVATIONS

Diagnostics of the severity of cervical intraepithelial neoplasia in women with infertility in the presence of papillomavirus infection

Kindrativ Elvira[1], Lenchuk Tetiana[2], Mytsyk Yulian[3], Matskevych Viktoriya[2], Vasylyk Volodymyr[4], Zoriana Huryk[1]

[1]*Department of Pathomorphology, Ivano-Frankivsk National Medical University, Ivano-Frankivsk, Ukraine.*
[2]*Department of Radiology and Radiation medicine, Ivano-Frankivsk National Medical University, Ivano-Frankivsk, Ukraine.*
[3]*Department of Urology, Danylo Halytsky Lviv National Medical University, Lviv, Ukraine.*
[4]*Pathology Department, Municipal Non-profit Enterprise «Regional Clinical Hospital of Ivano-Frankivsk Regional Council», Ivano-Frankivsk, Ukraine.*

Article info

PATHOLOGY

Original paper

Article history:
Accepted August 17, 2021

Published online
December 28, 2021

Keywords:
Cervical intraepithelial neoplasia,
squamous non-keratinized epithelium,
cervical infertility factors,
papillomavirus infection

Abstract

Objectives. To objectify the diagnosis of cervical intraepithelial neoplasia in the presence of papillomavirus infection in women with infertility by morphometric analysis of the cervical mucosa. Material and methods. The pieces of the cervix obtained during diagnostic biopsies of 157 infertile women with cervical intraepithelial neoplasia associated with papillomavirus infection were material for morphological examination. A specific quantitative diagnosis of real-time polymerase chain reaction with hybridization-fluorescence detection was used to identify papillomavirus infection. Immunohistochemical study was performed on paraffin sections of cervical tissue by conventional methods. Histological examination was performed on an AxioScop 40 (Zeiss) microscope. Metric parameters were calibrated on the tool for measuring "Mira". Results. Mild dysplastic ectocevix changes were generally characterized by preservation of anisomorphism and stratification of the surface and intermediate layers, focal basal cell hyperactivity with increasing nuclear-cytoplasmic ratio. The volumetric density of capillaries of a mucous membrane credibly increased in 2.8-times in moderate cervical intraepithelial neoplasia compared with the control group. The thickness of multilayered squamous non-keratinized epithelium with severe cervical intraepithelial neoplasia often did not differ from that with mild or moderate ones. Violation of histoarchitectonics due to loss of stratification and vertical anismorphism was noted in the ectocervix. There was a total basal hyperactivity, impaired maturation and differentiation of epithelial cells. Conclusions. The obtained morphometric data studies have revealed that disorders of the epithelial-stromal relationship especially in cases of severe cervical intraepithelial neoplasia may be one of the stages of carcinogenesis.

Corresponding author. Elvira Kindrativ, Department of Pathomorphology, Ivano-Frankivsk National Medical University, Halytska str., 2, Ivano-Frankivsk, 76000, +38(050)9921086, ekindrativ@ifnmu.edu.ua

Introduction.

The future of the state is determined by a set of political, economic, social factors that affect the demographic situation and health status of the population. Reproductive health is an integral part of the health of the nation as a whole and is of strategic importance for the sustainable development of society. According to the World Health Organization (WHO), reproductive health is a state of physical, mental and social well-being. Major reproductive health issues worldwide are: high maternal and infant mortality, high abortions, miscarriages, complications of pregnancy and childbirth, high prevalence of female and male infertility and sexually transmitted infections, including human immunodeficiency virus/acquired immunodeficiency syndrome, oncological morbidity of the reproductive sphere, etc [1, 2]. There is a tendency to increase the number of cases of female infertility in Ukraine. The cervical factor is among 22 causing factors of infertility, according to the WHO and occurs from 8 to 20% of infertility according to the literature [3, 4, 5, 6]. The greatest importance of cervical infertility belongs to hormonal disorders, cervicitis, cervical ectopia, polyps, cervical neoplasia and especially the consequences of aggressive treatment of cervical pathology [7, 8, 9, 10]. Cervical intraepithelial neoplasia (CIN), especially due to papillomavirus infection is considered a morphological substrate for the development of cervical cancer [11, 12, 13]. Analysis of recent studies shows the widespread use of molecular biological markers aimed at improving the diagnosis of CIN, as they can help to objectify the verification of the diagnosis [14, 15, 16, 17]. Despite the large number of studies on CIN, in particular in human papillomavirus infection (PVI), a number of issues remain under discussion, and the peculiarities of its morphology in women with infertility are absent.

Objectives.

To objectify the diagnosis of cervical intraepithelial neoplasia in the presence of papillomavirus infection in women with infertility by morphometric analysis of the cervical mucosa.

Material and methods (Case presentation).

The material for morphological examination were pieces of the cervix obtained during diagnostic biopsies of 157 women with infertility with PVI associated CIN, There were 62 patients with CIN of mild (CIN-I) severity, 53 patients with moderate CIN (CIN-II) and 42 patients with severe CIN (CIN-III) in this study. A specific quantitative diagnosis of real-time polymerase chain reaction with hybridization-fluorescence detection (Real-Nime PCR) was used to identify PVI with a set of reagents (PCR kit Russian Federation) to determine of 12 types of HPV DNA (16, 18, 31, 33, 35, 39, 45, 51, 52, 56, 58, 59) in scraping from the cervical canal, transformation zone and pathological areas of the cervix. The final result was calculated automatically in the logarithms of the viral genom equivalents (GE) normalized per 100 thousand (105) human genomes, distinguishing three types of viral load: 5 Ig GE per 105. Pieces of the cervix were fixed in 10% neutral formalin, dehydrated through a series of alcohols of growth increasing concentration poured into paraffin and prepared serial sections 5-6 µm thick, stained with hematoxylin and eosin, picrofuxin by Van Gieson for morphological examination. Immunohistochemical study was performed on paraffin sections of cervical tissue by conventional methods. Monoclonal antibodies to Ki-67 (clone MIB-1, Dako) and p63 (clone 4A4, Dako) were used. Control studies were performed for each marker to exclude false-positive or false-negative results. The proliferative activity of Ki-67 was evaluated depending on the number of cells with labeled nuclei to the total number of epithelial cells and the prevalence of cells with nuclear expression in the layers of the ectocervix. The expression level of Ki-67 was assessed by the prevalence in the epithelial layer: low - positively stained cells occupy <1/3 of the epithelial layer; medium - 1/3 - 2/3 epithelial layer and high >2/3 epithelial layer. Proliferative activity was considered high when staining more than 50% of cells, low - when staining less than 10%, the value of 10-50% was considered as an intermediate zone. Proliferation indices (PIs), p63 were calculated as the percentage of cells with a positive nuclear reaction, regardless of the intensity of staining, to the total number of cells on average according to the results of all studied areas. To assess the expression level of p63, the following range was used: low level - less than 30% of cells with a positive nuclear reaction; moderate - 30-75% of positively stained cells; high level - more than 75% of cells with positive expression.

Histological examination was performed on an AxioScop 40 (Zeiss) microscope at original magnification x 20. Metric parameters were calibrated on the tool for measuring "Mira" (test control) with image analysis based on the software UTHSC SA Image Tool for Windows. The height of the multilayered squamous non-keratinized epithelium (MSNE), the height of the basement membrane were measured, the density of the mucous membrane capillaries and the ratio of the height of the MSNE to the volumetric density of capillaries of a mucous membrane (VDCMM) were determined. The obtained results were subjected to statistical processing by methods of variance

statistics (arithmetic mean, standard error, standard deviation, confidence interval). Testing statistical hypotheses to determine the differences between nonparametric features was performed using the χ2-criterion and the z-criterion. Correlation analysis was performed based on the determination of the parametric correlation coefficient. Probability was assessed by Student's t test. Results with p <0.05 were considered statistically significant. Construction of a mathematical model, regression analysis, the values of multiple regression coefficients were determined using the program SPSS. The obtained data were processed using Microsoft Access software, Microsoft Excel 2010 (license № 01631-551-3027986-27852).

Results.

Mild CIN were generally characterized by preservation of anisomorphism and stratification of the surface and intermediate layers, focal basal cell hyperactivity with increasing nuclear-cytoplasmic ratio. The nuclei of cells of the basal and parabasal layer were with a clear chromatin structure of the nucleoli. Basal cell cytoplasm had basophilic color. There was an increase in mitotic activity in hyperplasia cells. The dominant morphological feature was an increase in the thickness of the MSNE with CIN-I. On average the thickness of MSNE increased 2.9 times compared with control samples of the cervix (p <0,05). The VDCMM increased in 2.9 times in comparison with the control group (6.93 ± 2.3 vs. 2.35 ± 0.4; p <0.05). The ratio of the thickness of the stratified squamous epithelium to the relative VDCMM increased from 94.03 ± 11.5 in the control group to 107.7 ± 14.3 (p <0.05). The thickness of MSNE with CIN-II increased in comparison with MSNE of control group and CIN-I (p <0,05). CIN-II was characterized by a violation of vertical anisomorphism and stratification of the lower layers of the stratified squamous epithelium due to basal cell hyperactivity. The basal layer was represented by 9-12 rows. Hyperplasia cells of the lower layers were oriented perpendicular to the basement membrane. The nuclei of basal cells were hyperchromic, surrounded by a narrow rim of the cytoplasm, but there were also normo- and hypochromic nuclei. A subnuclear vacuolation of the cytoplasm was observed in some cases. The number of cells with figures of mitosis increased in the direction to the basement membrane. The number of atypical mitoses increased slightly compared with CIN-I. Superficial and intermediate layers of the epithelial layer were with preserved stratification. The cells were placed horizontally in relation to the basement membrane. There were small cells with pyknotic nuclei of different shapes and sizes with intense eosinophilic cytoplasm (dyskeratocytes) in the cells of the upper and intermediate layers. Diskeratocytes were located mainly in complexes. The basement membrane was thickened in the form of a homogeneous oxyphilic layer, but it was also sharply tortuous in cases of condyloma vegetation or presence of acanthotic cords. It was represented by bundles of collagen fibers, which were sharply compacted or swollen. Collagen fibers were fibrous and fragmented in areas of edema. Sharply swollen fibroblasts with focal plasmolysis and karyolysis were found in such areas. The VDCMM credibly increased 2.8-times with moderate CIN compared with the control group (6.93 ± 2.6 vs. 2.73 ± 0.4). The ratio of the thickness of the stratified squamous epithelium to the VDCMM decreased to 83.7 ± 14.3 (p <0.05). The thickness of MSNE with severe CIN often did not differ from that with mild or moderate ones. But it was at the same level with the indicators of the control group in 35.2% of cases. Violation of histoarchitectonics due to loss of stratification and vertical anismorphism was noted in the ectocervix. There was a total basal hyperactivity, impaired maturation and differentiation of epithelial cells. Dysplastic cells occupied a larger thickness of the epithelial layer, with the exception of a few (2-3) surface layers, represented by mature cells that maintained a normal structure. The arrangement of cells was chaotic. Dysplastic cells were polymorphic and had different sizes. The majority of cells with large hyperchromic nuclei were surrounded by a narrow rim of the cytoplasm. The nuclear-cytoplasmic ratio changed in favor of the nucleus. The nuclei were deformed with multiple invaginations and protrusion of the nucleolema in some cells. Such cells were found in the upper layers of the epithelial layer. Severe CIN was characterized by an increase in the VDCMM in 4.9 times (13.63 ± 2.4 vs. 2.73 ± 0.4 in the control group). The ratio of MSNE height to VDCMM significantly decreased to 31.2 ± 13.6 (p <0.05) (Figure 1).

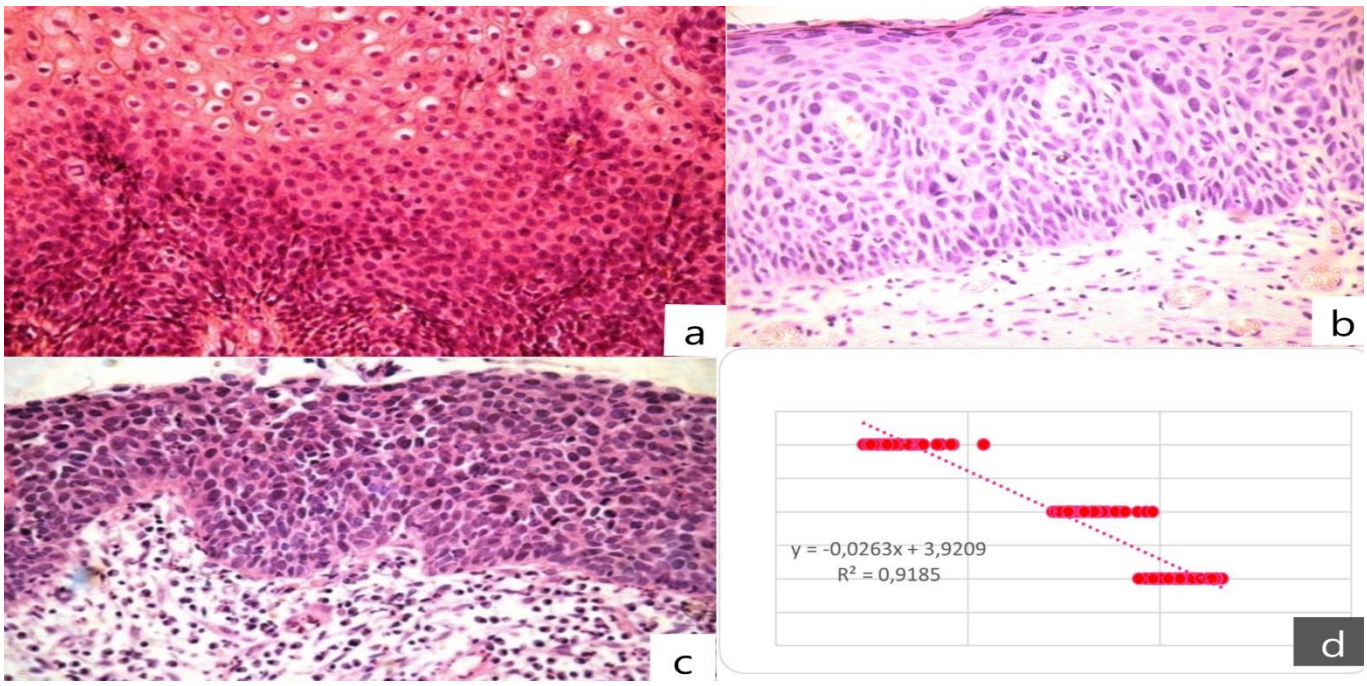

Figure 1. Cervical intraepithelial neoplasia (CIN), associated with papillomavirus infection in the infertile women: a – CIN of mild severity, b – CIN of moderate severity, c – severe CIN , d) connection between CIN severity and ratio of the multilayered squamous non-keratinized epithelium height to the volumetric density of capillaries of a mucous membrane. a-c – hematoxylin and eosin-stained section; original magnification x 20.

Immunohistochemical study of cervical tissue using the marker Ki-67 revealed a significant ($r = 0.96$, $p < 0.05$) increasing in expression according to an increase in severity of CIN. Analysis of the expression level showed that this marker contributed to a more complete determination of the severity, because the placement of Ki-67 positive cells corresponded to the general histological principle of CIN division. At the same time, at CIN variability of Ki-67 expression was noted. Thus, in the cervical biopsies of patients with CIN-I there was an increase in the intensity of binding of the proliferation marker of Ki-67 by epithelial cells of the basal and parabasal layers. This was characterized by a low level of expression and occupied no more than 1/3 of the of the integumentary layer. Also, a marker of cell proliferation was detected in the intermediate layer of the ectocervix, and it was also observed in the nuclei of superficial epitheliocytes in 4.8% of cases. Ki-67 was characterized by medium and high levels of expression with CIN-II (Figure 2).

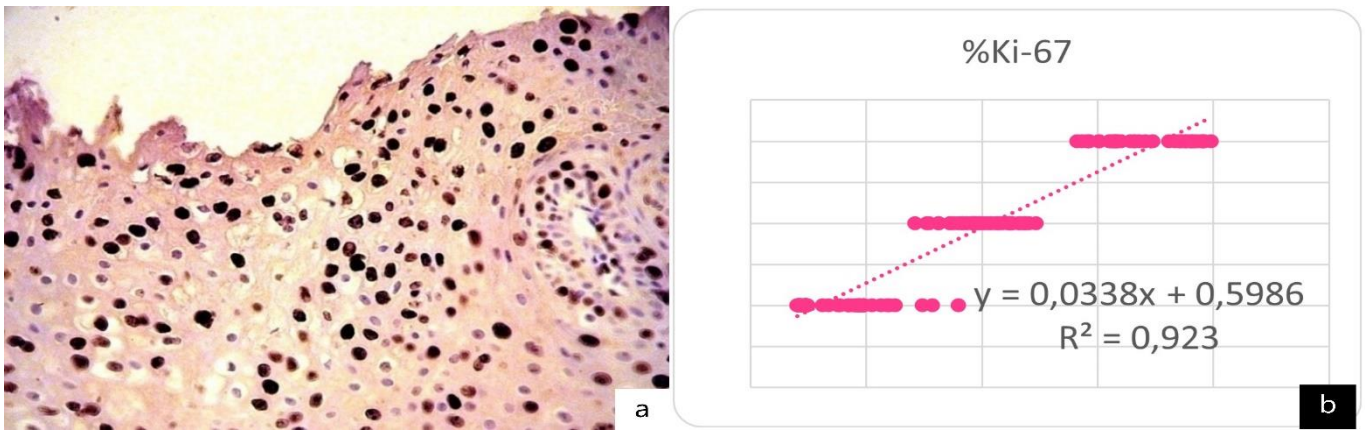

Figure 2. High level of Ki-67 expression with cervical intraepithelial neoplasia associated with papillomavirus infection of moderate severity. a - immunohistochemical study, original magnification x 20, b - connection between CIN severity and Ki-67 expression values.

Although the expression of Ki-67 was detected in the lower third of the epithelial layer in 13.2% of cases. Analysis by the method of χ2 - criterion revealed a significant effect of the severity of dysplasia on the proliferation index (χ2 = 9.48, p <0.05). The identified levels of oncoprotein p63 expression clearly correlated (r = 0.94, p <0.05) with the degree of CIN. The highest percentage (91.9%) with an expression level <30% was found in the group of patients with CIN-I. The expression level was 30-75% in 96.2% of cases with a moderate degree of CIN. The highest level (> 75%) of nuclear reaction was observed in 78.6% of patients with CIN-III (Figure 3). The results of the correlation analysis between the studied indicators showed the presence of a pronounced credible relationship between CIN and the ratio of MSNE / VDCMM (r = 0.95, p <0.05), the prevalence of Ki-67 expression in MSNE (r = 0.70, p <0.05), expression levels of Ki-67 (r = 0.96, p <0.05), p63 (r = 0.94, p <0.05). After a regression analysis, the regression equations of the dependence of the CIN severity on MSNE / VDCMM, Ki-67 and p63 were determined:

y = [-0,0263* X1+3,9209], coefficient of determination R^2 = 0,9185,

y = [0,0338* X2 + 0,5986], coefficient of determination R^2 = 0,9,

y = [0,03* X3 + 0,3088], coefficient of determination R^2 = 0,88,

when y – degree of CIN severity, X1 – value of MSNE / VDCMM,

X2 – value of Ki-67, %, X3 – value of p63, %.

A generalized regression model was created to determine the severity of CIN:

Y= [1,6094-0,00877*X1+0,011267*X2+0,01*X3]

The adequacy of the constructed mathematical model was proved by Fisher's criterion (F= 5123,064, F*=2,66, p=0,00000001). Coefficient of determination was R^2= 0,99.

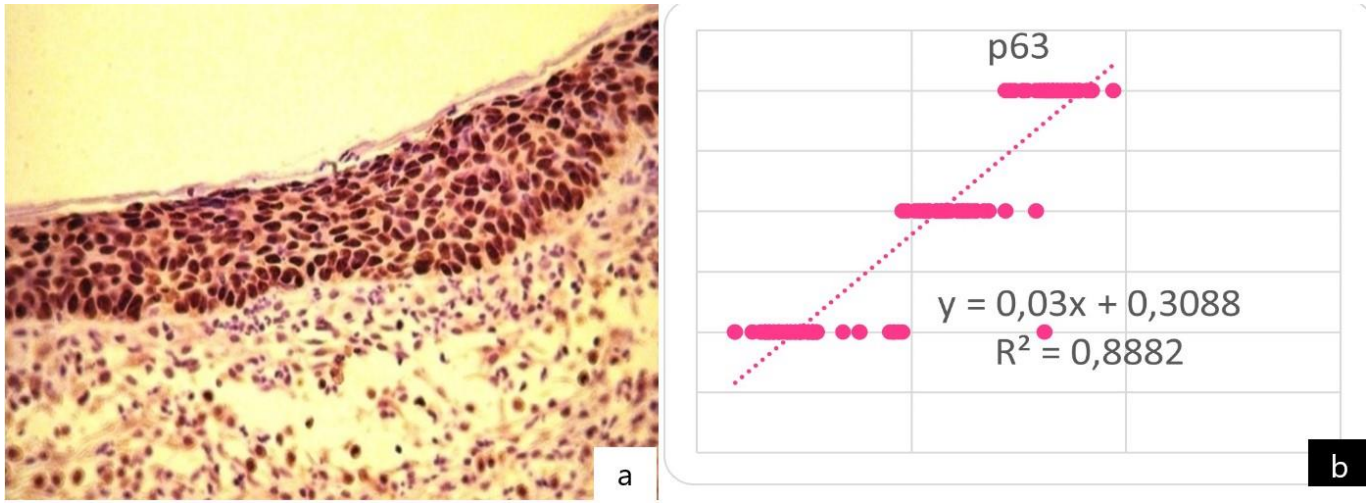

Figure 3. p63 hyperexpression in the cervical mucosa with positive reaction of cells groups in the cervical stroma with severe cervical intraepithelial neoplasia associated with papillomavirus infection. a - immunohistochemical study, original magnification x 20, b - connection between CIN severity and p63 expression values.

Conclusions.

The obtained morphometric data of the cervix with cervical intraepithelial neoplasia in women with infertility indicate changes in the epithelial-stromal relationship in the cervical mucosa. Disorders of the epithelial-stromal relationship especially in cases of severe cervical intraepithelial neoplasia may be one of the stages of carcinogenesis as evidenced by the ratio of multilayered squamous non-keratinized epithelium height to the volumetric density of capillaries of a mucous membrane and the expression of Ki-67 and p63.

The developed regression model which is based on the studied morphometric parameters reliably allows to determine the degree of CIN associated with papillomavirus infection in infertile women.

References.

[1] Sutton MY, Anachebe NF, Lee R, [et al.]. Racial and Ethnic Disparities in Reproductive Health Services and Outcomes, 2020. Obstet Gynecol 2021; 137 (2): 225-233.

[2] Farsimadan M, Motamedifar M. The effects of human immunodeficiency virus, human papillomavirus, herpes

simplex virus-1 and -2, human herpesvirus-6 and -8, cytomegalovirus, and hepatitis B and C virus on female fertility and pregnancy. Br J Biomed Sci 2021; 78 (1): 1-11.

[3] Moramazi F, Roohipoor M, Najafian M. Association between internal cervical os stenosis and other female infertility risk factors. Middle East Fertil Soc J 2018; 23 (4): 297–299.

[4] Brazdova A, Senechal H, Peltre G, [et al.]. Immune Aspects of Female Infertility. Int J Fertil Steril 2016; 10 (1): 1–10.

[5] Nakano FY, Leao RBF, Esteves SC. Insights into the role of cervical mucus and vaginal pH in unexplained infertility. MedicalExpress (São Paulo, online) 2015; 2 (2): M150207.

[6] Cooper TG, Noonan E, von Eckardstein S, [et al.]. World Health Organization reference values for human semen characteristics. Hum Reprod Update 2010; 16 (3): 231–245.

[7] Hofherr SE, Wiktor AE, Kipp BR, [et al.]. Clinical diagnostic testing for the cytogenetic and molecular causes of male infertility: the Mayo Clinic experience. J Assist Reprod Genet 2011; 28 (11) : 1091–1098.

[8] Tammy J. Lindsay, Kirsten R. Vitrikas. Evaluation and Treatment of Infertility. Am Fam Physician 2015; 91 (5): 308–314.

[9] Lian Y, Chen M, Qin L, [et al.]. A meta-analysis of the relationship between vaginal microecology, human papillomavirus infection and cervical intraepithelial neoplasia. Infect Agents Cancer 2019; 14 (29): 2–8.

[10] He ZH, Kou ZQ, Xu AQ. HPV infection and its immune prevention [J]. Chin J Prev Med 2018; 52 (1): 106 –112.

[11] Xiong Y, Cui L, Bian C, [et al.]. Clearance of human papillomavirus infection in patients with cervical intraepithelial neoplasia: a systemic review and meta-analysis. Medicine 2020; 99 (46): (e23155).

[12] Cohen PA, Jhingran A, Oaknin A, [et al.]. Cervical cancer. Lancet 2019 ; 393 (10167): 169–182.

[13] Zhang S, Batur P. Human papillomavirus in 2019: an update on cervical cancer prevention and screening guidelines. Cleve Clin J Med 2019; 86: 173–178.

[14] Cara M.Martin , John J.O'Leary. Histology of cervical intraepithelial neoplasia and the role of biomarkers. Best Pract Res Clin Obstet Gynaecol 2011; 25 (5): 605-615.

[15] Mitildzans A, Arechvo A, Rezeberga D, [et al.]. Expression of p63, p53 and Ki-67 in Patients with Cervical Intraepithelial Neoplasia. Turk Patoloji Derg 2017; 33: 9-16.

[16] Chen Li, Hao Chen, Xiaoyan Li, [et al.]. A review for cervical histopathology image analysis using machine vision approaches. Artif Intell Rev 2020; 53: 4821–4862.

[17] Arsenio A. Spinillo, Mattia M. Dominoni, Anna A. C. Boschi, [et al.]. Significance of the Interaction between Human Papillomavirus (HPV) Type 16 and Other High-Risk Human Papillomaviruses in Women with Cervical Intraepithelial Neoplasia (CIN) and Invasive Cervical Cancer. J Oncol 2020; 6508180.

WORLD JOURNAL OF MEDICAL INNOVATIONS

Promising strategies for overcoming cancer drug resistance: from nanomedicine to artificial intelligence

Martinelli Chiara[1], Biglietti Marco[2]

[1]*Istituto Italiano di Tecnologia, Smart Bio-Interfaces, Pontedera, Italy*
[2]*Independent Researcher, Milan, Italy*

Article info

ONCOLOGY

Review paper

Article history:
Accepted December 28, 2021

Published online January 2, 2022

Keywords:
nanomedicine,
artificial intelligence,
cancer,
drug resistance

Abstract

Cancer is one of the most diffused and deadly diseases worldwide. Unfortunately, due to the very heterogeneous nature of tumors, it has been very challenging finding efficient treatments. Standard clinical procedures present many adverse side effects and may often cause drug resistance with consequent therapy failure, onset of metastases and relapse. Combination therapy has demonstrated limited success due to the difficulties in matching different molecules pharmacokinetic properties and in tuning the best dosage in order to achieve the desired effects. Recently, innovations in the nanotechnology field have allowed to design *ad hoc* nanocarriers able to selectively deliver drugs to target cells and release them upon specific triggers. Artificial intelligence approaches have been also developed and advances in the computational modeling field have greatly impacted human healthcare. The possibility to exploit algorithms for predicting drug responsiveness based on data retrieved from databases is greatly improving clinical strategies and supporting therapeutic decisions. In this review, we report recent advances in the nanomedical and artificial intelligence fields and describe novel strategies adopted for counteracting cancer drug resistance. Limits and promises of these approaches are discussed, together with some examples of preclinical and clinical applications.

Corresponding author. Dr. Chiara Martinelli, Politecnico di Milano, Department of Chemistry, Materials and Chemical Engineering "Giulio Natta", Milan, Italy, chiara.martinelli@protonmail.com

Introduction.

Cancer is one of the leading causes of death worldwide and one of the costliest diseases. Standard therapeutic treatments are mainly based on surgery, chemotherapy, radiation therapy and, recently, on targeted immunotherapy. Unfortunately, these approaches present many undesirable side effects, they are invasive and very often do not display enough selectivity for cancer cells. One phenomenon that commonly arises in patients during and upon chemotherapy is drug resistance, namely the capacity of tumor cells to become tolerant to the administered chemical agents and sometimes also to unrelated drugs, leading to multidrug resistance (MDR) [1,2]. This situation is correlated to therapy failure and is responsible for the diffusion of metastatic cancer and tumor relapse [3,4]. In the last years, researchers have focused on unraveling the mechanisms involved in cancer drug resistance, such as apoptosis inhibition, DNA damage repair, drug inactivation, altered drug efflux and target modifications [1,5,6]. Many strategies have been adopted for circumventing drug resistance, for instance by administering drug combinations

and small molecule inhibitors or by performing gene therapy [7]. Nevertheless, complications with tuning the right doses for achieving an appreciable effect and the difficulty to match the pharmacokinetic profiles of the proposed drugs has led to many unpredictable outcomes [8,9]. Indeed, each patient presents unique responses to a specific drug and this is especially true in very heterogeneous disorders such as cancer, thus making diagnosis and treatment very challenging [10,11]. Recently, the concept of precision medicine has gained fundamental importance in the clinical context, for establishing specific treatments for each patient, based on their peculiar genetic and epigenetic features [12]. Currently, efforts are centered on two innovative approaches, nanomedicine and artificial intelligence (AI), which are developing as intertwined tools for counteracting cancer drug resistance through personalized medicine. Nanotechnology has provided the means for designing and engineering nanomaterials formulated for delivering multiple drugs, ameliorating their physicochemical properties, enhancing their effectiveness and reducing possible adverse side effects [13–15]. Both inorganic and organic nanocarriers have been developed and modified, making them not merely subjected to passive delivery but also able to actively reaching specific tumor cells by means of functionalization with targeting ligands [16–20]. Thanks to this feature, nanocarriers can circumvent cell membrane transporters and enter the cells by endocytosis [18]. Interestingly, nanomedicines responsive to external stimuli display the great advantage of releasing the drug on site and upon specific triggers [20]. The importance of predicting drug responsiveness in oncology is fundamental and many efforts have been focused on developing appropriate techniques, from cell culture based chemosensitivity tests [21] to computational models [22]. However, standard methods present limitations, partially overcome by the advent of DNA, RNA, and protein-based assays [23,24], which rely on predictions coming from a defined number of genes [22,25]. Despite the many successes in reducing mortality, however it remains relatively difficult to find the correct genes to be analyzed as prognostic markers of drug resistance [25]. Examples in this direction are the publicly available Gene Expression Omnibus (GEO) database and The Cancer Genome Atlas (TCGA) that have provided huge amounts of data [26]. This review reports innovative nanomedical and AI approaches for counteracting drug resistance in cancer. A special focus on the developments at the preclinical and clinical stages is made, discussing the advantages and limits of this vibrant field of research.

1. Nanomaterials for overcoming cancer drug resistance.

Nanomaterials are contributing to personalized medicine from diagnosis to therapy: improvements in many technologies have allowed to perform single molecule DNA sequencing [27] and to exploit nanosensors to detect biomarkers with femtomolar concentration sensitivities [28]. In particular, advances in the design of theranostic agents combining drug delivery and imaging agents have revolutionized the field of nanomedicine [29]. Multiple kinds of carriers have been developed, thanks to their intrinsic properties such as i) high surface to volume ratio, and ii) several possibilities of modification by specific ligand functionalization for responding to external stimuli (Figure 1).

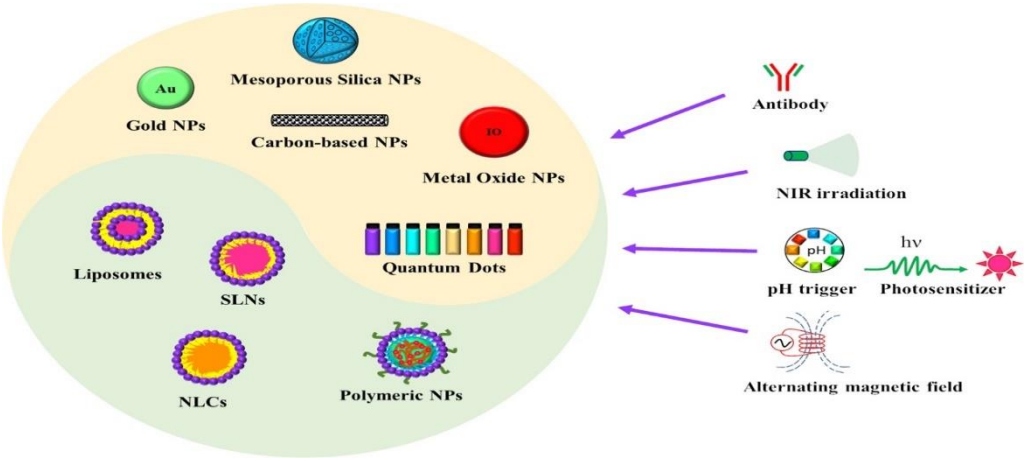

Figure 1. Scheme of the main inorganic and organic nanoparticles developed for counteracting cancer drug resistance. Possible functionalization with targeting ligand and external stimuli exploited for triggered drug release are reported. NPs: nanoparticles, IO: iron oxide, SLNs: solid lipid nanoparticles, NLCs: nanostructured lipid carriers, NIR: near-infrared.

Interestingly, nanoparticles (NPs) can easily penetrate cells by endocytic mechanisms, avoiding pump transporters involved in multidrug resistance. Considering inorganic nanomaterials, iron oxide NPs have been used for carrying chemotherapeutic molecules to drug resistant HeLa cells [30], and have displayed a more efficient behavior respect to the free molecule itself *in vivo* [31]. As mentioned before, the possibility to load NPs with multiple drugs for simultaneous delivery is of prominent importance for improving the potential of combination therapy, overcoming the limits due to pharmacokinetics and tumor microenvironment heterogeneity [32,33]. One further advantage of using metallic NPs is that they are responsive to alternating magnetic fields, generating localized hyperthermia, gaining drug release and efficient resistance reversal [34,35]. Similarly, to iron oxide, gold NPs have been synthetized and conjugated to specific drugs, achieving significant cytotoxic effects in drug resistant cancer cells [36,37]. Interestingly, a therapeutic approach, called photothermal therapy (PTT) has been adopted, based on the conversion of absorbed near-infrared (NIR) light to heat, specifically destroying cancer cells [38]. A recent study showed its efficacy upon administration of NPs to MDR tumor xenografts [39]. An interesting material used in nanomedicine is constituted by mesoporous silica nanoparticles (MSNs), excellent carriers of molecules inside drug resistant cancer cells [40]. When exploited for delivering siRNAs targeting P-glycoprotein (P-gp, also known as multidrug resistance protein 1) and doxorubicin, they showed accumulation due to enhanced permeability and retention effect, with resulting downregulation of specific protein expression [41]. Carbon based nanocarriers have been widely employed in nanomedicine for their high surface-to-volume ratio, thermal conductivity and ease of functionalization. For instance, i) carbon nanotubes, used in many applications such as imaging agents responsive to NIR irradiation [42] and as carriers for chemotherapeutics and P-gp inhibitors *in vitro* and *in vivo* [43–45], and ii) graphene oxide loaded with siRNAs and chemotherapeutic agents, that have revealed successful in targeting drug resistant tumor cells [46,47]. Concerning organic materials, they have raised increasing interest thanks to i) biocompatibility, due to the presence of natural components in their formulations, and ii) high biodegradability. In this section, some researches concerning the use of lipidic and polymeric NPs will be reported. Liposomes, thanks to their nature, can encapsulate hydrophilic and hydrophobic molecules [48], they easily accumulate into tumors and, when appropriately modified (i.e., by PEGylation), they can be made enough stable to enhance their circulation times [49] eluding transporters involved in MDR [50]. Liposomes loaded with multiple drugs revealed to be effective both *in vitro* and *in vivo*, efficiently overcoming MDR [51,52]. Modifications that made them responsive to external stimuli, further enhanced their efficacy [53]. Another kind of lipid NPs, constituted by lipids solid at body temperature and a stabilizing surfactant, are called solid lipid nanoparticles (SLNs) [54]. They present higher stability and a more sustained release respect to liposomes. MDR was successfully overcome in breast cancer cells upon SLNs administration [55] and in *in vitro* and *in vivo* models of hepatocellular carcinoma [56]. Nanostructured lipid carriers (NLCs) constituted by one or more liquid lipid allowing to encapsulate high amounts of drugs [57] have demonstrated efficient in combination therapy, delivering paclitaxel and indocyanine green, targeting tumor cells and releasing chemicals upon laser irradiation *in vitro* and *in vivo* [58]. NLCs mediated targeted delivery of doxorubicin and vincristine revealed effective *in vitro* and *in vivo* [59]. Highly biocompatible polymeric NPs have been successfully used for circumventing MDR in cancer [50]. Multifunctional NPs loaded with chemotherapeutic agents and responsive to external triggers have displayed effectiveness in MDR tumors [60,61]. Interestingly, modifications have been performed allowing to specifically downregulate the expression of proteins correlated to multidrug resistance [62]. The biopolymer poly lactide-co-glycolide (PLGA) has been widely explored for fabricating NPs carrying paclitaxel and siRNAs directed against focal adhesion kinase and for treating ovarian cancer *in vitro* and *in vivo* [63]. Interestingly, poloxamers, copolymers able to interfere with P-gp efflux pumps, have been combined to PLGA for obtaining docetaxel-loaded PLGA d-α-tocopheryl polyethylene glycol 1000 succinate (TPGS)/Poloxamer 235 NPs for breast cancer treatment [64]. In spite of the advantages of nanoparticle-based treatments, it is important to know that very few trials have been registered involving their clinical translation. Formulations of camptothecin conjugated to cyclodextrin-based polymers, have been reported for treating recurrent platinum-resistant ovarian, tubal and peritoneal cancer [65], castration resistant prostate cancer patients already treated with enzalutamide [66] and, combined with Olaparib, recurrent ovarian cancer [67]. Studies involving the administration of paclitaxel albumin-stabilized NPs, alone or in combination with other molecules, have been reported in platinum-resistant ovarian, fallopian tube, or primary peritoneal cancer [68–70], in taxol resistant patients with metastatic breast cancer [71] and in advanced gastric tumors [72]. Two clinical trials have been registered for studying the effects of the administration of docetaxel NPs in metastatic castration resistant prostate cancer [73] and in platinum-

resistant ovarian cancer patients [74]. Concerning liposomes as therapeutic agents, one study is expected to administer irinotecan liposomes and bevacizumab to patients with platinum resistant ovarian, fallopian tube, or primary peritoneal cancer and to subjects with recurrent and refractory cancer [75]. Another trial performing a treatment with anti-EGFR immunoliposomes carrying cytotoxic molecules, and specifically targeting solid tumors overexpressing EGFR, has been described [76].

2. Artificial intelligence for overcoming cancer drug resistance

In the last decades, AI has revolutionized many fields of human life [77] impacting with ground-breaking healthcare strategies and supporting problem solving and decision making in oncology [78]. Similarly to traditional medical approaches, where multidisciplinary teams integrating the most different competences are involved in finding the correct diagnosis, analyzing data and finally developing a treatment strategy, computational models are capable to learn and predict patterns, by mining and linking data, often walking along roads that researchers and physicians can't walk [79] (Figure 2). Computational strategies can drastically improve basic research and precision oncology [78], cancer medical imaging (i.e., radiographic imaging [80,81] and digital pathology [82,83]) and translational oncology (i.e., cancer therapy [84–86] and drug discovery [87,88]), allowing to plan personalized treatments. From a generic point of view, computational technologies allow to i) collect huge amounts of digital data, acquired from heterogeneous sources, such as different types of images, next generation sequencing, large scale clinical trials and patients health records, and ii), improve drug discovery, correct diagnosis and therapy by early detection, modeling-based predictions, pattern recognition and data correlations, based on "automatically improve through experience" algorithms[78].

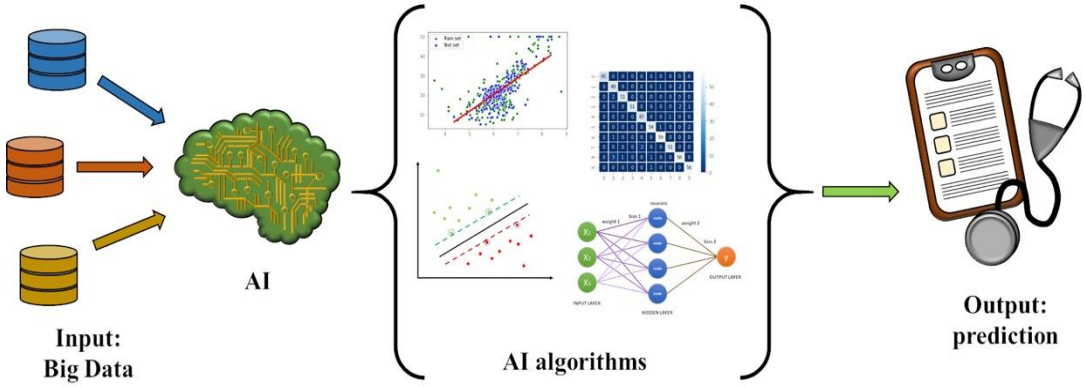

Figure 2. Scheme of an artificial intelligence algorithm. In input, Big Data are retrieved from different databases. The dataset collected is subsequently analyzed by artificial intelligence (AI) algorithms with specific architectures. In order to improve the result, several solutions can be combined in a single algorithm. The obtained output is a prediction able to improve medical strategies and therapeutic decisions.

Because the complexity and quantity of databases developed in the last decades are experimentally and economically not affordable by *in vitro* and *in vivo* researches, computational methods have revealed to be the most promising tools for supporting drug discovery and for screening drug combinations [89]. Machine learning (ML) algorithms are a subclass of AI, typically divided into different categories, depending on the signal or feedback provided to the learning system and on the statistical and probabilistic approach adopted [90,91]. Support-vector machines (SVMs) are a ML supervised approach, able to analyze data for classification and regression processes, very useful to recognize patterns in complex data [90]. Hazai et al., exploited a model of SVM to predict substrates of human breast cancer resistance protein (BCRP), involved in multidrug resistance onset, and demonstrated this method as an affordable system for the analysis of pharmacokinetics, efficacy and safety of specific drugs [92]. In a recent study, a SVM algorithm was implemented, presenting a high accurate solution in predicting drug responsiveness in many cancer cell lines. To train and test the model, datasets of gene expression and drug response collected in the National Cancer Institute panel of 60 human cancer cell lines (NCI-60) were used [93]. Another architecture exploited in the ML field is the Bayesian algorithm, a statistical model based on Bayes' theorem [90]. Costello et al., demonstrated its impact in predicting drug response by analyzing 44 drug sensitivity prediction algorithms trained on datasets collected from

genomic, epigenomic and proteomic analyses performed in human breast cancer cell lines [94]. In order to unravel the highly heterogeneous nature of a pathology such as cancer, Gönen et al., proposed computational algorithms able to mining genomic information for obtaining robust predictors of drug responses. They focused on a Bayesian algorithm with two main properties: i) developing a simultaneous predictive model for all the drugs considered, stressing their common parameters, and ii) handling missing data concerning drug susceptibility measurements, in order not to discard data with missing outputs [95]. It is well known that patients affected by the same tumor display heterogeneous behaviors towards the same kind of therapy. Therefore, computational models have developed the so-called ensemble methods, that use multiple learning algorithms to obtain a better predictive performance than using their learning algorithm alone. A typical example of an ensemble method is the "random forest" model, a ML strategy for classification using determined numbers of predictive sub-models called "decision trees". A recent work demonstrated that adopting a random forest it could be feasible mapping pharmacogenomics alterations in 1,001 human cancer cell lines and correlating the analysis with possible sensitivity to 265 drugs. The study showed the importance of different kinds of data in predicting drug response of specific tumor populations [96]. Cortés-Ciriano et al., applied the random forest integrating chemical and biological information for modelling 50% growth inhibition bioassay endpoint of thousands of compounds screened against 59 cancer cell lines. The algorithm was able to elaborate compound bioactivities in input and output, with the possibility to be extended to different cell lines, tissues and compounds, predicting drug-pathway associations and growth inhibition patterns [97]. Naulaerts et al., created a ML model for comparing commonly considered single-gene markers with multi-gene markers, exploiting genomic data for distinguishing sensitive *vs.* resistant cancer cell lines. The study demonstrated that sensitivity to specific drugs can be better predicted by these kinds of models [98]. Interestingly, it has been shown that is possible to overcome the "trial and error method" while looking for the identification of the best drug mixtures for circumventing drug resistance, by using a computational ensemble predictive model greatly reducing the complexity of combination therapy [99]. Very recently, Sharma et al., applied a modified rotation forest from a specific ensemble learning framework to Genomics of Drug Sensitivity in Cancer (GDSC) and Cancer Cell Line Encyclopedia (CCLE) drug screens, and obtained very robust drug-response predictions [100]. An artificial neural network is a ML network composed by nodes interconnected and controlled by a linear combination of weights and its name originates from the computational attempts to mimic a biological brain. Artificial neural networks can learn by training through datasets, allowing to obtain probabilistic responses moving through complex and apparently unrelated information. Menden et al., exploited an artificial neural network for designing *ad hoc* drug-cell screenings, suggesting an *in silico* massive test both for drug discovery and sensitivity evaluation [101]. As studies progress, new computational solutions have been gradually introduced to improve the efficiency of the process. Deep learning (DL) is a particular subclass of ML [90], specifically based on artificial neural networks [102,103], where the adjective "deep" refers to the multiple layers used in the construction of the network architecture. In many studies, DL algorithms have shown robust prediction of drug response when applied to pharmacological and cell line -omics data [104]. As for ML technology, DL can investigate huge amounts of multi factor and noisy data while defining nonlinear relations in datasets and bypassing the complexity of biological data [105]. Like for ML, different strategies can be used for elaborating a DL algorithm. The more intuitive is an artificial neural network with a large number of fully connected hidden layers, where the information flows through the nodes in one direction [106]. Regardless of its simplicity, this model has been already successfully used in drug response analysis [107]. Another type of DL model is the convolutional neural network where, in specific points of the network, the algorithm applies convolutions and the final layers result to be fully connected for a supervised classification or regression. Importantly, convolutional neural networks are used for drug response prediction based on input data like 2D compound structures, named "compound images" [108]. Finally, the network can present cycles connecting adjacent edges. In this case, the DL model is named recurrent neural network, whose main application is modeling sequential data. For instance, Oskooei et al., developed a prediction algorithm for anticancer compound sensitivity (PaccMann), integrating molecular structure of drugs, transcriptomic profiles of cancer cells and data related to protein-cell interactions [109]. DL methods with unsupervised architecture have been also described, analyzing both chemical structures and -omics data for elaborating a predictive model of drug interaction [110–112].

Conclusions.

Considering the reported researches on nanomaterials, it is possible to infer that further studies will be required before a broad diffusion of nanoparticles in the medical context. Although the application of nanotechnology for targeted drug delivery is clearly a very promising strategy for counteracting cancer drug resistance, however more knowledge is required concerning the behavior of the delivered drugs and the metabolism of nanomaterials inside human body, especially in the long-term [113]. Assessment of nanotoxicity and nanosafety is a fundamental prerequisite for clinical applications and it is at this point that innovative multidisciplinary approaches such as computational technologies, could help predicting and finely tuning the best treatment for achieving the best therapeutic result in very much intricate pathologies like tumors [114,115]. Although the vast majority of the artificial intelligence studies are performed at a preclinical stage, importantly the possibility to perform clinical trials aimed at collecting radiomics, metabolic, genetic, pathological data for establishing multi-omics AI systems for predicting the effect of neoadjuvant therapy and better explore drug resistance is now becoming reality [116]. Obviously, the success of the computational approaches in the clinical field will be determined in large part by the efforts to translate mathematical abstract models into healthcare strategies. Some issues have been already raised, such as i) standardization of databases and predictions, ii) difficulties in translating diagnostic tasks into Boolean values, and iii) necessity to overcome the gap between medical professionals and computer scientists [117,118]. Furthermore, data collection raises some ethical issues, because it determines a potential exposure to hacking attacks or illegal access to very sensitive data and personalized medicine exposes to the risk of profiling patients into their privacy [119]. In conclusion, even though surveillance by human specialists (i.e., ethical commissions, cyber security experts, bioinformatics and physicians) is still indispensable, however researches in the artificial intelligence field are exponentially growing, laying foundations for future integrations with medicine.

References.

[1] Housman G, Byler S, Heerboth S, [et al.]. Drug resistance in cancer: An overview. Cancers (Basel) 2014; 6(3):1769–1792.

[2] Rebucci M, Michiels C. Molecular aspects of cancer cell resistance to chemotherapy. Biochem Pharmacol 2013; 85:1219–1226.

[3] Wu Q, Yang Z, Nie Y, [et al.]. Multi-drug resistance in cancer chemotherapeutics: Mechanisms and lab approaches, Cancer Lett 2014; 347(2):159-66.

[4] Longley DB, Johnston PG. Molecular mechanisms of drug resistance. J Pathol 2005; 205(2):275-92.

[5] Kibria G, Hatakeyama H, Harashima H. Cancer multidrug resistance: Mechanisms involved and strategies for circumvention using a drug delivery system. Arch Pharm Res 2014; 37(1):4-15.

[6] Martinelli C, Biglietti M. Nanotechnological approaches for counteracting multidrug resistance in cancer. Cancer Drug Resist 2020; 3:1003–1020.

[7] Raguz S, Yagüe E. Resistance to chemotherapy: new treatments and novel insights into an old problem.. Br J Cancer 2008; 99:387–391.

[8] Yap TA, Omlin A, De Bono JS. Development of therapeutic combinations targeting major cancer signaling pathways. J Clin Oncol 2013; 31(12):1592-605.

[9] Lee MJ, Ye AS, Gardino AK, [et al.]. Sequential application of anticancer drugs enhances cell death by rewiring apoptotic signaling networks. Cell 2012; 149(4):780-94.

[10] Schork NJ. Personalized medicine: Time for one-person trials. Nature 2015; 520:609–611.

[11] McGranahan N, Swanton C. Clonal Heterogeneity and Tumor Evolution: Past, Present, and the Future. Cell 2017; 168:613–628.

[12] Collins FS, Varmus H. A New Initiative on Precision Medicine. N Engl J Med 2015; 372:793-795.

[13] Iyer AK, Singh A, Ganta S, [et al.]. Role of integrated cancer nanomedicine in overcoming drug resistance. Adv Drug Deliv Rev 2013; 65(13-14):1784-802.

[14] Vinogradov S, Wei X. Cancer stem cells and drug resistance: The potential of nanomedicine. Nanomedicine 2012; 7(4):597-615.

[15] Maeda H. The enhanced permeability and retention (EPR) effect in tumor vasculature: The key role of tumor-selective macromolecular drug targeting. Adv Enzyme Regul 2001; 41:189-207.

[16] Ali A, Zafar H, Zia M, [et al.]. Synthesis, characterization, applications, and challenges of iron oxide nanoparticles. Nanotechnol Sci Appl 2016; 9:49-67.

[17] Bertrand N, Wu J, Xu X, [et al.]. Cancer nanotechnology: The impact of passive and active targeting in the era of modern cancer biology. Adv Drug Deliv Rev 2014; 66:2-25.

[18] Cerqueira BBS, Lasham A, Shelling AN, [et al.]. Nanoparticle therapeutics: Technologies and methods for overcoming cancer. Eur J Pharm Biopharm 2015; 97(Pt A):140-51.

[19] Mura S, Nicolas J, Couvreur P. Stimuli-responsive nanocarriers for drug delivery. Nat Mater 2013; 12(11):991-

1003.
[20] Torchilin VP. Multifunctional, stimuli-sensitive nanoparticulate systems for drug delivery. Nat Rev Drug Discov 2014; 13(11):813-27.
[21] Cortazar P, Johnson BE. Review of the efficacy of individualized chemotherapy selected by in vitro drug sensitivity testing for patients with cancer. J Clin Oncol 1999; 17(5):1625-31.
[22] Lloyd KL, Cree IA, Savage RS. Prediction of resistance to chemotherapy in ovarian cancer: a systematic review. BMC Cancer 2015; 15:117.
[23] Sekine I, Minna JD, Nishio K, [et al.]. A literature review of molecular markers predictive of clinical response to cytotoxic chemotherapy in patients with lung cancer. J Thorac Oncol 2006; 1(1):31-7.
[24] Sekine I, Minna JD, Nishio K, [et al.]. Genes regulating the sensitivity of solid tumor cell lines to cytotoxic agents: a literature review. Jpn J Clin Oncol 2007; 37(5):329-36.
[25] Wu L, Qu X. Cancer biomarker detection: recent achievements and challenges. Chem Soc Rev 2015; 44(10):2963-97.
[26] Barrett T, Wilhite SE, Ledoux P, [et al.]. NCBI GEO: archive for functional genomics data sets--update. Nucleic Acids Res 2013; 41(Database issue):D991-5.
[27] Gupta PK. Single-molecule DNA sequencing technologies for future genomics research. Trends Biotechnol 2008; 26:602–611.
[28] Xia Z, Xing Y, So M-K, [et al.]. Multiplex detection of protease activity with quantum dot nanosensors prepared by intein-mediated specific bioconjugation. Anal Chem 2008; 80:8649–8655.
[29] Sumer B, Gao J. Theranostic nanomedicine for cancer. Nanomedicine (Lond) 2008; 3:137–140.
[30] Elumalai R, Patil S, Maliyakkal N, [et al.]. Protamine-carboxymethyl cellulose magnetic nanocapsules for enhanced delivery of anticancer drugs against drug resistant cancers. Nanomedicine 2015; 11(4):969-81.
[31] Kievit FM, Wang FY, Fang C, [et al.]. Doxorubicin loaded iron oxide nanoparticles overcome multidrug resistance in cancer in vitro. J Control Release 2011; 152(1):76-83.
[32] Cheng J, Wu W, an Chen B, [et al.]. Effect of magnetic nanoparticles of Fe3O4 and 5-bromotetrandrine on reversal of multidrug resistance in K562/A02 leukemic cells. Int J Nanomedicine 2009; 4:209-16.
[33] Cheng J, Cheng L, Chen B, [et al.]. Effect of magnetic nanoparticles of Fe3O4 and wogonin on the reversal of multidrug resistance in K562/A02 cell line. Int J Nanomedicine 2012; 7:2843-52.
[34] Kossatz S, Grandke J, Couleaud P, [et al.]. Efficient treatment of breast cancer xenografts with multifunctionalized iron oxide nanoparticles combining magnetic hyperthermia and anti-cancer drug delivery. Breast Cancer Res 2015; 17(1):66.
[35] Ren Y, Zhang H, Chen B, [et al.]. Multifunctional magnetic Fe3O4 nanoparticles combined with chemotherapy and hyperthermia to overcome multidrug resistance. Int. J. Nanomedicine 2012; ;7:2261-9.
[36] Gu YJ, Cheng J, Man CWY, [et al.]. Cheng, Gold-doxorubicin nanoconjugates for overcoming multidrug resistance. Nanomedicine 2012; 8(2):204-11.
[37] Wang F, Wang YC, Dou S, [et al.]. Doxorubicin-tethered responsive gold nanoparticles facilitate intracellular drug delivery for overcoming multidrug resistance in cancer cells. ACS Nano 2011; 5(5):3679-92.
[38] Cheng L, Wang C, Liu Z. Functional nanomaterials for phototherapies of cancer. Chem rev 2014; 114(21):10869-939.
[39] Lee SM, Kim HJ, Kim SY, [et al.]. Drug-loaded gold plasmonic nanoparticles for treatment of multidrug resistance in cancer. Biomaterials 2014; 35(7):2272-82.
[40] Gao Y, Chen Y, Ji X, [et al.]. Controlled intracellular release of doxorubicin in multidrug-resistant cancer cells by tuning the shell-pore sizes of mesoporous silica nanoparticles. ACS Nano 2011; 5(12):9788-98.
[41] Meng H, Mai WX, Zhang H, [et al.]. Codelivery of an optimal drug/siRNA combination using mesoporous silica nanoparticles to overcome drug resistance in breast cancer in vitro and in vivo. ACS Nano 2013; 7(2):994-1005.
[42] Kruss S, Hilmer AJ, Zhang J, [et al.]. Carbon nanotubes as optical biomedical sensors. Adv Drug Deliv Rev 2013; 65(15):1933-50.
[43] Bhirde AA, Chikkaveeraiah BV, Srivatsan A, [et al.]. Targeted therapeutic nanotubes influence the viscoelasticity of cancer cells to overcome drug resistance. ACS Nano 2014; 8(5):4177-89.
[44] Kumar M, Sharma G, Misra C, [et al.]. N-desmethyl tamoxifen and quercetin-loaded multiwalled CNTs: A synergistic approach to overcome MDR in cancer cells. Mater. Sci. Eng. C. Mater Biol Appl 2018; 89:274-282.
[45] Suo X, Eldridge BN, Zhang H, [et al.]. P-Glycoprotein-Targeted Photothermal Therapy of Drug-Resistant Cancer Cells Using Antibody-Conjugated Carbon Nanotubes. ACS Appl Mater Interfaces 2018; 10(39):33464-33473.
[46] Zhi F, Dong H, Jia X, [et al.]. Functionalized Graphene Oxide Mediated Adriamycin Delivery and miR-21 Gene Silencing to Overcome Tumor Multidrug Resistance In Vitro. PLoS One 2013; 8(3):e60034.
[47] Feng L, Li K, Shi X, [et al.]. Smart pH-responsive nanocarriers based on nano-graphene oxide for combined chemo- and photothermal therapy overcoming drug

resistance. Adv Healthc Mater 2014; 3(8):1261-71.
[48] Huang Y, Cole SPC, Cai T, [et al.]. Applications of nanoparticle drug delivery systems for the reversal of multidrug resistance in cancer. Oncol Lett 2016; 12(1):11-15.
[49] Yang T, De Cui F, Choi MK, [et al.]. Enhanced solubility and stability of PEGylated liposomal paclitaxel: In vitro and in vivo evaluation. Int J Pharm 2007; 338(1-2):317-26.
[50] Kapse-Mistry S, Govender T, Srivastava R, [et al.]. Nanodrug delivery in reversing multidrug resistance in cancer cells. Front Pharmacol 2014; 5:159.
[51] Meng J, Guo F, Xu H, [et al.]. Combination Therapy using Co-encapsulated Resveratrol and Paclitaxel in Liposomes for Drug Resistance Reversal in Breast Cancer Cells in vivo. Sci Rep 2016; 6:22390.
[52] Ashley JD, Quinlan CJ, Schroeder VA, [et al.]. Dual Carfilzomib and Doxorubicin-Loaded Liposomal Nanoparticles for Synergistic Efficacy in Multiple Myeloma. Mol Cancer Ther 2016; 15(7):1452-9.
[53] Vaidya B, Nayak MK, Dash D, [et al.]. Development and characterization of highly selective target-sensitive liposomes for the delivery of streptokinase: In vitro / in vivo studies. Drug Deliv 2016; 23(3):801-7.
[54] Rajpoot K. Solid Lipid Nanoparticles: A Promising Nanomaterial in Drug Delivery. Curr Pharm Des 2019; 25(37):3943-3959.
[55] Baek JS, Cho CW. Controlled release and reversal of multidrug resistance by co-encapsulation of paclitaxel and verapamil in solid lipid nanoparticles. Int J Pharm 2015; 478(2):617-24.
[56] Zhao X, Chen Q, Li Y, [et al.]. Doxorubicin and curcumin co-delivery by lipid nanoparticles for enhanced treatment of diethylnitrosamine-induced hepatocellular carcinoma in mice. Eur J Pharm Biopharm 2015; 93:27-36.
[57] Tamjidi F, Shahedi M, Varshosaz J, [et al.]. Nanostructured lipid carriers (NLC): A potential delivery system for bioactive food molecules. Innov Food Sci Emerg Technol 2013; 19:29-43.
[58] Ding X, Xu X, Zhao Y, [et al.]. Tumor targeted nanostructured lipid carrier co-delivering paclitaxel and indocyanine green for laser triggered synergetic therapy of cancer. RSC Adv 2017; 7, 35086-35095.
[59] Dong X, Wang W, Qu H, [et al.]. Targeted delivery of doxorubicin and vincristine to lymph cancer: evaluation of novel nanostructured lipid carriers in vitro and in vivo. Drug Deliv 2016; 23(4):1374-8.
[60] Shi Q, Zhang L, Liu M, [et al.]. Reversion of multidrug resistance by a pH-responsive cyclodextrin-derived nanomedicine in drug resistant cancer cells. Biomaterials 2015; 67:169-82.
[61] Dai Z, Yao Q, Zhu L. MMP2-Sensitive PEG-Lipid Copolymers: A New Type of Tumor-Targeted P-Glycoprotein Inhibitor. ACS Appl Mater Interfaces 2016; 8(20):12661-73.
[62] Yin Q, Shen J, Zhang Z, [et al.]. Multifunctional nanoparticles improve therapeutic effect for breast cancer by simultaneously antagonizing multiple mechanisms of multidrug resistance. Biomacromolecules 2013; 14(7):2242-52.
[63] Byeon Y, Lee JW, Choi WS, [et al.]. CD44-targeting PLGA nanoparticles incorporating paclitaxel and FAK siRNA overcome chemoresistance in epithelial ovarian cancer. Cancer Res 2018; 78(21):6247-6256.
[64] Tang X, Liang Y, Feng X, [et al.]. Co-delivery of docetaxel and Poloxamer 235 by PLGA-TPGS nanoparticles for breast cancer treatment. Mater Sci Eng C Mater Biol Appl 2015; 49:348-355.
[65] U.S. National Library of Medicine, https://beta.clinicaltrials.gov/study/NCT01652079?patient=NCT01652079&locStr=&distance=0&aggFilters=status:act com not rec (accessed December 26, 2021).
[66] U.S. National Library of Medicine, https://beta.clinicaltrials.gov/study/NCT03531827?patient=NCT03531827&locStr=&distance=0&aggFilters=status:act com not rec (accessed December 26, 2021).
[67] U.S. National Library of Medicine, https://beta.clinicaltrials.gov/study/NCT04669002?patient=NCT04669002&locStr=&distance=0&aggFilters=status:act com not rec (accessed December 26, 2021).
[68] U.S. National Library of Medicine, https://beta.clinicaltrials.gov/study/NCT03942068?patient=NCT03942068&locStr=&distance=0 (accessed December 26, 2021).
[69] U.S. National Library of Medicine, https://beta.clinicaltrials.gov/study/NCT00499252?patient=NCT00499252&locStr=&distance=0 (accessed December 26, 2021).
[70] U.S. National Library of Medicine, https://beta.clinicaltrials.gov/study/NCT00466960?patient=NCT00466960&locStr=&distance=0 (accessed December 26, 2021).
[71] U.S. National Library of Medicine, https://beta.clinicaltrials.gov/study/NCT00046514?patient=NCT00046514&locStr=&distance=0 (accessed December 26, 2021).
[72] U.S. National Library of Medicine, https://beta.clinicaltrials.gov/study/NCT01336062?patient=NCT01336062&locStr=&distance=0 (accessed December 26, 2021).
[73] U.S. National Library of Medicine, https://beta.clinicaltrials.gov/study/NCT01812746?patient=NCT01812746&locStr=&distance=0 (accessed December 26,

2021).
[74] U.S. National Library of Medicine, https://beta.clinicaltrials.gov/study/NCT03742713?patient=NCT03742713&locStr=&distance=0 (accessed December 26, 2021).
[75] U.S. National Library of Medicine, https://beta.clinicaltrials.gov/study/NCT04753216?patient=NCT04753216&locStr=&distance=0 (accessed December 26, 2021).
[76] U.S. National Library of Medicine, https://beta.clinicaltrials.gov/study/NCT01702129?patient=NCT01702129&locStr=&distance=0 (accessed December 26, 2021).
[77] Joshi AV Machine learning and artificial intelligence. [A:] Springer Nature, Switzerland 2020.
[78] Jiang F, Jiang Y, Zhi H, [et al.]. Artificial intelligence in healthcare: past, present and future. Stroke Vasc Neurol. 2017; 2(4):230-243.
[79] Topalovic M, Das N, Burgel P-R, [et al.]. Artificial intelligence outperforms pulmonologists in the interpretation of pulmonary function tests. Eur Respir J 2019; 53(4):1801660.
[80] Lewis SJ, Gandomkar Z, Brennan PC. Artificial Intelligence in medical imaging practice: looking to the future. J Med Radiat Sci. 2019; 66(4):292-295.
[81] Gore JC. Artificial intelligence in medical imaging. Magn Reson Imaging 2020; 68:A1-A4.
[82] Bera K, Schalper KA, Rimm DL, [et al.]. Artificial intelligence in digital pathology - new tools for diagnosis and precision oncology. Nat Rev Clin Oncol. 2019; 16(11):703-715.
[83] Parwani AV. Next generation diagnostic pathology: use of digital pathology and artificial intelligence tools to augment a pathological diagnosis. Diagn Pathol 2019;14(1):138.
[84] Pokhriyal R, Hariprasad R, Kumar L, [et al.]. Chemotherapy Resistance in Advanced Ovarian Cancer Patients. Biomark Cancer 11:1179299X19860815.
[85] Kigawa J. New strategy for overcoming resistance to chemotherapy of ovarian cancer. Yonago Acta Med 2013; 56(2):43-50.
[86] Robinson DR, Wu Y-M, Lonigro RJ, [et al.]. Integrative clinical genomics of metastatic cancer. Nature; 548(7667):297-303.
[87] Civita P, Franceschi S, Aretini P, [et al.]. Laser Capture Microdissection and RNA-Seq Analysis: High Sensitivity Approaches to Explain Histopathological Heterogeneity in Human Glioblastoma FFPE Archived Tissues. Front Oncol 2019; 9:482.
[88] Eswaran J, Horvath A, Godbole S, [et al.]. RNA sequencing of cancer reveals novel splicing alterations. Sci Rep 2013; 3:1689.
[89] Menden MP, Wang D, Mason MJ, [et al.]. Community assessment to advance computational prediction of cancer drug combinations in a pharmacogenomic screen. Nat Commun 2019; 10(1):2674.
[90] Russell SJ, Norvig P Artificial intelligence: a modern approach. [A:] Pearson Series in Artifical Intelligence. [ed]. Pearson College Div, USA 2020.
[91] Koza J.R., Bennett F.H., Andre D., Keane M.A. Automated Design of Both the Topology and Sizing of Analog Electrical Circuits Using Genetic Programming. Gero J.S., Sudweeks F [ed]. Artificial Intelligence in Design '96. Springer, Dordrecht 1996.
[92] Hazai E, Hazai I, Ragueneau-Majlessi I, [et al.]. Predicting substrates of the human breast cancer resistance protein using a support vector machine method. BMC Bioinformatics 2013; 14:130.
[93] Huang C, Mezencev R, McDonald JF, [et al.]. Open source machine-learning algorithms for the prediction of optimal cancer drug therapies. PLoS One 2017; 12(10):e0186906.
[94] Costello JC, Heiser LM, Georgii E, [et al.]. A community effort to assess and improve drug sensitivity prediction algorithms. Nat Biotechnol 2014; 32(12):1202-12.
[95] Gönen M, Margolin AA. Drug susceptibility prediction against a panel of drugs using kernelized Bayesian multitask learning. Bioinformatics 2014;30(17):i556-63.
[96] Iorio F, Knijnenburg TA, Vis DJ, [et al.]. A Landscape of Pharmacogenomic Interactions in Cancer. Cell 2016; 166(3):740-754.
[97] Cortés-Ciriano I, van Westen GJP, Bouvier G, [et al.]. Improved large-scale prediction of growth inhibition patterns using the NCI60 cancer cell line panel. Bioinformatics 2016; 32(1):85-95.
[98] Naulaerts S, Dang CC, Ballester PJ, Precision and recall oncology: combining multiple gene mutations for improved identification of drug-sensitive tumours. Oncotarget 2017; 8(57):97025-97040.
[99] Gayvert KM, Aly O, Platt J, [et al.]. A Computational Approach for Identifying Synergistic Drug Combinations. PLoS Comput Biol 2017; 13(1):e1005308.
[100] Sharma A, Rani R. Ensembled machine learning framework for drug sensitivity prediction. IET Syst Biol 2020; 14(1):39-46.
[101] Menden MP, Iorio F, Garnett M, [et al.]. Machine learning prediction of cancer cell sensitivity to drugs based on genomic and chemical properties. PLoS One2013; 8(4):e61318.
[102] Schmidhuber J. Deep learning in neural networks: an

overview. Neural Netw 2020; 131:251-275.
[103] LeCun Y, Bengio Y, Hinton G. Deep learning. Nature 2015; 521(7553):436-44.
[104] Goh GB, Hodas NO, Vishnu A. Deep learning for computational chemistry. J Comput Chem 2017; 38:1291–1307.
[105] Koutsoukas A. Monaghan KJ, Li X, [et al.]. Deep-learning: investigating deep neural networks hyper-parameters and comparison of performance to shallow methods for modeling bioactivity data. J Cheminform 2017; 9(1):42.
[106] Goodfellow I, Bengio Y, Courville A Deep learning. [A:] Adaptive Computation and Machine Learning series [ed]. The MIT Press, USA 2016.
[107] Preuer K, Lewis RPI, Hochreiter S, [et al.]. DeepSynergy: predicting anti-cancer drug synergy with Deep Learning. Bioinformatics 2018; 34(9):1538-1546.
[108] Cortés-Ciriano I, Bender A. KekuleScope: prediction of cancer cell line sensitivity and compound potency using convolutional neural networks trained on compound images. J Cheminform 2019;11(1):41.
[109] Oskooei A, Born J, Manica M, [et al.]. PaccMann: Prediction of anticancer compound sensitivity with multi-modal attention-based neural networks. ArXiv. 2018; http://arxiv.org/abs/1811.06802.
[110] Ding MQ, Chen L, Cooper GF, [et al.]. Precision Oncology beyond Targeted Therapy: Combining Omics Data with Machine Learning Matches the Majority of Cancer Cells to Effective Therapeutics. Mol Cancer Res 2018;16(2):269-278.
[111] Li M, Wang Y, Zheng R, [et al.]. DeepDSC: A Deep Learning Method to Predict Drug Sensitivity of Cancer Cell Lines. IEEE/ACM Trans Comput Biol Bioinform 2021; 18(2):575-582.
[112] Chiu Y.-C, Chen H-IH., Zhang T, [et al.]. Predicting drug response of tumors from integrated genomic profiles by deep neural networks. BMC Med Genomics 2019; 12(Suppl 1):18.
[113] Teresa Villanueva M. Therapeutic resistance: Paradox breaking. Nat Rev Cancer 2015; 15(2):71.
[114] Patel P, Shah J. Safety and Toxicological Considerations of Nanomedicines: The Future Directions. Curr Clin Pharmacol 2017; 12(2):73-82.
[115] Dickinson AM, Godden JM, Lanovyk K, [et al.]. Assessing the Safety of Nanomedicines: A Mini Review. Appl Vitr Toxicol 2019; 5:114–122.
[116] U.S. National Library of Medicine, https://beta.clinicaltrials.gov/study/NCT04541251?patient=cancer drug resistance artificial intelligence&locStr=&distance=0 (accessed December 26, 2021).
[117] Kelly CJ, Karthikesalingam A, Suleyman M, [et al.]. Key challenges for delivering clinical impact with artificial intelligence. BMC Med 2019; 17:195.
[118] Tizhoosh HR, Pantanowitz L. Artificial Intelligence and Digital Pathology: Challenges and Opportunities. J Pathol Inform 2018; 9: 38.
[119] Gerke S, Minssen T, Cohen G. Ethical and legal challenges of artificial intelligence-driven healthcare. Artif Intell Healthc 2020; 295–336.

WORLD JOURNAL OF MEDICAL INNOVATIONS

The effect of 5-a-reductase inhibitor on apparent diffusion coefficient of MRI in the differential diagnosis of prostate cancer

Kobilnyk Yuriy[1], Mytsyk Yulian[1], Dutka Ihor[2], Pasichnyk Serhiy[1], Borzhyevskyy Oleksander[1], Dats Ihor[3], Makagonov Ihor[3], Komnatska Iryna[2], Matskevych Viktoriya[4], Borzhyevskyy Andriy[1]

[1]*Department of Urology, Danylo Halytsky Lviv National Medical University, Lviv, Ukraine.*
[2]*Medical center "Euroclinic", Lviv, Ukraine.*
[3]*Department of Radiology, Danylo Halytsky Lviv National Medical University, Lviv, Ukraine.*
[4]*Department of Radiology and Radiation medicine, Ivano-Frankivsk National Medical University, Ivano-Frankivsk, Ukraine.*

Article info

UROLOGY

Original paper

Article history:
Accepted September 21, 2021

Published online January 9, 2022

Keywords:
magnetic resonance imaging,
apparent diffusion coefficient,
prostate cancer,
5-a-reductase inhibitor,
finasteride

Abstract

Objectives. To study the effect of 5-a-reductase inhibitor on the parameter of the apparent diffusion coefficient of MRI in the differential diagnosis of prostate cancer. Material and methods. In total, the study involved 219 persons. The study included patients with histologically verified PCa and BPH, all patients before MRI and PBP were treated with 5-ARI - finasteride for lower urinary tract symptoms, 5 mg once daily for at least 4 months. The main group receiving finasteride treatment included patients of the following subgroups: 20 patients with PCa, of which 11 with clinically nonsignificant variant (nsPCa) and 9 with clinically significant variant (csPCa) of the disease and 12 patients with BPH. The comparison group included patients of the following subgroups: 102 patients with PCa, of which 23 with nsPCa, 79 with csPCa and 70 patients with BPH. In all patients MRI of the prostate (1.5 T) and biopsy were performed. Results. In patients treated with finasteride in both the subgroup with PCa and BPH, the mean ADC values were lower than in the corresponding comparison subgroups. At the same time, the statistical analysis did not reveal significant differences between the main and comparison subgroups of patients with PCa ($p > 0.05$) and between the respective subgroups of patients with nsPCa and csPCa ($p > 0.05$). In contrast, we observed significant differences between the mean values of ADC in subgroups of patients with BPH who did not receive and received finasteride treatment for lower urinary tract symptoms before MRI and biopsy: 1.16 ± 0.16 vs $0.84 \pm 0.12 \times 10^{-3}$ mm^2/s (<0.001). Conclusions. There is a link between administration of 5-ARI (finasteride) for symptoms of lower urinary tract and/or BPH, and values of ADC, which had a significant impact on the differential diagnosis between PCa and benign prostate disease using MRI.

Corresponding author. Mytsyk Yulian, Department of Urology, Lviv National Medical University, Lviv, 79000, Ukraine, +380677722806, mytsyk.yulian@gmail.com

Introduction.

Prostate cancer (PCa) is the second most common diagnosis of malignancy in men. On average, about 1.1 million cases of PCa are diagnosed worldwide each year, which is 15% of all newly diagnosed cancers [1]. In addition, PCa is the second most common cause of death in men from cancer in the world [2]. The incidence of PCa in men aged 30-74 in Europe is growing by about 10-20% every 5 years, and in the USA - more than 25%[3]. The success of the treatment of PCa largely depends on the accurate diagnosis of this disease. With the introduction into clinical practice of active surveillance tactics in selected patients with very low and low risk PCa (ISPU 1, GS 6), accurate stratification into one group or another based on pre-op research methods is crucial to avoid over-treatment of patients in this category.[4-6]. However, given the above data and despite existing screening methods and diagnostic algorithms, the detection of PCa is still a serious and unresolved clinical problem.[7-9]. Significant shortcomings in the methods of diagnosis and screening of this pathology is a disease which in 44.7% of cases is detected in the late stages (III-IV), when radical treatment is no longer indicated [9]. In turn, overdiagnosis often leads to overt treatment of PCa, for example, when patients of very low and low risk (with a small localized tumor with a high degree of differentiation - 6 points on the Gleason scale) undergoes highly traumatic surgery with potentially disabling and minor complications [10]. According to numerous current studies, cross-sectional screening methods such as multidetector spiral contrast-enhanced CT and contrast-enhanced MRI play a leading role in the detection and local staging of cancer. High efficiency of MRI in local stage of PCa is proved: MRI had high accuracy of diagnosis of invasion of seminal vesicles according to histopathology data, which added value to clinical models of prediction based on Partin tables [11]. As previously demonstrated, apparent diffusion coefficient (ADC) of the of diffusion-weighted MRI images (DWI) is a valuable tool for non-invasive differential diagnosis of PCa with benign prostatic lesions [12]. It is known that treatment with 5-α-reductase inhibitors (5-ARI) for benign prostatic hyperplasia due to its mechanism of action has a significant effect on prostate tissue, causing apoptosis of epithelial cells, which leads to a decrease in prostate size, especially with prolonged use. In addition, according to recent data, finasteride has some effect on prostate vascularization [13.14]. In this context, an important and insufficiently studied issue is the impact on the detection and differentiation of PCa with potential imaging markers of MRI in patients previously treated with 5-ARI inhibitors for benign prostatic hyperplasia (BPH). Because, in clinical practice, it is not uncommon for a patient to be treated with 5-ARI for lower urinary tract symptoms and/or BPH before being diagnosed with PCa, it has been suggested that the use of these agents may affect ADC in prostate MRI and may be important in the detection and differential diagnosis of PCa.

Objectives.

To study the effect of 5-a-reductase inhibitor on the parameter of the ADC of MRI in the differential diagnosis of prostate cancer.

Material and methods.

Multiparametric MRI of the prostate was performed using a Signa HDxt 1.5T (General Electric®, USA) and an eight-channel coil based on Euroclinic medical centers (Lviv, Ukraine). Patients did not eat 5 hours before the examination. In the evening before the examination, a micro-enema (Microlax or similar) was used in all cases. Prostate PI-RADS version 2.1 recommended by the American College of Radiology and Clinical Guidelines was used to assess the results of prostate MRI. From the maps of diffusion-weighted images, which were automatically generated on the workstation, their quantitative parameter – ADC was calculated, which was used as a measure of diffusion of healthy and affected tissues. In total, the study involved 219 persons. In order to create the main group, the study included patients with histologically verified PCa and BPH, all patients before MRI and PBP were treated with 5-ARI - finasteride for lower urinary tract symptoms, 5 mg once daily for at least 4 months (average duration of treatment - 0.6 ± 0.9 years). We analyzed the indicators of ADC in subgroups of patients with PCa and BPH who were not treated with 5-ARI (comparison group), as well as in 15 healthy individuals without prostate pathology (control group). In the main group of patients when assessing the level of PSA used a factor of × 2, due to the ability of finasteride to reduce approximately 2 times the level of this marker. Baseline clinical data (mean age, mean prostate size, mean PSA levels after application of the coefficient) of the main and comparison groups were comparable and did not differ significantly. Thus, the main group receiving finasteride treatment included patients of the following subgroups: 20 patients with PCa, of which 11 with clinically nonsignificant variant (nsPCa) and 9 with clinically significant variant (csPCa) of the disease and 12 patients with BPH. The comparison group included patients of the following

subgroups: 102 patients with PCa, of which 23 with nsPCa, 79 with csPCa and 70 patients with BPH.

Results.

When analyzing the mean values of ADC in the studied groups and subgroups of patients, the following data were obtained: in patients treated with finasteride in both the subgroup with PCa and BPH, the mean ADC values were lower than in the corresponding comparison subgroups. At the same time, the statistical analysis did not reveal significant differences between the main and comparison subgroups of patients with PCa (p> 0.05) and between the respective subgroups of patients with nsPCa and csPCa (p> 0.05). In contrast, we observed significant differences between the mean values of ADC in subgroups of patients with BPH who did not receive and received finasteride treatment for lower urinary tract symptoms before MRI and biopsy: 1.16 ± 0.16 vs 0.84 ± 0.12× 10^{-3} mm^2/s (<0.001). Moreover, there were no significant differences in the mean values of ADC between the subgroups of patients with BPH who received 5-ARI, and subgroups of patients with nsPCa and csPCa who did not received finasteride (p>0.05), as well as with a subgroup of patients with nsPCa who received such treatment (p>0.05); at the same time, there was a significant difference in mean ADC values compared with the subgroup of patients with csPCa who received finasteride (p=0.001). It is especially important that the value of ADC of the suspicious areas of the prostate in patients with BPH who received treatment with 5-ARI to a large extent overlap with the indicators of ADC in patients with PCa, regardless of the use of finasteride. Given the above data, it should be noted that reducing the value of ADC under the influence of treatment 5-ARI in patients with BPH will increase the score when assessing a suspicious area of the prostate according to the PI-RADS system on diffusion-weighted MRI images, which in turn will increase the frequency of unnecessary biopsies. To avoid this, we should take into account the full range of patient clinical data, including the range of PSA-based markers, to determine the indications for biopsy. In addition, it was estimated that the mean value of ADC in the subgroup of BPH patients receiving finasteride was 27.59% lower, in the subgroup with BPH without such treatment, and the ratio between this indicator in these subgroups was 1.38 (1.66 / 0.84).

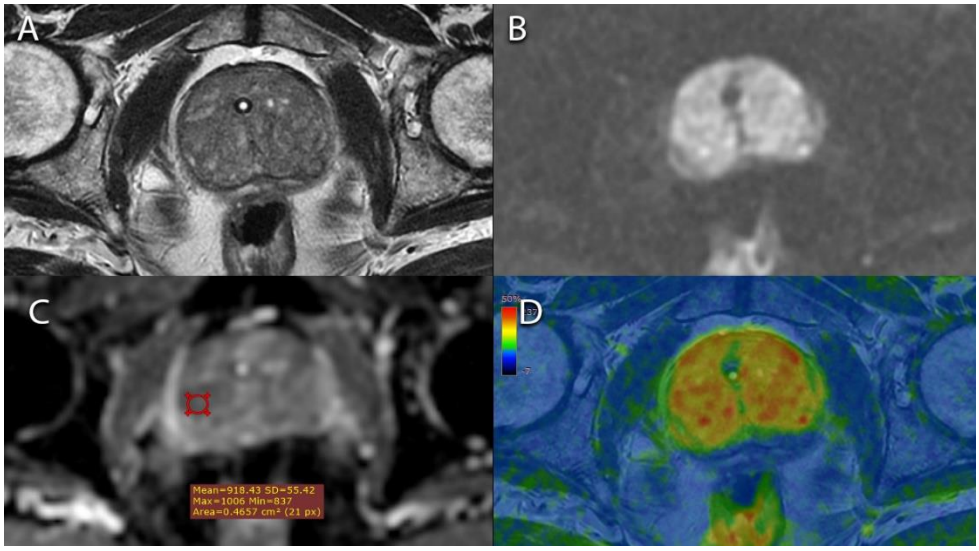

Figure 1. MRI of the prostate, axial images. A: T2-WW FRFSE; B: diffusion-weighted image (DWI), the areas of greatest restriction of diffusion have the brightest representation; C: ADC-map, ROI (red circle) is located above the zone of the greatest hypointensity of the MR signal, the ADC is 0.92 × 10^{-3} mm^2 / s; D: fusion map T2-WW and DWI, red color corresponds to the area of the greatest restriction of diffusion.

Discussion.

Our work was performed in order to study the effect of 5-a-reductase inhibitor on the parameter of the ADC of MRI in the differential diagnosis of prostate cancer. There is a lack of literature data on this topic. In a small study by Starobinets et al. (n = 17), it was reported that the increase in the homogeneity of prostate tissue in benign and malignant low-risk peripheral areas after administration of 5-ARI, reduced the variability of MR measurements after treatment. Discrimination of cancer was lower using T2-

weighted imaging, but was higher in functional MRI scores in the cohort receiving 5-ARI compared with controls, which contributed to the detection of PCa. However, a major drawback of this study was the lack of data on the transition zone of the prostate, the distinction of PCa in which is usually much more difficult compared to the peripheral zone, regardless of other factors [15]. In contrast, Kim et al. Demonstrated no such effect in the analysis of MRI data: there were no significant differences in the detection of PCa / csPCa between the 5-ARI and non-5-ARI groups (P> 0.05) [16]. In our study we found that there were no differences in the mean values of ADC between the subgroups of patients with BPH who received 5-ARI, and subgroups of patients with nsPCa and csPCa who did not received finasteride, as well as with a subgroup of patients with nsPCa who received such treatment; nevertheless, there was a significant difference in mean ADC values compared with the subgroup of patients with csPCa who received finasteride (p=0.001). We demonstrated the existence of a link between drug treatment with 5-ARI (finasteride) for symptoms of lower urinary tract and / or BPH, and values of ADC, which had a significant impact on the representation of prostate lesions on MRI images and hindered the differential diagnosis between PCa and benign prostate disease, due to the fact that the value of ADC suspicious areas of the prostate in patients with BPH who received treatment 5-ARI were superimposed with the indicators of ADC in patients with PCa, regardless of the intake of finasteride. To solve this problem, it is proposed to use a coefficient of × 1.38 when calculating the ADC value, which will allow to obtain a more accurate value of ADC for differential diagnosis with PCa.

Conclusions.

There is a link between administration of 5-ARI (finasteride) for symptoms of lower urinary tract and/or BPH, and values of ADC, which had a significant impact on the differential diagnosis between PCa and benign prostate disease using MRI.

References.

[1] Barsouk A, Padala SA, Vakiti A, Mohammed A, Saginala K, Thandra KC, et al. Epidemiology, Staging and Management of Prostate Cancer. Med Sci (Basel). 2020 Jul 20;8(3):28.

[2] Pilleron S, Soto-Perez-de-Celis E, Vignat J, Ferlay J, Soerjomataram I, Bray F, et al. Estimated global cancer incidence in the oldest adults in 2018 and projections to 2050. Int J Cancer. 2021 Feb 1; 148(3):601-8.

[3] Siegel RL, Miller KD, Jemal A. Cancer statistics, 2020. CA Cancer J Clin. 2020 Jan;70 (1):7-30.

[4] Hamdy FC, Donovan JL, Lane JA, Mason M, Metcalfe C, Holding P, et al. 10-Year Outcomes after Monitoring, Surgery, or Radiotherapy for Localized Prostate Cancer. N Engl J Med. 2016 Oct 13;375 (15):1415-24.

[5] Tosoian JJ, Mamawala M, Epstein JI, Landis P, Wolf S, Trock BJ, et al. Intermediate and Longer-Term Outcomes From a Prospective Active-Surveillance Program for Favorable-Risk Prostate Cancer. J Clin Oncol. 2015 Oct 20;33(30):3379-85.

[6] Bruinsma SM, Roobol MJ, Carroll PR, Klotz L, Pickles T, Moore CM, et al. Expert consensus document: Semantics in active surveillance for men with localized prostate cancer - results of a modified Delphi consensus procedure. Nat Rev Urol. 2017 May;14(5):312-22.

[7] Egevad L, Swanberg D, Delahunt B, Ström P, Kartasalo K, Olsson H, et al. Identification of areas of grading difficulties in prostate cancer and comparison with artificial intelligence assisted grading. Virchows Arch. 2020 Dec;477(6):777-86.

[8] Mishra SC. A discussion on controversies and ethical dilemmas in prostate cancer screening. J Med Ethics [Internet]. 2020 Jul 6. Available from: https://doi.org/10.1136/medethics-2019-105979.

[9] Brönimann S, Pradere B, Karakiewicz P, Abufaraj M, Briganti A, Shariat SF. An overview of current and emerging diagnostic, staging and prognostic markers for prostate cancer. Expert Rev Mol Diagn. 2020 Aug;20(8):841-50.

[10] Masaoka H, Ito H, Yokomizo A, Eto M, Matsuo K. Potential overtreatment among men aged 80 years and older with localized prostate cancer in Japan. Cancer Sci. 2017 Aug;108(8): 1673-80.

[11] Grivas N, Hinnen K, Jong J de, Heemsbergen W, Moonen L, Witteveen T, et al. Seminal vesicle invasion on multi-parametric magnetic resonance imaging: Correlation with histopathology. Eur J Radiol. 2018 Jan 1;98:107-12.

[12] Stabile A, Giganti F, Rosenkrantz AB, Taneja SS, Villeirs G, Gill IS, et al. Multiparametric MRI for prostate cancer diagnosis: current status and future directions. Nat Rev Urol. 2020;17(1):41-61.

[13] Khwaja MA, Nawaz G, Muhammad S, Jamil MI, Faisal M, Akhter S. The Effect of Two Weeks Preoperative Finasteride Therapy in Reducing Prostate Vascularity. J Coll Physicians Surg Pak. 2016 Mar;26(3):213-5.

[14] Bansal A, Arora A. Transurethral Resection of Prostate and Bleeding: A Prospective, Randomized, Double-Blind Placebo-Controlled Trial to See the Efficacy of Short-Term Use of Finasteride and Dutasteride on Operative Blood Loss

and Prostatic Microvessel Density. J Endourol. 2017 Sep;31(9):910-7.

[15] Starobinets O, Kurhanewicz J, Noworolski SM. Improved Multiparametric MRI Discrimination Between Low-Risk Prostate Cancer and Benign Tissues in a Small Cohort of 5-alpha Reductase Inhibitor Treated Individuals as Compared to an Untreated Cohort. NMR Biomed [Internet]. 2017 May [cited 2021 Jun 15]; 30(5). Available from: https://www.ncbi.nlm.nih.gov/pmc/articles/PMC5522750/

[16] Kim JK, Lee HJ, Hwang SI, Choe G, Kim HJ, Hong SK. The effect of 5 alpha-reductase inhibitor therapy on prostate cancer detection in the era of multi-parametric magnetic resonance imaging. Sci Rep. 2019 Nov 28;9(1):17862.

WORLD JOURNAL OF MEDICAL INNOVATIONS

MicroRNAs as Potential Biomarkers and Therapeutic Targets in Renal Cell Carcinoma

Xuanyu Chen

Department of Neuroscience & Regenerative Medicine, Medical College of Georgia at Augusta University, Augusta, Georgia, the United States of America

Article info

GENETICS

Review paper

Article history:
Accepted
December 30, 2021

Published online
January 10, 2022

Keywords:
microRNA,
renal cell carcinoma,
biomarkers

Abstract

Optimal management of patients will be guided by ideal biomarkers, which can help clinicians to implement early detection, prognosis, prediction of benefit from therapies, recurrence or progression of human cancers, although biomarkers have not yet become clinically routine, especially in renal cell carcinoma (RCC). microRNAs (miRNAs) are chemically stable and can thus be detected in a broad range of clinical samples and hence, have diagnostic and prognostic value in many human malignancies. The discovery that miRNAs function as key regulators of carcinogenesis and tumor progression has initiated extensive research in the cancer field, leading to the development of newer anti-cancer therapies. Growing studies have identified some miRNAs as promising biomarkers and therapeutic targets of RCC. This review discusses the current status of miRNAs in RCC, focusing on miRNAs as potential diagnostic, prognostic, and predictive biomarkers and their therapeutic potential.

Corresponding author. Xuanyu Chen, MD & PhD, Department of Neuroscience & Regenerative Medicine, Medical College of Georgia at Augusta University, 1120 15th Street, Rm. CA4059, Augusta, GA 30912, 706-667-4824, xuachen@augusta.edu

Introduction.

Renal cell carcinoma (RCC) is the most lethal urological malignancy with the highest mortality rate at over 30%, and the incidence of RCC is increasing by 2~4% each year [1]. In Early stage RCC confined to the kidney can be cured in approximately 90% of patients by surgery, but these rates drop substantially in patients with advanced disease [1]. Unexpectedly, 30% of RCC have advanced disease at diagnosis and 30% of patients with organ-confined RCCs will subsequently develop metastatic recurrence resistant to conventional cytotoxic chemotherapy and die of their disease [2]. Recently, an improved understanding of genetic changes in RCC has produced pharmaceuticals based on specific molecular targets. However, eventually the vast majority of treated patients with mRCC develop progressive disease due to acquired resistance or for other reasons. Hence, biomarkers for early detection, follow-up and predicting treatment efficacy and new strategies to treat this disease are urgently needed. Until now, DNA, RNA and protein profiles of cancer research have not fully elucidated the pathogenesis of RCC. miRNA has been identified as a crucial regulator of human cancer pathogenesis from initiation to metastasis [3-7], which suggests that miRNA has therapeutic potential against RCC. Intriguingly, growing evidence have showed that miRNAs are chemically stable

and can be detected in a broad range of body fluids and hence, have diagnostic and prognostic value in many malignancies [8-11]. This review summarizes miRNAs potentially serving as biomarkers and therapeutic targets for RCC.

Sorting out small RNAs.

Small RNAs are short (approximately 18~30 nts), non-coding RNA molecules that can regulate gene expression in both the cytoplasm and the nucleus via post-transcriptional gene silencing (PTGS), chromatin-dependent gene silencing (CDGS) or RNA activation (RNAa) [12]. Endogenous small RNAs are diverse and comprise miRNAs, small interfering RNAs (siRNAs), and piwi-interacting RNAs (piRNAs) [13]. miRNAs in association with Argonaute (AGO) and GW182 proteins, forming the RNA-induced silencing complex (RISC), mediate fine tuning of gene expression and are involved in various biological key processes. Each miRNA is predicted to target hundreds of mRNAs thus influencing key regulatory mechanisms of cells. Consequently, deregulated miRNA expression has been described to contribute to the initiation and progression of human cancer and other diseases [14]. SiRNAs are oligonucleotides of around 21~23 nts in length. SiRNAs, generated from double-stranded RNAs (dsRNAs), trigger sequence-specific mRNA decay also known as RNA interference (RNAi). The third developmentally vital class of small RNAs is the piwi-interacting (pi) RNAs, which play a role in the formation of the germ line. In mammals, these ~27 nt ssRNAs are expressed in the reproductive organs, mainly the testis [15]. Research has indicated that small RNAs play important roles in cellular processes such as cell differentiation, growth, migration, apoptosis, metabolism and defense. Accordingly, miRNAs as a representative of small RNAs are critical regulators of development, physiology and disease [12].

Differential expression of miRNAs in RCC.

In order to develop further understanding of the molecular mechanism involved in the pathogenesis of RCC, increasing groups investigate miRNA expression profiles in the RCC tissues [16-22] and serum [23, 24]. These studies suggest the miRNA expression profiles or even single miRNA could become useful biomarkers for RCC diagnosis, prognosis, and treatment optimization. The first study in this setting was done by Gottardo et al. They reported 4 human miRNAs (miR-28, miR-185, miR-27, and let-7f-2) significantly up-regulated and no down-regulated through studying the expression of 248 miRNA clusters (161 human, 84 mouse, and 3 Arabidopsis) in a set of 27 kidney specimens [16]. However, the most of latter research showed that dysregulated miRNAs in RCC are reduced. These altered miRNAs in RCC in each study are not consistent. The inconsistencies may be caused by the different discovery microarray platforms, samples themselves, experimental conditions, and so on [16-20, 22]. Clear cell RCC (ccRCC), the most common subtype of RCC, originates from the epithelial cells of the proximal tubulus of the kidney. Recently, through analyzing the miRNA expression profiles of 10 ccRCC-derived cell lines and the renal proximal tubular epithelial cells (PTECs), Gerben et al. [25] reported 15 miRNAs were markedly reduced and 8 miRNAs increased in ccRCC cells. Some of deregulated miRNAs in ccRCC cells were consistently reported in ccRCC tissues, such as the miR-200 family and miR-205 [25, 26].

miRNAs as biomarkers in RCC.

miRNAs as diagnostic biomarkers in RCC.

Identification of stable biomarkers for diagnosis remains a major challenge in cancer research, especially RCC. Following the discovery of the existence of circulating miRNAs in the plasma and serum of cancer patients [8-10], growing evidence show that circulating miRNAs are promising biomarkers for noninvasive diagnosis in various tumor entities. Recent studies have suggested that the deregulated miRNA expression profiles and the identification of their targets in RCC offer the opportunity to develop new diagnostic strategies. The miRNA expression profiles may be helpful 1) to distinguish normal from malignant tissues, 2) to identify the tissue of origin in poorly differentiated tumors or tumors of unknown origin and 3) to differentiate tumors from the same organ with different histology [27, 28]. miRNA profiles offer some important potential advantages over standard mRNA or other protein-based profiles. miRNAs have been shown to be very stable in tissues and biological fluids, including serum, plasma, stool and urine and are protected from endogenous RNase by virtue of their small size and perhaps by packaging within exosomes [9]. Jung et al.[29] observed the significant distinction of miRNA expression profiles between ccRCC and normal kidney tissues. Their further investigation showed that combination of miR-141 and miR-155 had 97% accuracy for identification of ccRCC. miR-141 or miR-200c alone could yield 93% or 94% accuracy in discriminating ccRCC tissues from normal kidney tissues, respectively. This is the first ccRCC/normal classifier constructed with miRNAs. Despite each type of RCC has distinct histological appearance, many cases in which the morphological criteria are not conclusive.

As RCC subtype is a major determinant for their prognosis and the sensitivity to targeted therapies, accurate classification is very important. Some reports have showed the ability of miRNAs to distinguish between RCC subtypes [30-33]. Petillo et al.[30] showed the overexpression of miR-424 and miR-203 in ccRCC relative to pRCC, as well as the lower expression of miR-203 in the benign oncocytomas (where it is underexpressed relative to normal kidney) than the malignant chRCC (where it is overexpressed relative to normal kidney). A high degree of similarity in microRNA expression between ccRCC and pRCC and between chRCC and oncocytoma, and a lower degree of similarity between these pairs were reported [31, 32]. Fridman et al. [32] defined a two-step decision-tree classifier that used expression levels of six microRNAs: the first step uses expression levels of miR-210 and miR-221 to distinguish between the two pairs of subtypes; the second step uses either miR-200c with miR-139-5p to identify oncocytoma from chRCC, or miR-31 with miR-126 to identify ccRCC from pRCC. Identification sensitivity of the classifier was 94% for oncocytoma, 86% for chRCC, 94% for ccRCC, and 100% for pRCC, with overall accuracy of 93% [32]. Another study provided a stepwise decision tree to distinguish between normal and each of the subtypes in a maximum of four steps based on miRNA microarray analysis [31]. The system had a sensitivity of 97% in distinguishing normal from RCC, 100% for ccRCC subtype, 97% for pRCC subtype, and 100% accuracy in distinguishing oncocytoma from chRCC subtype. This system was cross-validated and showed an accuracy of about 90%. The classification system provided accurate classification (an accuracy of about 98%) between any given subtype pair. miR-21 is up-regulated in a variety of cancers, including RCC [33-37]. Expression of miR-21 is higher in both ccRCC and pRCC subtypes than that of healthy kidney and both chRCC and oncocytoma [33, 38]. Furthermore, miR-21 could distinguish ccRCC and pRCC subtypes from chRCC and oncocytoma with the sensitivity of 83% and specificity 90% [33]. Growing evidence are available on circulating miRNAs as biomarkers of RCC. Wulfken et al.[39] reported that miR-1233 was upregulated in RCC tissue and serum, and serum miR-1233 could detect RCC with 77.4% sensitivity and 37.6% specificity. Redova et al. [40] showed that combination of serum miR-378 (overexpression in RCC patients) and miR-451 (downexpression in RCC patients) could yields a ROC curve area of 0.86 with 81% sensitivity and 83% specificity in discriminating RCC patients from healthy controls. Wang et al. [41] demonstrated that the panel of 5 serum miRNAs (upregulated miR-193a-3p, miR-362 and miR-572, and downregulated miR-28-5p and miR-378 in RCC) could serve as an early detection marker for RCC with the accuracy of 0.807. Theoretically, urinary miRNAs may be filtered and excreted by, or directly from, the kidney and/or urinary tract. Therefore, it is possible that urinary miRNAs are promising noninvasive biomarkers of RCC. Melkonyan et al. [23] detected 22 different urinary miRNAs, but none was kidney-specific. Hanke et al. [24] showed that analysis of miRNA species in single urine samples revealed the miRNA ratios miR-126 : miR-152 and miR-182 : miR-152 were significantly elevated in urine of urothelial bladder cancer patients compared with urine of healthy donors and patients with urinary tract infections, enabling a separation of tumor patients from the control groups. The expression of miR-15 and miR-15a in urine from patients with RCC was significantly higher than that of oncocytoma and urinary tract inflammation [42, 43]. More recently, the panel of urinary miR-122, miR-1271 and miR-15b was identified as urinary biomarkers of ccRCC [44]. Thus, these studies have revealed a new possibility in the development of non-invasive investigation of RCC by using specific urinary miRNAs as diagnostic biomarkers.

miRNAs as prognostic biomarkers in RCC.

Therapeutic decision-making of RCC largely depends on defining the prognosis. Currently, tumor–node–metastasis (TNM) stage, Fuhrman nuclear grade, and RCC subtype are used to evaluate the prognosis of RCC. However, all prognostic models are not yet optimal [45]. Recent studies showed that individual miRNAs have prognostic relevance in RCC. High miR-21 expression levels in RCC are associated with late stages, higher tumor grades, larger tumor size, and shorter disease-free survival (DFS) and overall survival (OR) [33, 36]. Petillo et al.[30] investigated miRNA expression profiles that distinguish ccRCC cases with poor vs. good prognosis. This study showed S-has-miR-32 was over-expressed in poor prognosis cases relative to good prognosis cases. The significantly lower level of miR-106b in RCC patients who developed metastasis has been observed [46]. Wang et al. showed that miR-100 was overexpressed in RCC and associated with poor prognosis in patients with RCC [47]. However, several studies have consistently identified that miR-100 was downregulated in RCC [21, 48]. These miRNAs may be incorporated into existing models to improve their accuracy after validation on a larger group of patients. To date, there are very few indicators that can predict which RCC patients will develop a recurrence. RCC patients who developed a recurrence had a significant increase in hypermethylated miR-9-1, miR-9-3 and miR-124-3 in their primary tumor [49, 50]. What's more, methylation of miR-9-3 and miR-124-3 was significantly associated with an

increased risk of recurrence and high methylation levels of either miR-9-1 or miR-9-3 resulted in a significant, nearly 30-month decrease in recurrence-free survival time (miR-9-1 and miR-9-3) [49, 50]. Tumor metastasis and grade was positively correlated with methylation of miR-124-3 in RCC [50]. These results suggested miR-9 and miR-124-3 function as a tumor suppressor for RCC tumorigenesis, and methylation status of miR-9-1, miR-9-3 and miR-124-3 could be a biomarker for a poor prognosis due to the development of metastatic recurrence [49]. Gleadle and colleagues showed, for the first time, the effect of the VHL tumor suppressor gene on miRNA expression in RCC [51]. A significant increase in miR-210 expression was observed in the tumor tissue by some studies. MiR-210 levels also showed a correlation with a HIF-regulated mRNA, carbonic anhydrase IX (CAIX), and with VHL mutation or promoter methylation. The expression of miR-210 was shown to be a prognostic marker as its expression correlated with sarcomatoid changes, Fuhrman nuclear grade, lymph node metastasis, patient survival [51-53]. Moreover, miR-210 could effectively distinguish malignant from non-malignant tissues with a classification accuracy rate of 88% [54].

miRNAs as predictive biomarkers in RCC.

Metastatic dissemination is the most significant prognostic factor for patients with RCC. Moreover, predicting recurrences early can improve patient outcome. Preliminary evidence suggests that miRNAs can serve as predictive markers and indicators of cancer metastasis and relapse. Recent studies suggest that miRNAs dysregulated in metastatic RCC may be decreased [55-57]. Heinzelmann et al. found that 33 miRNAs altered in metastatic RCC compared with non-metastatic RCC are all downregulated, 20 out of which were associated with progression-free survival [55]. In another research, 56 miRNAs downregulated and only 9 miRNAs upregulated in metastatic RCC were reported [56]. Notably, miR-10b, miR-27b, miR-26a/b, miR-29a, miR-181a, miR-151-5p, miR-130a, let-7 family and miR-30 family were consistently decreased. Moreover, many downregulated miRNAs (miR-204, miR-200a/b, miR-215, miR-26a, miR-10b, miR-196a and miR-194) in RCC were further downregulated in metastatic RCC. Even some overexpression miRNAs (miR-16, miR-155, miR-122 and let-7f/g) in RCC were decreased in metastatic RCC. In addition, miRNAs (miR-10b, miR-126, miR-196a, miR-204, miR-215, miR-192 and miR-194) were decreased in metastatic RCC compared with matched primary tumors [57]. Lower expression of miR-215 is related to RCC patients with short disease-free survival time [58]. Upregulation of miR-106b and miR-122 and downregulation of miR-514 in RCC were significantly lower in tumors of patients who developed metastasis compared with non-metastatic tumors [46, 54]. In relation to the TNM stage of RCCs, a general tendency for miR-106b, miR-122 and miR-708 levels to decrease from earlier stages towards advanced was observed [5, 46, 54]. Further investigation showed that miR-122 and miR-514 were related to RCC relapse [54]. To identify miRNA signature of tumor relapse in RCC patients after nephrectomy, Slaby et al. [59] analyzed miRNA expression profiles in tumor tissues of RCC patients with relapse or relapse-free and found 20 miRNAs were upregulated and 44 miRNAs were downregulated in RCC patients developing early recurrence. Many of these dysregulated miRNAs, including miR-143, miR-10b, miR-26a, miR-195, miR-145 and miR-126, are also associated with metastasis [55-57]. Higher miR-127-3p, miR-145 and miR-126 were significantly correlated with relapse-free survival [59]. Accordingly, miRNAs in RCC were gradually regressed during tumor progression. These results suggest miRNAs may be potential predictive marker of early metastasis and relapse after nephrectomy in RCC patients. Therapy targeted at the vascular endothelial growth factor (VEGF) and mammalian target of rapamycin (mTOR) pathways has been the standard of care in metastatic renal cell carcinoma (mRCC). At present, seven such agents have been approved for the treatment of mRCC, including sunitinib, sorafenib, pazopanib, axitinib, temsirolimus, everolimus, and bevacizumab in combination with IFNa. Existing investigation shows that most patients with mRCC gain significant benefit from these drugs. However, 11-29% of patients exhibit progressive disease during treatment with VEGF target therapy [60]. Furthermore, eventually the vast majority of treated patients acquire resistance. Thus, biomarkers are urgently needed to predict drug response and monitor therapeutic response. Examining miRNA expression in the peripheral leukocytes of 38 patients with advanced RCC receiving sunitinib, Gamez-Pozo et al. recently identified 28 miRNAs associated with poor response and 23 miRNAs associated with prolonged response to sunitinib [60]. The predictive models established according to miRNA expression could effectively distinguish the prolonged response group from the poor response group [60].The prolonged response group's median time to progression and overall survival (OS) is significantly longer (14 and 24 months) than the poor response group's (3.5 and 8.5 months) [60]. More recently, miRNA expression in cytoreductive nephrectomy specimens of 20 patients with metastatic ccRCC receiving sunitinib treatment was assessed using a quantitative miRNA PCR-primer array platform [61].

The miR-141 expression in poor responders was markedly lower than that in good responders, and miR-141 down-regulation was related to the presence of sarcomatoid features associated with a poor prognosis [61]. Through enhancing ZEB1/2 protein and reducing E-cadherin, downregulation of miR-141 regulated the epithelial-to-mesenchymal transition (EMT), which contributes to treatment resistance and metastases [61-63]. Moreover, miR-141 inhibited the p38α pathway and subsequently increased the sensitivity to reactive oxygen species (ROS)-producing therapeutic agents in ovarian cancer [64]. Collectively, these results indicate miRNAs may be used as predictive biomarkers for therapy response in the future.

miRNAs as therapeutic targets in RCC.

miRNAs are important biological regulators and therefore can serve as novel therapeutic targets for cancer. For miRNAs with oncogenic capabilities, potential therapies include anti-miRNA oligonucleotides, miRNA sponges, miRNA masking, and small molecule inhibitor. Inhibition of miR-122, a liver-specific miRNA contributing to the replication of HCV and hepatocellular carcinoma, significantly repressed HCV replication [65]. For tumor-suppressor miRNAs, restoring suppressor miRNAs by forced expression of those miRNAs may be a useful strategy [66]. Furthermore, miRNAs could enhance response to standard cancer therapies. There are several promising potential therapeutic miRNA candidates in RCC.

Inhibition of oncogenic miRNAs.

miR-21 is up-regulated in a variety of cancers, including RCC [33-37]. Creating a transgenic mouse carrying miR-21 was reported by Frank Slack and co-workers [67]. Genetic machinery, inserted along with miR-21, allowed them to turn miR-21expression on or off by changing the animals' diet. In Slack's experimental model, when they turned on miR-21 expression, the animals quickly developed a pre–B-cell lymphoid malignancy. When the expression of miR-21 was turned off, the animals' tumors completely regressed within a few days. miR-155 is regarded as an oncogenic miRNA on the basis of the finding that B cell malignancies occurred in miR-155-overexpressing transgenic mice [68]. miR-21 and miR-155 have repeatedly been identified through microarray profiling as up-regulated in RCC relative to normal kidney tissue. Knockdown of miR-21 in ccRCC suppressed cell proliferation, migration and invasion, and promoted cell apoptosis [34-37]. Further investigation showed that miR-21 regulated multiply genes, including PTEN/Akt/TORC1, fas ligand (FASL), metalloproteinase inhibitor 3 (TIMP3), p21 and p38 MAP kinases, cyclin E2, transcription factor TCF21 [34-37]. These studies supported an interesting hypothesis that miR-21 and miR-155 may have oncogenic function in RCC. Abrogated ubiquitin-mediated degradation due to VHL inactivation in more than 70% of ccRCC causes accumulation of HIF1α and HIF2α, which increases expression of VEGF and glucose transporter type 1 (GLUT1), consequently promoting angiogenesis and metabolic disorders [6]. It has been well documented that miR-210 could be induced under hypoxic conditions and modulated by HIFs in various solid cancers, including ccRCC [6]. However, the biological significance of miR-210 in RCC is controversial. miR-210 overexpression caused multipolar spindle formation and aneuploidy through centrosome amplification, and reduced cell viability via G2/M-phase arrest in RCC cells [6]. Inhibition of miR-210 did not alter RCC cell viability and cycle [6]. In contrast, Redova et al. reported that inhibition of miR-210 leaded to the decrease of cell viability via G2/M-phase arrest, cell migration and invasion [69]. Thus, further studies regarding the role of miR-210 in RCC in vitro and in vivo is needed. Despite several studies have consistently identified that miR-34a was upregulated in RCC [19, 21, 48], Vogt et al. found inactivation of miR-34a by CpG methylation in 58% RCC [70]. An increase of miR-34a expression during rat oxidative stress-induced renal carcinogenesis and a significant decrease of cellular proliferation in RCC cells after knockdown of miR-34a were observed [71]. In contrast, Yamamura and coworkers showed that miR-34a suppressed cell growth and invasion in RCC cells by indirectly modulating RhoA via targeting c-Myc and downregulating c-Myc–P-TEFb complex [7].The effects of miR-17-92 over expression have been examined in multiple animal models, human cancers, and cell culture systems for its ability to regulate a number of cellular processes that favor malignant transformation [72, 73]. Chow et al.[74] showed that the miR-17-92 cluster was also over expressed in RCC and had an important role in promoting tumor cell proliferation. If the levels of these miRNAs could be manipulated in vivo, effects relevant for RCC progression and treatment efficacy could be obtained.

Restoration of tumor suppressor miRNAs.

The miRNA microarray analysis has revealed that most of miRNAs deregulated in RCC tissues and cell lines were reduced. Notably, the miR-200 family consisting of five members, miR-200a/miR-200b/ miR-429 and miR-200c/miR-141, localized in 1p36.33 and 12p13.31 respectively, were all significantly downregulated in RCC [19, 25, 26]. Furthermore, among the miRNAs differentially expressed in

ccRCC, miR-141 and miR-200c are the most significantly down-regulated [20, 22, 25, 26, 29, 46]. Both miR-200c and miR-141 are mechanistically associated with the process of epithelial-mesenchymal transition (EMT). EMT is characterized by a decrease of E-cadherin, loss of cell adhesion, and increased cell motility leading to promotion of metastatic behavior of cancer cells (including RCC) [75]. Zinc-finger E-box binding homeobox 1(ZEB1) is a crucial inducer of EMT in various human tumors directly suppressing transcription of miR-141 and miR-200c, which strongly activate epithelial differentiation in pancreatic, colorectal and breast cancer cells [76]. Nakada et al. found that over-expression of miR-141 and miR-200c caused down-regulation of ZEB2 and up-regulation of E-cadherin in two renal carcinoma cell lines, ACHN and 786-O [20]. ZEB2 was identified as the common target of miR-141 and miR-200c. It already has been reported that ZEB2 up-regulated in a variety of human carcinomas may function as a transcriptional repressor for E-cadherin [75]. More recently, Berkers et al. and Yu et al. [61, 77] showed that overexpression of miR-141 in RCC cells reversed EMT and inhibited cell growth in normoxic and hypoxic conditions by targeting CDC25B. BY using xenograft orthotopic implantations, Chen et al.[78] demonstrated that miR-141 effectively suppressed tumor growth, local invasion, and metastatic colonization by targeting EphA2. On the basis of these data, miR-141 and miR-200c may have a tumor suppressor function in cancer cells and could be a promising treatment in anticancer therapy [22]. Other downregulated miRNAs in RCC also contribute to the development of RCC. Through inhibiting the proto-oncogenic SFKs, miR-205 overexpression in RCC cells markedly suppressed cell growth, migration and invasion, and induced cell apoptosis in vitro and in vivo [4]. miR-708 also had similar role in RCC by targeting survivin, ZEB2 and BMI1 [5]. Moreover, intratumoral delivery of synthetic miR-708 oligonucleotides successfully inhibited tumorigenicity in established renal tumor xenografts [5]. Similar results were also seen in miR-508-3p, miR-509-3p [79], miR-99a [80], miR-145 [81], miR-1826 [82], miR-584 [83], miR-30d [84], miR-138 [85], miR-1285 [26], miR-135a [86]. In addition to angiogenesis related to the loss of VHL gene in ccRCC as a source of nutrients for tumor growth, autophagy that eliminates cellular defective organelles and proteins and recycles nutrients for survival also provides nutrients necessary. Mikhaylova and co-workers [3] demonstrated that RCC cell growth depended on LC3B-mediated autophagy and VHL gene induced the expression of miR-204 in RCC cells, which suppressed tumor growth through inhibition of LC3B-mediated autophagy.

Enhancing of responsiveness of tumors to standard therapy.

Schickel et al. [87] showed that miR-200c affected sensitivity to CD95-mediated apoptosis, and validated FAP-1 as a miR-200 target that regulates CD95-mediated apoptotic signaling in tumor cells, including RCC cells CAKI-1 and ACHN. When miR-200c was highly over-expressed, CAKI-1 and ACHN cells were found to be more sensitive to TRAIL-induced apoptosis, and CAKI-1 cells were also more sensitive to TNFa-induced apoptosis [87]. miR-145 did not directly induce cell apoptosis but enhance the sensitivity to cisplatin of RCC cells [81].

Conclusions and further aspects.

Although we are in the early phases of miRNA research in RCC, it is anticipated that miRNAs will have a significant impact on improving the patient's diagnosis and management. Based miRNA profiles in RCC, we may identify biomarkers for early detection, follow-up of the disease and predicting treatment efficacy, which will improve patient outcome. Following the discovery of the existence of circulating miRNAs in the plasma and serum of cancer patients, growing evidence shows that circulating miRNAs are promising biomarkers for noninvasive diagnosis and prognosis in various tumor entities. The global expression patterns of miRNAs in patient - matched RCC and normal kidney tissues contribute to the growing understanding of the role that miRNAs play in RCC. Therefore, miRNAs can serve as novel therapeutic targets for RCC. Further studies are needed in larger samples of RCC and further investigation is needed to clarify the roles of identified miRNAs in the pathogenesis of RCC. Moreover, further studies of in vitro and in vivo models are necessary to elucidate miRNAs' targets and role in RCC. The study of miRNAs in RCC will play an important role in prospective clinical medicine as diagnostic, prognostic and predictive biomarkers, and therapeutic strategies.

References.

[1] Cairns P. Renal cell carcinoma. Cancer Biomark 2010;9: 461-73.

[2] Protzel C, Maruschke M, Hakenberg OW. Epidemiology, Aetiology, and Pathogenesis of Renal Cell Carcinoma. Eur Urol Suppl. 2012;11:52-9.

[3] Mikhaylova O, Stratton Y, Hall D, et al. VHL-Regulated MiR-204 Suppresses Tumor Growth through Inhibition of LC3B-Mediated Autophagy in Renal Clear Cell Carcinoma. Cancer Cell. 2012;21:532-46.

[4] Majid S, Saini S, Dar AA, et al. MicroRNA-205 Inhibits Src-Mediated Oncogenic Pathways in Renal Cancer. Cancer

Research. 2011;71:2611-21.
[5] Saini S, Yamamura S, Majid S, et al. MicroRNA-708 Induces Apoptosis and Suppresses Tumorigenicity in Renal Cancer Cells. Cancer Research. 2011;71:6208-19.
[6] Nakada C, Tsukamoto Y, Matsuura K, et al. Overexpression of miR-210, a downstream target of HIF1α, causes centrosome amplification in renal carcinoma cells. J Pathol. 2011;224:280-8.
[7] Yamamura S, Saini S, Majid S, et al. MicroRNA-34a suppresses malignant transformation by targeting c-Myc transcriptional complexes in human renal cell carcinoma. Carcinogenesis. 2011;33:294-300.
[8] Lawrie CH, Gal S, Dunlop HM, et al. Detection of elevated levels of tumour-associated microRNAs in serum of patients with diffuse large B-cell lymphoma. Br J Haematol. 2008;141: 672-5.
[9] Mitchell PS, Parkin RK, Kroh EM, et al. Circulating microRNAs as stable blood-based markers for cancer detection. Proc Natl Acad Sci U S A. 2008;105:10513-8.
[10] Chen X, Ba Y, Ma L, et al. Characterization of microRNAs in serum: a novel class of biomarkers for diagnosis of cancer and other diseases. Cell Res. 2008;18:997-1006.
[11] Weber JA, Baxter DH, Zhang S, et al. The microRNA spectrum in 12 body fluids. Clin Chem. 2010; 56: 1733-41.
[12] Zhang C. Novel functions for small RNA molecules. Curr Opin Mol Ther. 2009;11:641-51.
[13] Kim, V.N. Sorting out small RNAs. Cell 2008; 133: 25-6.
[14] Riedmann, L.T. and R. Schwentner. miRNA, siRNA, piRNA and argonautes: news in small matters. RNA Biol. 2010;7: 133-9.
[15] Linsen SE, de Wit E, de Bruijn E, et al. Small RNA expression and strain specificity in the rat. BMC Genomics 2010;11:249.
[16] Gottardo F, Liu CG, Ferracin M, et al. Micro-RNA profiling in kidney and bladder cancers. Urol Oncol. 2007;25:387-92.
[17] Chow TF, Youssef YM, Lianidou E, et al. Differential expression profiling of microRNAs and their potential involvement in renal cell carcinoma pathogenesis. Clin Biochem. 2010;43:150-8.
[18] Huang Y, Dai Y, Yang J, et al. Microarray analysis of microRNA expression in renal clear cell carcinoma. Eur J Surg Oncol. 2009;35:1119-23.
[19] White NM, Bao TT, Grigull J, et al. miRNA profiling for clear cell renal cell carcinoma: biomarker discovery and identification of potential controls and consequences of miRNA dysregulation. J Urol. 2011;186:1077-83.
[20] Nakada C, Matsuura K, Tsukamoto Y, et al. Genome-wide microRNA expression profiling in renal cell carcinoma: significant down-regulation of miR-141 and miR-200c. J Pathol. 2008;216:418-27.
[21] Juan D, Alexe G, Antes T, et al. Identification of a microRNA panel for clear-cell kidney cancer. Urology. 2010;75:835-41.
[22] Yi Z, Fu Y, Zhao S, et al. Differential expression of miRNA patterns in renal cell carcinoma and nontumorous tissues. J Cancer Res Clin Oncol. 2010;136:855-62.
[23] Melkonyan HS, Feaver WJ, Meyer E, et al. Transrenal nucleic acids: from proof of principle to clinical tests. Ann N Y Acad Sci. 2008;1137:73-81.
[24] Hanke M, Hoefig K, Merz H, et al. A robust methodology to study urine microRNA as tumor marker: microRNA-126 and microRNA-182 are related to urinary bladder cancer. Urol Oncol. 2010;28:655-61.
[25] Duns G, van den Berg A, van Dijk MC, et al. The entire miR-200 seed family is strongly deregulated in clear cell renal cell cancer compared to the proximal tubular epithelial cells of the kidney. Genes Chromosomes Cancer 2013;52:165-73.
[26] Hidaka H, Seki N, Yoshino H, et al. Tumor suppressive microRNA-1285 regulates novel molecular targets: aberrant expression and functional significance in renal cell carcinoma. Oncotarget 2012;3:44-57.
[27] Schaefer A, Jung M, Kristiansen G, et al. MicroRNAs and cancer: current state and future perspectives in urologic oncology. Urol Oncol. 2010;28:4-13.
[28] Metias SM, Lianidou E, Yousef GM. MicroRNAs in clinical oncology: at the crossroads between promises and problems. J Clin Pathol. 2009;62:771-6.
[29] Jung M, Mollenkopf HJ, Grimm C, et al. MicroRNA profiling of clear cell renal cell cancer identifies a robust signature to define renal malignancy. J Cell Mol Med. 2009;13:3918-28.
[30] Petillo D, Kort EJ, Anema J, et al. MicroRNA profiling of human kidney cancer subtypes. Int J Oncol. 2009;35:109-14.
[31] Youssef YM, White NMA, Grigull J, et al. Accurate Molecular Classification of Kidney Cancer Subtypes Using MicroRNA Signature. Eur Urology. 2011 May;59(5):721-30.
[32] Fridman E, Dotan Z, Barshack I, et al. Accurate Molecular Classification of Renal Tumors Using MicroRNA Expression. J Mol Diagn. 2010;12:687-96.
[33] Faragalla H, Youssef YM, Scorilas A, et al. The clinical utility of miR-21 as a diagnostic and prognostic marker for renal cell carcinoma. J Mol Diagn 2012;14:385-92.
[34] Pal S, Dey N, Das F, et al. microRNA-21 Governs TORC1 Activation in Renal Cancer Cell Proliferation and Invasion. PLoS One 2012;7 e37366.
[35] Zhang A, Liu Y, Shen Y, et al. miR-21 Modulates Cell Apoptosis by Targeting Multiple Genes in Renal Cell Carcinoma. Urology 2011;78:474.e13-474.e19.
[36] Zaman MS, Shahryari V, Deng G, et al. Up-regulation of microRNA-21 correlates with lower kidney cancer survival.

PLoS One 2012;7:e31060.
[37] Zhang H, Guo Y, Shang , et al. miR-21 Downregulated TCF21 to Inhibit KISS1 in Renal Cancer. Urology 2012;80:1298-1302.e1.
[38] Powers MP, Alvarez K, Kim HJ, et al. Molecular classification of adult renal epithelial neoplasms using microRNA expression and virtual karyotyping. Diagn Mol Pathol 2011;20:63-70.
[39] Wulfken LM, Moritz R, Ohlmann C, et al. MicroRNAs in renal cell carcinoma: diagnostic implications of serum miR-1233 levels. PLoS One 2011;6:e25787.
[40] Redova M, Poprach A, Nekvindova J, et al. Circulating miR-378 and miR-451 in serum are potential biomarkers for renal cell carcinoma. J Transl Med 2012;10:55.
[41] Wang C, Hu J, Lu M, et al. A panel of five serum miRNAs as a potential diagnostic tool for early-stage renal cell carcinoma. Sci Rep 2015;5:7610.
[42] von Brandenstein M, Pandarakalam JJ, Kroon L, et al. MicroRNA 15a, inversely correlated to PKCalpha, is a potential marker to differentiate between benign and malignant renal tumors in biopsy and urine samples. Am J Pathol 2012;180:1787-97.
[43] Mytsyk Y, Dosenko V, Borys Y, et al. MicroRNA-15a expression measured in urine samples as a potential biomarker of renal cell carcinoma. Int Urol Nephrol 2018;50:851-859.
[44] Cochetti G, Cari L, Nocentini G, et al. Detection of urinary miRNAs for diagnosis of clear cell renal cell carcinoma. Sci Rep 2020;10:21290.
[45] Eichelberg C, Junker K, Ljungberg B, et al. Diagnostic and prognostic molecular markers for renal cell carcinoma: a critical appraisal of the current state of research and clinical applicability. Eur Urol 2009;55:851-63.
[46] Slaby O, Jancovicova, J Lakomy R, et al. Expression of miRNA-106b in conventional renal cell carcinoma is a potential marker for prediction of early metastasis after nephrectomy. J Exp Clin Cancer Res 2010;29:90.
[47] Wang G, Chen L, Meng J, et al. Overexpression of microRNA-100 predicts an unfavorable prognosis in renal cell carcinoma. International Urology and Nephrology 2013;45:373-9.
[48] Liu H, Brannon AR, Reddy AR, et al. Identifying mRNA targets of microRNA dysregulated in cancer: with application to clear cell Renal Cell Carcinoma. BMC Systems Biology 2010;4:51.
[49] Hildebrandt MA, Gu J, Lin J, et al. Hsa-miR-9 methylation status is associated with cancer development and metastatic recurrence in patients with clear cell renal cell carcinoma. Oncogene. 2010;29:5724-8.
[50] Gebauer K, Peters I, Dubrowinskaja N, et al. Hsa-mir-124-3 CpG island methylation is associated with advanced tumours and disease recurrence of patients with clear cell renal cell carcinoma. Br J Cancer. 2013;108:131-8.
[51] Neal CS, Michael MZ, Rawlings LH, et al. The VHL-dependent regulation of microRNAs in renal cancer. BMC Med. 2010;8:64.
[52] Valera VA, Walter BA, Linehan WM, et al. Regulatory Effects of microRNA-92 (miR-92) on VHL Gene Expression and the Hypoxic Activation of miR-210 in Clear Cell Renal Cell Carcinoma. J Cancer. 2011;2:515-26.
[53] Wang X, Wang T, Chen C, et al. Serum exosomal miR-210 as a potential biomarker for clear cell renal cell carcinoma. J Cell Biochem. 2018.
[54] Wotschofsky Z, Busch J, Jung M, et al. Diagnostic and prognostic potential of differentially expressed miRNAs between metastatic and non-metastatic renal cell carcinoma at the time of nephrectomy. Clin Chim Acta. 2013;416:5-10.
[55] Heinzelmann J, Henning B, Sanjmyatav J, et al. Specific miRNA signatures are associated with metastasis and poor prognosis in clear cell renal cell carcinoma. World J Urol. 2011;29:367-73.
[56] White NM, Khella HW, Grigull J, et al. miRNA profiling in metastatic renal cell carcinoma reveals a tumour-suppressor effect for miR-215. Br J Cancer. 2011;105:1741-9.
[57] Khella HW, White NM, Faragalla H, et al. Exploring the role of miRNAs in renal cell carcinoma progression and metastasis through bioinformatic and experimental analyses. Tumour Biol. 2012;33:131-40.
[58] Khella HW, Bakhet M, Allo G, et al. miR-192, miR-194 and miR-215: A Convergent miRNA Network Suppressing Tumor Progression in Renal Cell Carcinoma. Carcinogenesis 2013.
[59] Slaby O, Redova M, Poprach A, et al. Identification of MicroRNAs associated with early relapse after nephrectomy in renal cell carcinoma patients. Genes Chromosomes Cancer 2012;51:707-16.
[60] Gamez-Pozo A, Anton-Aparicio LM, Bayona C, et al. MicroRNA expression profiling of peripheral blood samples predicts resistance to first-line sunitinib in advanced renal cell carcinoma patients. Neoplasia 2012; 14:1144-52.
[61] Berkers J, Govaere O, Wolter P, et al. A Possible Role for MicroRNA-141 Down-Regulation in Sunitinib Resistant Metastatic Clear Cell Renal Cell Carcinoma Through Induction of Epithelial-to-Mesenchymal Transition and Hypoxia Resistance. J Urol. 2013;189:1930-8.
[62] Sun L, Yao Y, Liu B, et al. MiR-200b and miR-15b regulate chemotherapy-induced epithelial-mesenchymal transition in human tongue cancer cells by targeting BMI1. Oncogene 2012;31:432-45.
[63] Lopez-Lago MA, Thodima VJ, Guttapalli A, et al. Genomic deregulation during metastasis of renal cell

carcinoma implements a myofibroblast-like program of gene expression. Cancer Res. 2010;70:9682-92.
[64] Mateescu B, Batista L, Cardon M, et al. miR-141 and miR-200a act on ovarian tumorigenesis by controlling oxidative stress response. Nat Med. 2011;17:1627-35.
[65] Fusco DN, Chung RT. Novel therapies for hepatitis C: insights from the structure of the virus. Annu Rev Med. 2012;63:373-87.
[66] Li C, Feng Y, Coukos G, et al. Therapeutic microRNA strategies in human cancer. AAPS J 2009;11:747-57.
[67] Medina PP, Nolde M, and Slack FJ. OncomiR addiction in an in vivo model of microRNA-21-induced pre-B-cell lymphoma. Nature. 2010;467:86-90.
[68] Costinean S, Zanesi N, Pekarsky Y, et al. Pre-B cell proliferation and lymphoblastic leukemia/high-grade lymphoma in E(mu)-miR155 transgenic mice. Proc Natl Acad Sci U S A. 2006;103:7024-9.
[69] Redova M, Poprach A, Besse A, et al. MiR-210 expression in tumor tissue and in vitro effects of its silencing in renal cell carcinoma. Tumour Biol. 2013;34:481-91.
[70] Vogt M, Munding J, Grüner M, et al. Frequent concomitant inactivation of miR-34a and miR-34b/c by CpG methylation in colorectal, pancreatic, mammary, ovarian, urothelial, and renal cell carcinomas and soft tissue sarcomas. Virchows Archiv. 2011;458:313-322.
[71] Dutta KK, Zhong Y, Liu YT, et al. Association of microRNA-34a overexpression with proliferation is cell type-dependent. Cancer Science. 2007;98:1845-52.
[72] Wong P, Iwasaki M, Somervaille TC, et al. The miR-17-92 microRNA polycistron regulates MLL leukemia stem cell potential by modulating p21 expression. Cancer Res. 2010;70:3833-42.
[73] Yu J, Ohuchida K, Mizumoto K, et al. MicroRNA miR-17-5p is overexpressed in pancreatic cancer, associated with a poor prognosis and involved in cancer cell proliferation and invasion. Cancer Biol Ther. 2010;10.
[74] Chow TF, Mankaruos M, Scorilas A, et al. The miR-17-92 cluster is over expressed in and has an oncogenic effect on renal cell carcinoma. J Urol 2010;183:743-51.
[75] Gibbons DL, Lin W, Creighton CJ, et al. Contextual extracellular cues promote tumor cell EMT and metastasis by regulating miR-200 family expression. Genes Dev. 2009;23:2140-51.
[76] Burk U, Schubert J, Wellner U, et al. A reciprocal repression between ZEB1 and members of the miR-200 family promotes EMT and invasion in cancer cells. EMBO Rep 2008;9:582-9.
[77] Yu XY, Zhang Z, Liu J, et al. MicroRNA-141 is downregulated in human renal cell carcinoma and regulates cell survival by targeting CDC25B. Onco Targets Ther. 2013;6:349-54.
[78] Chen X, Wang X, Ruan A, et al. miR-141 is a key regulator of renal cell carcinoma proliferation and metastasis by controlling EphA2 expression. Clin Cancer Res. 2014;20:2617-30.
[79] Zhai Q, Zhou L, Zhao C, et al. Identification of miR-508-3p and miR-509-3p that are associated with cell invasion and migration and involved in the apoptosis of renal cell carcinoma. Biochem Biophys Res Commun. 2012;419:621-6.
[80] Cui L, Zhou H, Zhao H, et al. MicroRNA-99a induces G1-phase cell cycle arrest and suppresses tumorigenicity in renal cell carcinoma. BMC Cancer. 2012;12:546.
[81] Doberstein K, Steinmeyer N, Hartmetz AK, et al. MicroRNA-145 targets the metalloprotease ADAM17 and is suppressed in renal cell carcinoma patients. Neoplasia. 2013;15:218-30.
[82] Hirata H, Hinoda Y, Ueno K, et al. MicroRNA-1826 directly targets beta-catenin (CTNNB1) and MEK1 (MAP2K1) in VHL-inactivated renal cancer. Carcinogenesis, 2011;33:501-508.
[83] Ueno K, Hirata H, Shahryari V, et al. Tumour suppressor microRNA-584 directly targets oncogene Rock-1 and decreases invasion ability in human clear cell renal cell carcinoma. Br J Cancer 2011;104:308-15.
[84] Wu C, Jin B, Chen L, et al. MiR-30d induces apoptosis and is regulated by the Akt/FOXO pathway in renal cell carcinoma. Cell Signal. 2013;25:1212-21.
[85] Yamasaki T, Seki N, Yamada Y, et al. Tumor suppressive microRNA138 contributes to cell migration and invasion through its targeting of vimentin in renal cell carcinoma. Int J Oncol. 2012;41:805-17.
[86] Yamada Y, Hidaka H, Seki N, et al. Tumor-suppressive microRNA-135a inhibits cancer cell proliferation by targeting the c-MYC oncogene in renal cell carcinoma. Cancer Sci. 2013;104:304-12.
[87] Schickel R, Park SM, Murmann AE, et al. mir-200c Regulates Induction of Apoptosis through CD95 by Targeting FAP-1. Molecular Cell. 2010;38:908-915.

WORLD JOURNAL OF MEDICAL INNOVATIONS

Efficiency of febuxostat (Adenuric®) in preventing of further GFR decline in patients with hyperuricemia with and without diabetic nephropathy associated and chronic kidney disease

Mytsyk Yulian[1], Pasichnyk Serhiy[1], Borzhyevskyy Oleksander[1], Makagonov Ihor[2], Kozlovska Hrystyna[3], Matskevych Viktoriya[4], Kovalsky Vasyl[5], Borzhyevskyy Andriy[1]

[1]*Department of Urology, Danylo Halytsky Lviv National Medical University, Lviv, Ukraine.*
[2]*Department of Radiology, Danylo Halytsky Lviv National Medical University, Lviv, Ukraine.*
[3]*Department of Endocrinology, Danylo Halytsky Lviv National Medical University, Lviv, Ukraine.*
[4]*Department of Radiology and Radiation medicine, Ivano-Frankivsk National Medical University, Ivano-Frankivsk, Ukraine.*
[5]*Department of Oncology and Radiology, Danylo Halytsky Lviv National Medical University, Lviv, Ukraine.*

Article info

NEPHROLOGY

Original paper

Article history:
Accepted
December 11, 2021

Published online
February 10, 2022

Keywords:
chronic kidney disease,
hyperuricemia,
diabetic nephropathy,
glomerular filtration rate,
Febuxostat,
Adenuric

Abstract

Objectives. To assess the efficiency of Febuxostat in preventing of further GFR decline in patients with hyperuricemia with and without diabetic nephropathy (DN) associated and chronic kidney disease (CKD). Material and methods. The prospective study enrolled 73 adult patients with hyperuricemia and CKD of 3A-4 stages (34 patients with DN and 39 without DN). In all cases, baseline and 6 months after beginning of the treatment uric acid serum levels, estimated glomerular filtration rate (eGFR). All patients with DN were randomized into two groups: treatment with febuxostat 40 mg daily (n=16) or placebo (n=18). Patients without DN were similarly randomized: treatment with the same dose of febuxostat (n=20) or placebo (n=19). Statistical significance was considered when P value was <0.05. Results. In patients with DN who received febuxostat or placebo and in patients without DN who received febuxostat or placebo mean baseline eGFR showed no difference (p>0.05). Six months after treatment with febuxostat, eGFR in patients with and without DN changed insignificantly and was 41.63±3.48 and 41.3±7.92 respectively (p>0.05). In patients with and without DN, who received placebo, there was a significant decrease in mean eGFR six months after the treatment: 24.0± 6.51 and 33.26±4.78 correspondingly (p<0.01). On 6-th month there was a statistically substantial difference in mean eGFR between subgroups of patients treated and not treated with febuxostat (p<0.05). Moreover, there was more pronounced decline in mean eGFR in patients with DN who received placebo, compared with subgroup without DN taking placebo (p<0.01). Conclusions. The study demonstrated promising ability of febuxostat to prevent eGFR decline in patients with hyperuricemia with and without diabetic nephropathy associated with chronic kidney disease.

Corresponding author. Mytsyk Yulian, Department of Urology, Lviv National Medical University, Lviv, 79000, Ukraine, +380677722806, mytsyk.yulian@gmail.com

Introduction.

Chronic kidney disease (CKD) is considered to be an irreversible pathologic process, and patients who have it are expected to experience a progressively worsening course [1]. The rate of disease progression varies with the cause, and various therapeutic interventions, such as control of hypertension and proteinuria, have been shown to decrease it [2]. Hyperuricemia has been associated with adverse outcomes in CKD. Increasing level of uric acid in blood may lead to acute kidney injury and hence at risk for development of CKD [3]. Moreover, hyperuricemia has been linked to macrovascular heart disease in diabetic CKD [4]. High uric acid levels have been reported to be associated with increased rates of decline in glomerular filtration rate (GFR) in cross-sectional studies [1,5]. Another well-known risk factor of CKD development is diabetic nephropathy (DN). Simultaneously, type 2 diabetes is the most common cause of CKD and end-stage renal disease worldwide [6]. In the United States 40% of the 29 million individuals with type 2 diabetes have diabetic kidney disease [7]. The classic description of DN involved progressive stages of glomerular hyperfiltration, microalbuminuria, overt proteinuria, and a decline in the GFR, eventually leading to dialysis [8,9]. Febuxostat is a xanthine oxidase inhibitor shown to be efficacious in hyperuricemia and gout [10,11]. It does not require dose modification in patients with kidney failure. Therapy with febuxostat has been shown to prevent renal damage in 5/6 nephrectomized rats [12]. One randomized controlled trial has demonstrated the efficacy of allopurinol in reducing the rate of decline in GFR in patients with CKD with estimated GFRs (eGFRs) < 60 mL/min/1.73 m2 [13]. It was confirmed that febuxostat is able to slow down CKD progression and reduce GFR decline in patients without DN [11]. However, the difference in febuxostat potential to prevent further GFR decline in patients with hyperuricemia, with and without DN associated with CKD was not comprehensively evaluated. In this context, we hypothesized that febuxostat might retard the progression of kidney disease in patients with hyperuricemia and CKD associated with DN.

Objectives.

To assess the efficiency of Febuxostat in preventing of further GFR decline in patients with hyperuricemia with and without diabetic nephropathy associated and chronic kidney disease.

Material and methods.

The prospective study enrolled 73 adult patients with hyperuricemia and CKD of 3A-4 stages (34 patients with DN and 39 without DN). The mean age was 62.4±10.3 years. In all cases, baseline and 6 months after beginning of the treatment uric acid serum levels, estimated glomerular filtration rate (eGFR) and urine protein creatinine index were calculated. In patients with DN mean eGFR was 39.68±8.86 ml/min/1.72 m^2, while in patients without DN it was 42.31±8.54 ml/min/1.72 m^2 (figure 1).

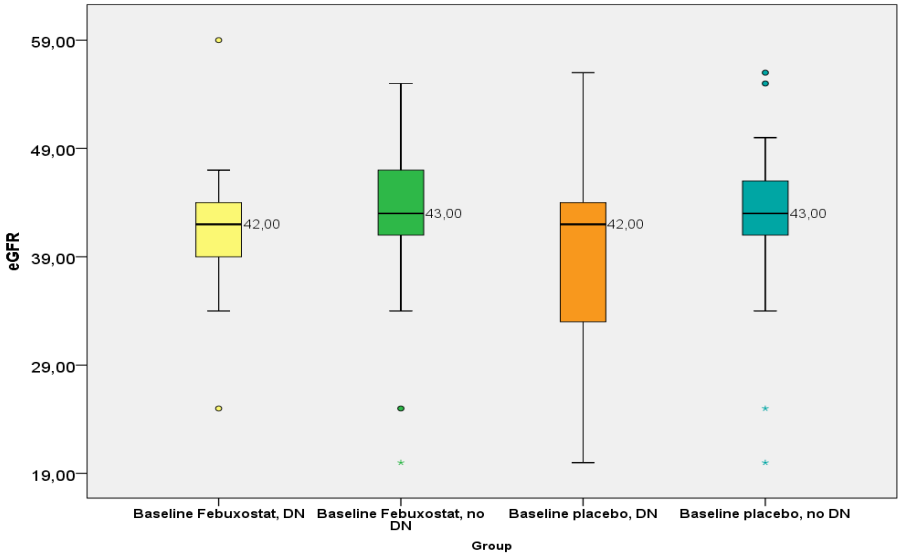

Figure 1. The box plot of the baseline eGFR (ml/min/1.72 m^2) in groups of patients. Notes: DN = diabetic nephropathy.

All patients with DN were randomized into two groups: treatment with febuxostat (Adenuric®) 40 mg daily (n=16) or placebo (n=18). Patients without DN were similarly randomized: treatment with the same dose of febuxostat (n=20) or placebo (n=19). Statistical significance was considered when P value was <0.05.

Results.

In patients with DN who received febuxostat or placebo and in patients without DN who received febuxostat or placebo mean baseline eGFR showed no difference and was 40.31±9.62, 39.11±8.37, 42.45±8.6, 42.16±8.7 accordingly (p>0.05). Six months after treatment with febuxostat, eGFR in patients with and without DN changed insignificantly and was 41.63±3.48 and 41.3±7.92 respectively (p>0.05). Conversely, in patients with and without DN, who received placebo, there was a significant decrease in mean eGFR six months after the treatment: 24.0± 6.51 and 33.26±4.78 correspondingly (p<0.01). On 6-th month there was a statistically substantial difference in mean eGFR between subgroups of patients treated and not treated with febuxostat (p<0.05). Moreover, there was more pronounced decline in mean eGFR in patients with DN who received placebo, compared with subgroup without DN taking placebo (p<0.01) table 1, figure 2.

Table 1. Detailed statistic characteristics of the eGFR (ml/min/1.72 m^2) dynamics in groups of patients

	N	Mean, ml/min/1.72 m^2	Std. Deviation	Std. Error	95% Confidence Interval for Mean		Minimum	Maximum
					Lower Bound	Upper Bound		
Baseline Febuxostat, DN	16	40.31	9.62	2.41	35.18	45.44	15.0	59.0
On 6 MO Febuxostat, DN	16	39.81	2.07	0.52	38.71	40.92	34.0	43.0
Baseline Febuxostat, no DN	20	42.45	8.60	1.92	38.43	46.47	20.0	55.0
On 6 MO Febuxostat, no DN	20	41.30	7.92	1.77	37.59	45.01	20.0	54.0
Baseline placebo, DN	18	39.11	8.37	1.97	34.95	43.27	20.0	56.0
On 6 MO placebo, DN	18	31.61	3.29	0.78	29.97	33.25	25.0	38.0
Baseline placebo, no DN	19	42.16	8.70	2.00	37.96	46.35	20.0	56.0
On 6 MO placebo, no DN	19	38.74	5.43	1.25	36.12	41.36	32.0	45.0

Notes: DN = diabetic nephropathy, MO = month

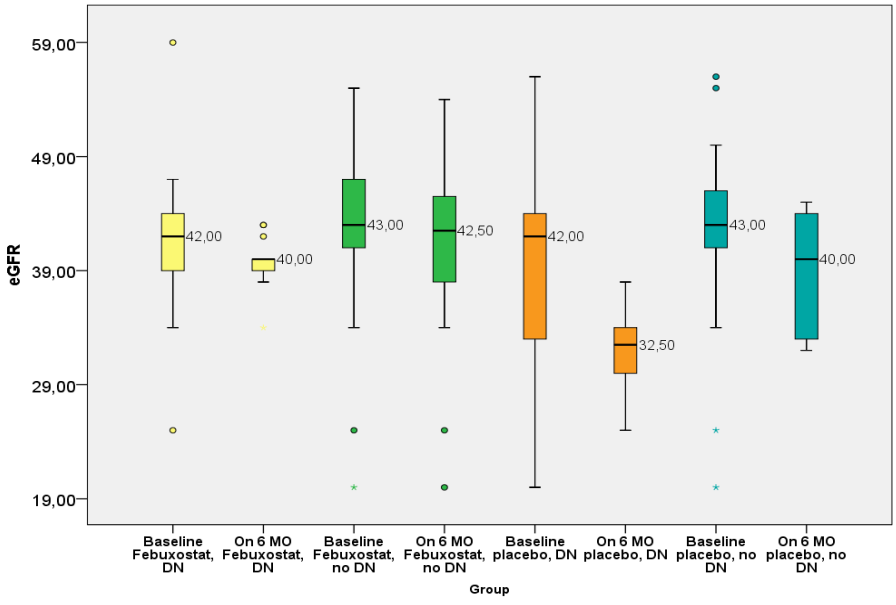

Figure 2. The box plot of the eGFR (ml/min/1.72 m^2) in groups of patients before and after treatment. Notes: DN = diabetic nephropathy, MO = month.

The dynamics of mean uric acid serum levels in all subgroups of patients demonstrated similar to eGFR tendency. However, there were no significant changes in urine protein creatinine index 6 months after the treatment compared to baseline in all subgroups. We observed no serious complications in subgroups treated with febuxostat.

Discussion.

There is a solid evidence that hyperuricemia is associated with adverse outcomes in CKD: increasing level of uric acid in blood may lead to acute kidney injury and to development of CKD [3]. Another well-known risk factor of CKD development is diabetic nephropathy [6]. Our study was dedicated to investigation of the efficiency of Febuxostat in preventing of further GFR decline in patients with hyperuricemia with and without diabetic nephropathy associated and chronic kidney disease. According to a literature analysis, there is a paucity of conflicting data dedicated to dedicated topic. In Sánchez-Lozada et al. work Febuxostat prevented renal injury in 5/6 nephrectomized rats with and without coexisting hyperuricemia. Because Febuxostat helped to preserve preglomerular vessel morphology, normal glomerular pressure was maintained even in the presence of systemic hypertension [12]. According to Kimura et al. data, among 443 patients who were randomly assigned, 219 and 222 assigned to febuxostat and placebo, respectively, were included in the analysis. There was no significant difference in mean eGFR slope between the febuxostat (0.23 ± 5.26 mL/min/1.73 m^2 per year) and placebo (−0.47 ± 4.48 mL/min/1.73 m^2 per year) groups (difference, 0.70; 95% CI, −0.21 to 1.62; P = 0.1). Subgroup analysis demonstrated a significant benefit from febuxostat in patients without proteinuria (P = 0.005) and for whom serum creatinine concentration was lower than the median (P = 0.009). The incidence of gouty arthritis was significantly lower (P = 0.007) in the febuxostat group (0.91%) than in the placebo group (5.86%). Adverse events specific to febuxostat were not observed [11]. Conversely, in another study 45 patients in the febuxostat group and 48 in the placebo group were analyzed. Mean eGFR in the febuxostat group showed a nonsignificant increase from 31.5±13.6 (SD) to 34.7±18.1mL/min/1.73 m^2 at 6 months. With placebo, mean eGFR decreased from a baseline of 32.6±11.6 to 28.2±11.5mL/min/1.73 m^2 (P=0.003). The difference between groups was 6.5 (95% CI, 0.08-12.81) mL/min/1.73 m^2 at 6 months (P=0.05). 17 of 45 (38%) participants in the febuxostat group had a >10% decline in eGFR over baseline compared with 26 of 48 (54%) from the placebo group (P<0.004), febuxostat slowed the decline in eGFR in CKD stages 3 and 4 compared to placebo [14]. There is another ongoing trial dedicated to this topic [15]. In our study application of febuxostat on dose 40 mg daily in patients with hyperuricemia and CKD of 3A-4 stages associated with DN allowed to prevent further eGFR decline. However, we observed no such effect in patients without DN, we explain such phenomena by relatively small number of cases and it was a main limitation of our study. Moreover, in multicenter open-label study of long-term administration of febuxostat in patients with hyperuricemia including gout demonstrated no noteworthy adverse events or adverse drug reactions in the patients with renal dysfunction, and no differences in drug efficacy up to 60 mg/d were noted between the patients with moderate or mild renal dysfunction and those with normal renal function [16]. In our study application of febuxostat also demonstrated excellent safety profile: there were no serious complications in all groups of patients.

Conclusions.

The study demonstrated promising ability of febuxostat (Adenuric®) to prevent eGFR decline in patients with hyperuricemia with and without diabetic nephropathy associated with chronic kidney disease. There was no difference in eGFR 6 months after treatment with febuxostat in patients with and without DN, which enlights its renoprotective equivalence in both subgroups. Treatment with febuxostat demonstrated no serious complications. However, there is an urge in further confirmation of such results in larger long-term studies.

References.

[1] Satirapoj B, Supasyndh O, Nata N, Phulsuksombuti D, Utennam D, Kanjanakul I, et al. High levels of uric acid correlate with decline of glomerular filtration rate in chronic kidney disease. J Med Assoc Thai. 2010 Nov;93 Suppl 6:S65-70.

[2] Johnson RJ, Bakris GL, Borghi C, Chonchol MB, Feldman D, Lanaspa MA, et al. Hyperuricemia, Acute and Chronic Kidney Disease, Hypertension, and Cardiovascular Disease: Report of a Scientific Workshop Organized by the National Kidney Foundation. Am J Kidney Dis. 2018 Jun;71(6):851-65.

[3] Ramirez-Sandoval JC, Madero M. Treatment of Hyperuricemia in Chronic Kidney Disease. Contrib Nephrol. 2018;192:135-46.

[4] Tanaka K, Hara S, Kushiyama A, Ubara Y, Yoshida Y, Mizuiri S, et al. Risk of macrovascular disease stratified by stage of chronic kidney disease in type 2 diabetic patients: critical level of the estimated glomerular filtration rate and the significance of hyperuricemia. Clin Exp Nephrol. 2011 Jun;15(3):391-7.

[5] Ben-Dov IZ, Kark JD. Serum uric acid is a GFR-independent long-term predictor of acute and chronic renal insufficiency:

the Jerusalem Lipid Research Clinic cohort study. Nephrol Dial Transplant. 2011 Aug;26(8):2558-66.

[6] Doshi SM, Friedman AN. Diagnosis and Management of Type 2 Diabetic Kidney Disease. Clin J Am Soc Nephrol. 2017 Aug 7;12(8):1366-73.

[7] Bailey RA, Wang Y, Zhu V, Rupnow MFT. Chronic kidney disease in US adults with type 2 diabetes: an updated national estimate of prevalence based on Kidney Disease: Improving Global Outcomes (KDIGO) staging. BMC Res Notes. 2014 Jul 2;7:415.

[8] Pena MJ, Lambers Heerspink HJ, Hellemons ME, Friedrich T, Dallmann G, Lajer M, et al. Urine and plasma metabolites predict the development of diabetic nephropathy in individuals with Type 2 diabetes mellitus. Diabet Med. 2014 Sep;31(9):1138-47.

[9] Pugliese G, Penno G, Natali A, Barutta F, Di Paolo S, Reboldi G, et al. Diabetic kidney disease: New clinical and therapeutic issues. Joint position statement of the Italian Diabetes Society and the Italian Society of Nephrology on "The natural history of diabetic kidney disease and treatment of hyperglycemia in patients with type 2 diabetes and impaired renal function." Nutr Metab Cardiovasc Dis. 2019 Nov;29(11):1127-50.

[10] Cicero AFG, Fogacci F, Kuwabara M, Borghi C. Therapeutic Strategies for the Treatment of Chronic Hyperuricemia: An Evidence-Based Update. Medicina (Kaunas). 2021 Jan 10;57(1):58.

[11] Kimura K, Hosoya T, Uchida S, Inaba M, Makino H, Maruyama S, et al. Febuxostat Therapy for Patients With Stage 3 CKD and Asymptomatic Hyperuricemia: A Randomized Trial. American Journal of Kidney Diseases. 2018 Dec 1;72(6):798-810.

[12] Sánchez-Lozada LG, Tapia E, Soto V, Avila-Casado C, Franco M, Wessale JL, et al. Effect of febuxostat on the progression of renal disease in 5/6 nephrectomy rats with and without hyperuricemia. Nephron Physiol. 2008;108(4):69-78.

[13] Goicoechea M, de Vinuesa SG, Verdalles U, Ruiz-Caro C, Ampuero J, Rincón A, et al. Effect of allopurinol in chronic kidney disease progression and cardiovascular risk. Clin J Am Soc Nephrol. 2010 Aug;5(8):1388-93.

[14] Sircar D, Chatterjee S, Waikhom R, Golay V, Raychaudhury A, Chatterjee S, et al. Efficacy of Febuxostat for Slowing the GFR Decline in Patients With CKD and Asymptomatic Hyperuricemia: A 6-Month, Double-Blind, Randomized, Placebo-Controlled Trial. Am J Kidney Dis. 2015 Dec;66(6):945-50.

[15] Hosoya T, Kimura K, Itoh S, Inaba M, Uchida S, Tomino Y, et al. The effect of febuxostat to prevent a further reduction in renal function of patients with hyperuricemia who have never had gout and are complicated by chronic kidney disease stage 3: study protocol for a multicenter randomized controlled study. Trials. 2014 Jan 16;15:26.

[16] Kamatani N, Fujimori S, Hada T, Hosoya T, Kohri K, Nakamura T, et al. Multicenter, open-label study of long-term administration of febuxostat (TMX-67) in Japanese patients with hyperuricemia including gout. J Clin Rheumatol. 2011 Jun;17(4 Suppl 2):S50-56.